



This is to certify that the

dissertation entitled

Analysis of air flow patterns in potato storage

presented by Zai-chun Yang

has been accepted towards fulfillment of the requirements for

PhD degree in Agri. Engineering

Date 150ct 91

LIBRARY Michigan State University

PLACE IN RETURN BOX to remove this checkout from your record.

TO AVOID FINES return on or before date due.

DATE DUE	DATE DUE	
<u>वटार ५ ५ ५०८ ।</u>		-
SIP 2 0 LSC		

MSU Is An Affirmative Action/Equal Opportunity Institution c:/circ/datedus.pm3-p.1

ANALYSIS OF AIR FLOW PATTERNS IN POTATO STORAGE

By

Zai-chun Yang

A DISSERTATION

Submitted to
Michigan State University
in partial fulfillment of the requirements
for the degree of

DOCTOR OF PHILOSOPHY

Department of Agricultural Engineering

ABSTRACT

ANALYSIS OF AIR FLOW PATTERNS IN POTATO STORAGE

By

Zai-chun Yang

In a modern potato production system, potatoes are placed in a storage immediately after harvest to reduce losses and to preserve quality for later marketing or processing.

During storage, the quality of potato tubers is strongly affected by the temperature, relative humidity and composition of the air within the potato pile. Therefore, maintenance of a uniform air flow in the duct system and through the storage is important. To serve this purpose, the effect on air flow patterns of various factors, such as the characteristics of potato tubers, the air properties and air flow parameters, and the configurations of the duct system and the potato storage, should be thoroughly understood.

By taking into consideration the roles of the above factors, general and abstract mathematical models were established based on physical principles and experimental data. Because of their nonlinearity, these mathematical models could not be solved analytically. The finite element method was used to facilitate the solution processes. It was an effective method for dealing with nonlinear partial differential equations in the present study.

Following the concepts of the mathematical models and the procedures of applying

the finite element method, the computer programs were written in Fortran code.

The calculated results included pressure, velocity and air flow direction at any point in two- and three-dimensional potato piles, and were plotted as iso-pressure lines, streamlines and velocity profiles.

It was found that uniform air flow usually existed in the upper region of the potato pile where the depth of the pile was equal to or greater than the spacing between two adjacent ducts. Nonuniform air flow dominated the lower region of the potato pile where the depth of the pile was less than the duct spacing.

The region above the lateral duct had reasonable ventilation. But the lower region between two adjacent ducts had the poorest ventilation condition. Here, the pressure showed considerable variation, and the velocity was the lowest at the mid-point between ducts where temperature control would be the most difficult.

Duct spacing had a significant effect on air flow patterns in the potato pile.

Decreasing duct spacing resulted in more uniform air distribution in the pile and improved the air ventilation conditions in the middle lower region between two adjacent ducts.

Duct size had a marked effect on air flow patterns. Increased duct size achieved similar results to decreased duct spacing.

A lower potato pile depth was favorable for having more efficient air ventilation and circulation through the pile.

Duct pressure had little effect on the iso-pressure lines and the streamlines.

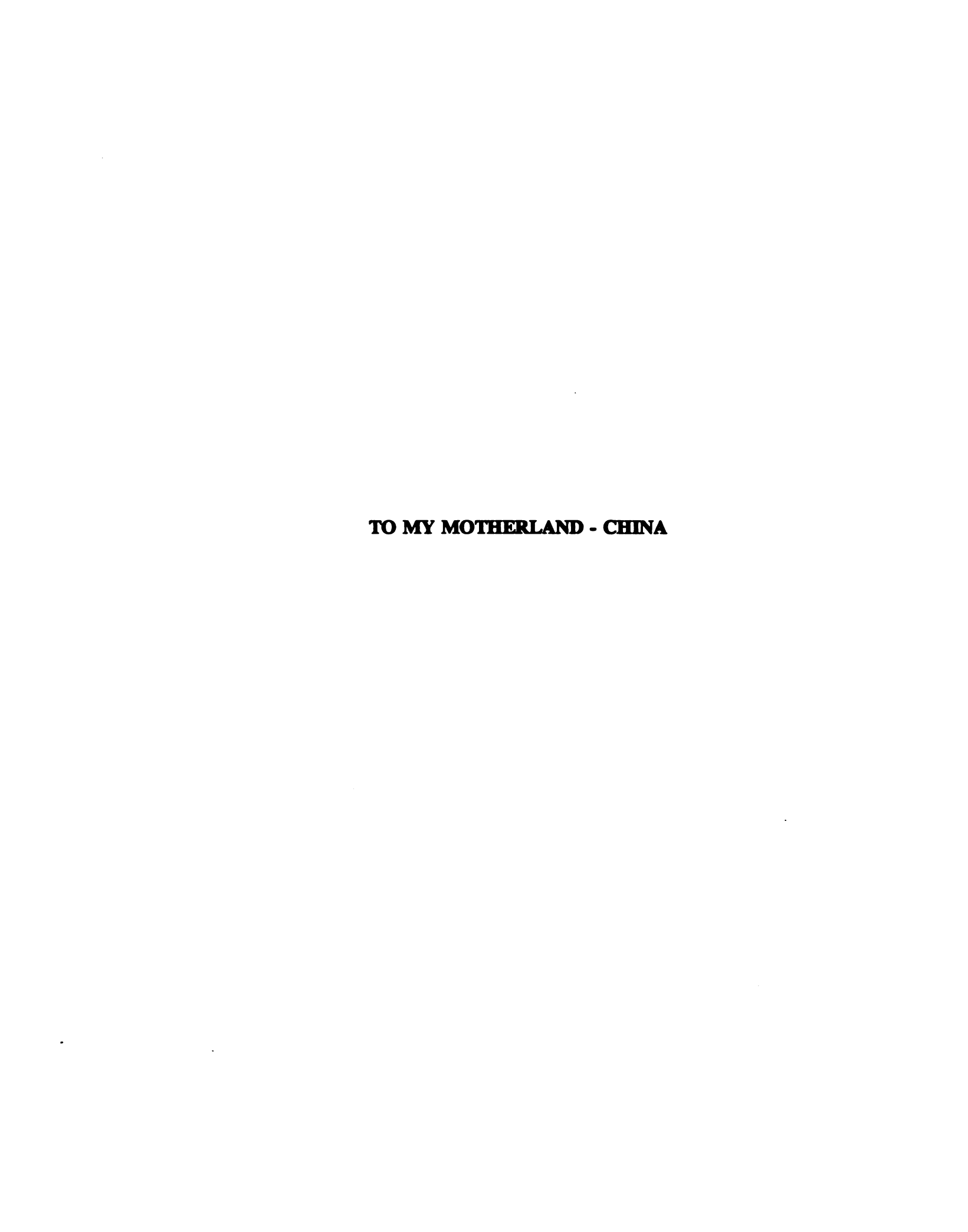
The general air ventilation condition in the middle lower region between two adjacent ducts was independent of the duct shapes studied when ducts with different shapes have

equivalent diameters. However, in-floor rectangular duct tended to have a more uniform air distribution in the pile than ducts with triangular, circular and semicircular shapes.

In a potato storage, air flow distribution along the duct axial direction was generally nonuniform. The effect on air flow patterns of the distance from a given cross-section to the duct entrance was equivalent to that of different duct pressures on air flow patterns.

Approved

Department Chairman



ACKNOWLEDGMENTS

The author wishes to express his sincere appreciation to Dr. Roger C. Brook (Professor and Extension Specialist, Department of Agricultural Engineering) for his encouragement, guidance and support as the major professor and chairman of the doctoral advisory committee.

The author is very grateful to Dr. Larry J. Segerlind (Professor, Department of Agricultural Engineering), Dr. Amritlal M. Dhanak (Professor, Department of Mechanical Engineering) and Dr. Jerry N. Cash (Professor and Extension Specialist, Department of Food Science and Human Nutrition) for their serving on the doctoral advisory committee and for their help and guidance.

Special thanks are extended to Dr. Thomas H. Burkhardt (Professor, Department of Agricultural Engineering), Dr. John F. Foss (Professor, Department of Mechanical Engineering) and Dr. Charles A. Petty (Professor, Department of Chemical Engineering) for their help and advice during the author's graduate study in Michigan State University.

The author is indebted to the faculty, staff and students in the Department of Agricultural Engineering for their friendship and help.

TABLE OF CONTENTS

Page
LIST OF TABLESxi
LIST OF FIGURESxii
LIST OF SYMBOLS xvi
Chapter
1 INTRODUCTION1
1.1 Background
1.2 Objectives
2 LITERATURE REVIEW4
2.1 The potato crop4
2.2 Causes and control of deterioration of stored potato
2.2.1 Physical problems8
2.2.2 Physiological problems9
2.2.2.1 Water loss9
2.2.2.2 Respiration10
2.2.2.3 Sugar level
2.2.2.4 Sprouting
2.2.3 Pathological problems

Chapter	Page
2.3 Air ventilation systems for potato storage	18
2.3.1 Types of air ventilation system	18
2.3.2 Structures of ventilation system	19
2.3.3 Duct spacing and duct size	21
2.3.4 Duct opening and its location	22
2.3.5 Ventilation rate for potato storage	25
2.4 Equations of predicting the behavior of fluid flow through porous media	27
2.4.1 Darcy's equation	27
2.4.2 Muskat's equation	29
2.4.3 Shedd's equation	33
2.4.4 Hukill's equation	35
2.4.5 Sheldon's equation	37
2.4.6 Bear's eqaution	39
2.4.7 Brooker's equation	40
2.4.8 Segerlind's equation	41
2.4.9 Other equations	43
2.5 Representing fluid flow through porous media	45
3 ANALYSIS METHODS	68
3.1 Establishment of mathematical models	68
3.1.1 Models of pressure and velocity distributions	68
3.1.2 Models of streamlines and flow rates	71
3.2 Application of finite element method	73

Chapter	Page
3.2.1 Applying the Galerkin method	74
3.2.2 Applying the Green-Gauss theorem	75
3.2.3 Jacobian transformation	77
3.2.4 Gauss-Legendre quadrature	81
3.2.5 Applying the direct stiffness method	82
3.2.6 Applying the Newton-Raphson method	82
3.3 Compilation of computer programs	85
3.3.1 Calculation of nodal pressure values	85
3.3.2 Calculation of pressure and velocity for the selected cross-sec	tion88
3.3.3 Calculation of streamlines and flow rate for the selected cross	s-section90
4 ANALYSIS OF AIR FLOW PATTERNS	93
4.1 Preparation of basic data	93
4.1.1 Basic data of duct system and potato storage	93
4.1.2 Selection of variables and their levels	94
4.1.3 Coefficients in Shedd's equation	96
4.1.4 Defining boundary conditions	97
4.1.5 Calculation of duct pressures	99
4.1.6 Mesh generation	102
4.2 The effect on air flow patterns of variables under study	107
4.2.1 The effect of duct spacing on air flow patterns	108
4.2.2 The effect of duct size on air flow patterns	124
4.2.3 The effect of potato pile depth on air flow patterns	136

Chapter	Page
4.2.4 The effect of duct pressure on air flow patterns	140
4.2.5 The effect of duct shape on air flow patterns	141
4.2.6 The effect of the distance to the duct entrance on air flow patterns	142
5 CONCLUSIONS AND RECOMMENDATIONS	144
5.1 Conclusions	144
5.2 Recommendations	147
LIST OF REFERENCES	148

LIST OF TABLES

Tabl	le	Page
1	Total potato production, utilization, and shrinkage and loss in the United States for five selected years	6
2	The nutrient composition of potatoes	7
3	Respiration rate of potato tubers for the British cultivars Arran Consul, King Edward and Majestic	11
4	Potato bed depth vs the required length of 1.9 cm slot for in-floor rectangular duct in the Pacific Northwest	23
5	Potato bed depth vs spacing of discharge hole for circular duct in the Pacific Northwest	23
6	Selected variables and their levels as used in the computer programs	95
7	Coefficients A and B of Equation [13] for air flow through potato storage	97
8	The effect of duct spacing on air flow patterns: related data and Figure numbers	111
9	The effect of duct size on air flow patterns: related data and Figure numbers	127

LIST OF FIGURES

Figu	Page Page
1	The relationship between storage temperature and sugar contents of potato tubers (cv. Majestic)
2	The typical changes in sucrose concentration during growth and storage of potato tubers
3	Typical arrangements of main plenum and lateral ducts for potato storage
4	Effect of equivalent diameter on the uniformity of air discharge21
5	Effect of the ratio of discharge area to duct cross-sectional area on the uniformity of air discharge
6	Patterns of temperature, moisture, pressure and streamline distribution in a grain drying bin
7	Air flow patterns in the section of an oat drying bin47
8	Air distribution patterns for different duct shapes and spacings48
9	Pressure patterns established by numerical method and by experimental data
10	Iso-flow lines, iso-pressure lines and streamlines for different duct openings
11	Velocity distribution in the lower portion of the bin for three duct pressures
12	Calculated pressure patterns expressed as percentage of duct pressure54
13	Pressure patterns obtained from experimental data for different duct pressures
14	Air pressure and flow path patterns for different grain repose angles

rigi	ure	Page
15	Air pressure and flow path patterns for a section of a conical shaped pile	57
16	Calculated iso-pressure lines in a grain drying bin with different duct shapes and openings	59
17	Pressure contour lines in the entrance region	61
18	Pressure distribution for Y-shaped duct	62
19	Velocity distribution for Y-shaped duct	63
20	Pressure contour lines for grain bed with different duct pressures	65
21	Velocity vector fields for bins with semicircular and rectangular ducts	66
22	Air flow patterns for flat grain storage with three circular ducts	68
23	Sketch of twenty-node solid element with natural coordinates	78
24	The flow chart of the computer program for the calculation of nodal pressure values in 3-D space	87
25	The flow chart of the computer program for the calculation of pressure and velocity in 2-D space	89
26	The flow chart of the computer program for the calculation of streamline and flow rate in 2-D space	92
27	Sketch of boundary conditions for potato storage	98
28	Friction coefficient as a function of Reynolds number for round pipes of various relative roughness ratio ε _s /d	101
29	Mesh generation for potato storage with triangular duct	103
30	Mesh generation for potato storage with circular duct	104
31	Mesh generation for potato storage with semicircular duct	105

Figu	ure	Page
32	Mesh generation for potato storage with rectangular duct	106
33	Iso-pressure lines and streamlines (left) and velocity profiles (right) for triangular duct with duct spacing of 1.8 m	112
34	Iso-pressure lines and streamlines (left) and velocity profiles (right) for triangular duct with duct spacing of 2.4 m	113
35	Iso-pressure lines and streamlines (left) and velocity profiles (right) for triangular duct with duct spacing of 3.1 m	114
36	Iso-pressure lines and streamlines (left) and velocity profiles (right) for circular duct with duct spacing of 1.8 m	115
37	Iso-pressure lines and streamlines (left) and velocity profiles (right) for circular duct with duct spacing of 2.4 m	116
38	Iso-pressure lines and streamlines (left) and velocity profiles (right) for circular duct with duct spacing of 3.1 m	117
39	Iso-pressure lines and streamlines (left) and velocity profiles (right) for semicircular duct with duct spacing of 1.8 m	118
40	Iso-pressure lines and streamlines (left) and velocity profiles (right) for semicircular duct with duct spacing of 2.4 m	119
41	Iso-pressure lines and streamlines (left) and velocity profiles (right) for semicircular duct with duct spacing of 3.1 m	120
42	Iso-pressure lines and streamlines (left) and velocity profiles (right) for rectangular duct with duct spacing of 1.8 m	121
43	Iso-pressure lines and streamlines (left) and velocity profiles (right) for rectangular duct with duct spacing of 2.4 m	122
44	Iso-pressure lines and streamlines (left) and velocity profiles (right) for rectangular duct with duct spacing of 3.1 m	123
45	Iso-pressure lines and streamlines (left) and velocity profiles (right) for triangular duct with duct size of $h_t \times a_t = 0.64 \text{ m} \times 0.36 \text{ m}$	128
46	Iso-pressure lines and streamlines (left) and velocity profiles (right) for triangular duct with duct size of h. × a. = 0.67 m × 0.39 m	129

Figu	ire	Page
47	Iso-pressure lines and streamlines (left) velocity profiles (right) for circular duct with duct size of $d_c = 0.54 \text{ m}$	130
48	Iso-pressure lines and streamlines (left) velocity profiles (right) for circular duct with duct size of $d_e = 0.58 \text{ m}$	131
49	Iso-pressure lines and streamlines (left) velocity profiles (right) for semicircular duct with duct size of $r_a = 0.38 \text{ m}$	132
50	Iso-pressure lines and streamlines (left) velocity profiles (right) for semicircular duct with duct size of $r_s = 0.41 \text{ m}$	133
51	Iso-pressure lines and streamlines (left) velocity profiles (right) for rectangular duct with duct size of $a_r \times b_r = 0.34 \text{ m} \times 0.34 \text{ m}$	134
52	Iso-pressure lines and streamlines (left) velocity profiles (right) for rectangular duct with duct size of $a_r \times b_r = 0.36 \text{ m} \times 0.36 \text{ m}$	135
53	Iso-pressure lines and streamlines (left) velocity profiles (right) for triangular duct with depth of potato pile of 3.1 m	138
54	Iso-pressure lines and streamlines (left) velocity profiles (right) for triangular duct with depth of potato pile of 5.5 m	139

LIST OF SYMBOLS

Dimensions: L=Length, M=Mass, t=Time, and T=Temperature

- A Constant in Equation [3], [4], [5], [7], [10], [12], [13], [15], [17], [18], [27]
- A Cross-sectional area in Equation [1] (L²)
- A_c Flow cross-sectional area in Equation [73] (L^2)
- A_c Lateral duct opening area (L^2)
- A_1 Cross-sectional area of lateral duct (L^2)
- A_p Cross-sectional area of main plenum (L²)
- [A] Jacobian matrix in Equation [67], [68]
- a, Half of the width of rectangular duct (L)
- a, Half of the base length of triangular duct (L)
- adj Notation of adjoint matrix in Equation [59]
- B Constant in Equation [3], [4], [5], [6], [7], [8], [9], [10], [12], [13], [15], [17], [18], [25], [27], [30]
- [B] Row vector of the first order derivatives of [N] in Equation [52], [53], [58], [61], [63]
- [B]^T Transposed [B] in Equation [52], [61], [63]
- b_r Height of rectangular duct (L)
- C Constant in Equation [3], [8], [10], [12], [28], [29]
- C State of flow factor in Equation [6]
- C. Potato storage capacity (M)
- $\cos \alpha$ Direction cosine in Equation [50]

- $\cos\beta$ Direction cosine in Equation [50]
- $\cos \gamma$ Direction cosine in Equation [50]
- cosh Hyperbolic cosine in Equation [16]
- D Equivalent diameter in Equation [18] (L)
- D_h Hydraulic diameter in Equation [73] (L)
- [D] Diagonal matrix in Equation [52]
- d Diameter of duct in Equation [70], [71] (L)
- d Effective diameter of granular particle in Equation [4], [6] (L)
- d Notation of differential in Equation [38], [39], [42], [43], [47], [50], [52], [60], [61]
- d. Diameter of circular duct (L)
- det Notation of determinant in Equation [59], [60], [61], [63]
- div Notation of divergence
- (e) Notation of element in Equation [47], [49], [51], [52], [61], [62]
- exp Exponent in Equation [30]
- F_i Function of natural coordinates in Equation [65], [66], [67], [68]
- {F} Force vector in Figure 24
- f Friction factor in Equation [70], [72]
- f_P Friction factor in Equation [18]
- f₁ Leva's friction factor in Equation [6]
- f_m percentage distribution of fine materials in Equation [12], [17]
- f_s Particle shape factor in Equation [6]
- g Acceleration of gravity in Equation [4], [6], [69], [70] (Lt²)

- g Specific gravity of potato (ML-3)
- H Height of packed bed in Equation [1] (L)
- H Depth of grain bed in Equation [18], [28] (L)
- H Height of potato storage (L)
- H_P Depth of potato pile (L)
- h₁ Hydraulic head in Equation [1] (L)
- h₂ Hydraulic head in Equation [1] (L)
- h_f Friction loss in Equation [69], [70] (L)
- h, Height of triangular duct (L)
- [J] Jacobian matrix in Equation [56], [57], [59], [60], [61], [63]
- [J]⁻¹ Inverse matrix of [J] in Equation [58], [59]
- K Constant in Equation [28], [29], [31]
- K Hydraulic conductivity in Equation [1] (Lt⁻¹)
- K Permeability in Equation [21]
- [K^(e)] Element stiffness matrix in Equation [51], [52], [61], [62]
- [K] Global stiffness matrix in Equation [64]
- K_E Modified Ergun product constant in Equation [7]
- K_G Granular permeability in Equation [26], [27], [36], [37], [47]
- K_v Function of velocity in Equation [17]
- K_x Permeability related to local coordinate in Equation [20]
- K, Permeability related to local coordinate in Equation [20]
- K₂ Permeability related to local coordinate in Equation [20]
- k Permeability of porous media in Equation [2] (L²)

- L Length of potato storage (L)
- L_d Duct spacing (L)
- In Natural logarithm in Equation [15], [17], [19]
- log Common logarithm in Equation [14]
- M Function of pump work in Equation [69] (L)
- m Coefficient in Equation [25]
- m_e Moisture content in Equation [19]
- N₁ Number of lateral duct
- [N] Row vector of shape function
- [N]^T Transposed [N] in Equation [47]
- n Notation of normal direction
- P Pressure $(ML^{-1}t^{-2})$
- P_d Lateral duct pressure (ML⁻¹t⁻²)
- P_w Wetted perimeter in Equation [73] (L)
- p Dimensionless pressure parameter in Equation [14]
- Q Volumetric flow rate in Equation [1] (L^3t^1)
- Q Function of Cartesian coordinates in Equation [50]
- Q_1 Air flow rate in lateral duct (L^3t^{-1})
- q Air flow rate per unit mass $(L^3t^1M^{-1})$
- R Function of Cartesian coordinates in Equation [50]
- R Ratio of open area of duct system to floor area served by duct system
- R_m Source strength in Equation [16]
- R^(e) Contribution of element to the residual equation in Equation [47]

Reynolds number in Equation [71], [72] Re_D Radius of semicircular duct (L) r, S Curved surface in Equation [50] sinh Hyperbolic sine in Equation [16] Time t T Function of Cartesian coordinates in Equation [50] ប្រា Upper triangular matrix in Figure 24 V Velocity vector V Velocity (Lt¹) V Volume in Equation [47], [52], [60] (L^3) V. Air flow velocity exiting lateral duct (Lt^{-1}) V_1 Air flow velocity in the lateral duct (Lt^{-1}) V_m Mean fluid velocity over duct cross-section in Equation [71] V. Velocity in normal direction (Lt1) V_{p} Air flow velocity in main plenum (Lt^1) V_{x} Velocity component in Cartesian coordinates (Lt1) ٧, Velocity component in Cartesian coordinates (Lt^1) V, Velocity component in Cartesian coordinates (Lt1) W Width of bin in Equation [16] (L) W Width of potato storage **(L)** W.G. Water gauge **(L)** W_{iik} Weighting coefficients in Equation [62]

(L)

X

Cartesian coordinates

- x Cartesian coordinates (L)
- Y Cartesian coordinates (L)
- y Cartesian coordinates (L)
- y₁ Elevation head in Equation [69] (L)
- y₂ Elevation head in Equation [69] (L)
- Z Cartesian coordinates (L)
- z Cartesian coordinates (L)
- ϵ Porosity of porous media in Equation [4], [6]
- ϵ Preset comparative value in Figure 24
- ϵ_s Roughness in Equation [70] and Figure 28 (L)
- Y Natural coordinate
- η Natural coordinate
- μ Dynamic viscosity of fluid in Equation [2], [4], [5], [71] (ML⁻¹t⁻¹)
- ξ Natural coordinate
- ξ_i Natural coordinates of sampling points
- π The ratio of the circumference of a circle to its diameter in Equation [16]
- π_i The π numbers in Equation [11]
- ρ Density of fluid in Equation [4], [5], [6], [32], [69], [71] (ML⁻³)
- ρ_b Dry matter bulk density in Equation [19] (ML⁻³)
- Σ Summation in Equation [62]
- ¥ Stream function in Equation [41], [42], [43], [45], [46]
- ∂ Notation of partial derivative

CHAPTER 1

INTRODUCTION

1.1 Background

Potatoes are an important agricultural crop and are a main food in the daily diet of the United States. In 1987 potato production reached 17.7 million metric tons, among which 50.3%, 33.5% and 8.1% were used for processing, for table stock and for other usages (such as seed and feed), respectively. However 8.2% were lost due to damage, shrinkage, deterioration or other factors (USDA Agricultural Statistics, 1989).

In a modern potato production system, potatoes will be put in storage immediately after harvest to reduce losses and to preserve quality for later marketing or processing. During storage, the quality of potato tubers may deteriorate due to physical, physiological and pathological problems. The extent of deterioration, among other things, is closely related to the temperature, relative humidity and composition of the air within the potato storage.

To maintain a suitable temperature, relative humidity and air composition, forced air ventilation systems are commonly used in commercial potato storages. A uniform air flow through the potatoes in storage is desirable to achieve ideal air conditions and consequently to help maintain the quality of the stored potato tubers. Therefore, the investigation of pressure and velocity distributions within stored potatoes becomes an

important research subject.

Fluid flow through porous media, such as air flow through a potato pile, is a simple physical process. Yet, numerous researchers in various fields have analyzed the factors that affect this process and have attempted to formulate mathematical prediction models. This fact not only indicates the importance of the subject of fluid flow through porous media in the relevant engineering areas, but also implies the difficulty in describing the phenomena of fluid flow through porous media.

Air flowing through a potato pile will encounter resistance from potato tubers or dirt, causing a pressure drop to develop. Air flow patterns in a potato storage are strongly affected not only by characteristics of potato itself such as tuber size, porosity, orientation and cleanness, but also by air properties and flow parameters, and by the configurations of the air duct system and the storage. Because of the inhomogeneous distribution of potato size and porosity, and the nonuniform distribution of air flow along the duct length, air flow phenomena in a potato pile will show nonuniformity both in two- and three-dimensional spaces. By taking into consideration these factors and their mutual relationships, mathematical models based on physical principles and experimental data can be built. These models, which govern the relationship between pressure gradient and air velocity, will provide a useful means for studying air flow patterns in a potato pile and for evaluating the effect of various factors on these patterns.

Since these models involve nonlinear partial differential equations, they can not be solved analytically (Ames, 1965). The finite element method, which has been proved to be an effective numerical method for solving field problems (Segerlind, 1984), was used in this study to facilitate the solution process. The pressure, velocity and air flow

direction at any point within the pile in two- and three-dimensional domains can be calculated and the air flow patterns in the forms of iso-pressure lines, streamlines and velocity profiles can be plotted.

1.2 Objectives

The general purpose of this study was to analyze air flow patterns within a potato pile in two- and three-dimensional spaces. In order to reach this goal, mathematical models of the process were developed. Using the finite element method, computer programs were written to calculate the specific solutions for the mathematical models.

The specific objectives for analyzing the calculated results were:

- 1. To present graphically the iso-pressure lines, streamlines and velocity profiles;
- 2. To predict the common tendency of air flow patterns in a potato pile;
- To analyze the effect on air flow patterns of duct spacing, duct size, duct pressure, duct shape, depth of potato pile and the distance from a selected cross-section to the duct entrance.

CHAPTER 2

LITERATURE REVIEW

2.1 The potato crop

The potato is an ancient domesticated crop. It originates from the Andes of Peru and Bolivia in South America. This crop was first introduced into the North American continent from England via Bermuda in 1621 (Hawkes, 1978).

There are two main cropping seasons in the United States: early-crop potatoes and late-crop potatoes. The early-crop potatoes are mostly planted in the Southern and Western states and harvested during the spring and summer months. The late-crop potatoes are planted in the Northern half of this country and are harvested during the late summer and fall months. Most of the late-crop potatoes are stored, with about half of the stored potatoes used for processing purposes (Hardenburg et al. 1986). The total production for each of five selected years is shown in Table 1 (USDA Agricultural Statistics, 1989).

The utilization of the potato has changed, with potatoes processed for food increasing significantly. The processed potato, including potato chips, frozen french fries, dehydration, etc., accounted for only 10.1 percent of the total production and 13.7 percent of the total use for food in 1956, but it reached 50.3 percent and 60.0 percent

in 1987, respectively. In contrast, potatoes used for fresh food has declined markedly as shown in Table 1.

The potato is rich in nutrients. It provides significant quantities of food energy, protein and vitamin C. Table 2 gives the nutritional values in percentages of the U.S. Recommended Daily Allowances established in 1973 (revised in 1980). It is obvious that potato can provide an important source of vitamin C in the daily diet.

To provide a common language for commerce and to set a minimum quality level, the United States Department of Agriculture developed the Potato Grade Standards. These standards specify U.S. extra #1, U.S. #1, U.S. commercial and U.S. #2 grades. Among these grades U.S. #1 is the principal trading grade. Visual inspection is used most often to evaluate the quality of potatoes. Potatoes of any kind and size should have a relatively smooth, clean and well shaped appearance without badly cut and bruised skin and without any green part from light exposure. They also should have a firm texture without wilt and sprouting (Seelig, 1972). Besides the above visual qualities, stored potatoes for processing purpose should be mature, not stressed, free from imperfections, low in reducing sugars (less than 0.25 percent) and high in specific gravity (Gould, 1984).

Table 1. Total potato production, utilization, and shrinkage and loss in the United States for five selected years.

Source: USDA Agricultural Statistics, 1989

(Unit: 1,000 metric ton)

Year	1956	1960	1970	1980	1987
Total production	11,159	11,673	14,782	13,797	17,675
Total for fresh food	7,054	7,006	5,950	4,516	5,912
Total for processed food	1,123	2,224	5,811	6,857	8,883
Total shrinkage and loss	69 6	589	1,088	1,055	1,448
Total for other usages	2,286	1,854	1,933	1,369	1,432
Fresh food to total production	63.2 %	60.0 %	40.3 %	32.7 %	33.5 %
Fresh food to total potato used for food	86.3 %	75.9 %	50.6 %	39.7 %	40.0 %
Processed to total production	10.1 %	19.1 %	39.3 %	49.7 %	50.3 %
Processed to total potato used for food	13.7 %	24.1 %	49.4 %	60.3 %	60.0 %
Shrinkage and loss to total production	6.2 %	5.1 %	7.4 %	7.7 %	8.2 %
Other usages to total Production	20.5 %	15.9 %	13.1 %	9.9 %	8.1 %

Table 2. The nutrient composition of potatoes Source: Thornton and Sieczka, 1980

Nutrient	Nutrient Values	% U.S. RDA in medium potato (about 150g)	% U.S. RDA in large potato (about 250g)
Calories		About 110, approx. 4% of total calories for adult male	About 180, approx. 7% of total calories for adult male
Vitamin C	13.2 - 54.2 mg	56.6 %	93.3 %
Iodine	0.05 - 0.04 mg	15.2 %	25.3 %
Vitamin B ₆	0.20 - 0.60 mg	16.4 %	27.3 %
Niacin	1.00 - 3.50 mg	12.1 %	20.2 %
Copper	0.10 - 0.50 mg	16.9 %	28.2 %
Magnesium	0.03 - 0.04 g	7.8 %	13.0 %
Thiamin(B ₁)	0.07 - 0.15 mg	8.7 %	14.5 %
Phosphorus	0.05 - 0.10 g	7.3 %	12.2 %
Protein	2.50 - 3.60 g	4.7 %	7.8 %
Folic Acid	7.80 - 32.5 mg	4.9 %	8.2 %
Iron	0.40 - 2.10 mg	5.2 %	8.7 %
Riboflavin(B ₂)	0.03 - 0.10 mg	3.6 %	6.0 %
Zinc	0.50 - 0.80 mg	3.9 %	6.5 %

2.2 Causes and control of deterioration of stored potatoes

2.2.1 Physical problems

Potatoes that are mechanically harvested may be injured by blades, chains and other moving parts. The injured potato tubers, if left unprotected, will have high evaporation losses and will be easily affected by diseases. The rate and extent of the wound healing process are mainly affected by temperature, humidity and composition of the air surrounding the tubers. Wilson (1967) suggested that, immediately after being placed in storage, potatoes be cured by holding at a temperature of about 10° to 15.6° C and a relative humidity of above 90 percent for 10 to 14 days to permit suberization and wound periderm formation. Earl (1976) proposed a higher temperature of 15.6° to 21.1° C and a higher relative humidity of 95 percent. Although wound periderm formation is most rapid at about 21° C, Hardenburg et al. (1986) maintained that a temperature of 10° to 15.6° C would be preferable, as decay to the injured part is more likely to occur at a higher temperature.

While temperature plays an important role in the process of suberization, the relative humidity level has more influence than temperature on a desirable new dense periderm. Potatoes stored in an environment with a high relative humidity of 95 percent will suberize at temperatures of 7.2° to 18.3° C (Cargill, 1976).

Hammerschmidt and Cameron (1986 and 1987) investigated the effect of CO₂ level on wound healing. They found that as the CO₂ level increased from 0.0% to 8.0% the rate of wound healing gradually declined and the degrees of the soft rot decay gradually

increased. Therefore, increases in CO₂ during the early phase of storage can have a very negative effect on the potato tubers.

During the loading and unloading processes in the potato storage, potatoes may also suffer injury. Cargill (1976) recommended that the drop height be limited to 30 to 40 cm and that conveyor speeds not exceed 40 m/min. Cargill (1976) and Rastovski et al. (1987) also noted that during storage, pressure bruise will pose a serious problem to the lower layer of potatoes, since the deformed or damaged tissue is particularly sensitive to blue-grey discoloration. To help reduce pressure bruise, Cargill (1976) recommended that the depth of the potato storage be limited to 3.7 to 4.6 m, and the relative humidity in the storage should be kept at 92 to 95 percent.

2.2.2 Physiological problems

2.2.2.1 Water loss

The potato tuber contains 74 to 82 percent water (Burton, 1989). Water loss will directly affect both the weight loss and the appearance of the potato. Shrinkage and loss account for 5 to 8 percent of the total potato production as presented previously in Table 1. Cargill (1976) observed that if potato weight loss reaches 5 percent of the original weight, the potato will shrink; if this loss reaches 10 percent of the original weight, the potato will become wrinkled and spongy, difficult to peel and virtually unsalable.

Water loss from stored potato tubers is mainly through evaporation and respiration.

It is closely related to the temperature and humidity of the air in the storage, in addition

to factors such as cultivar, tuber size, maturity and injury condition. Under constant humidity conditions, higher temperatures result in a higher vapor pressure deficit and higher water loss. Under constant temperature conditions, lower humidities result in a higher vapor pressure deficit and higher water loss. Therefore, potato weight loss can be minimized by reducing the storage temperature to reduce vapor pressure deficit and tuber respiration rate, and by increasing the storage relative humidity to reduce vapor pressure deficit and moisture exchange. Hardenburg et al. (1986) recommended that to minimize weight loss the optimum temperature range for storing most cultivars of potatoes to be processed into chips or french fries be between 10° and 13° C and the desirable relative humidity be 95 percent. Rastovski et al. (1987) proposed a lower temperature for long term storage: 7° to 10° C for chipping potatoes and 5° to 8° C for french frying potatoes.

2.2.2.2 Respiration

The potato is a living organism, and respiration is the metabolic process necessary for maintaining the life of the potato tuber. During this process the sugars in the tuber are converted into carbon dioxide, water and heat energy through the consumption of oxygen. The whole process can be described by the following relationship:

$$C_6H_{12}O_6 + 6O_2 \Rightarrow 6CO_2 + 6H_2O + Energy$$

Under standard conditions, for example, the oxidation of 180 g (1 mole) of glucose with 192 g (6 mole) of oxygen will release 264 g (6 mole) of carbon dioxide, produce 108 g (6 mole) of water and yield 2,880 kJ of energy among which about 30% is fixed in ATP (metabolic energy) and 68% is released into surrounding media in the form of heat

(Stryer, 1975 and Rastovski et al. 1987). Obviously, respiration will directly result in the loss of dry matter from the potato tuber. But the main problems related to respiration of the stored potatoes are temperature increases, the accumulation of CO_2 and the depletion of O_2 . As respiration rate increases, more heat will be released, which will increase decay and senescence of the stored potatoes. A high accumulation of CO_2 and the depletion of O_2 are harmful to the potato tubers (Burton, 1989).

Respiration rate is strongly affected by temperature. The classical concept of the effect of temperature is that the respiration rate for biological materials will generally double for every 10° C rise in temperature. This tendency can be seen very clearly in Table 3, in which Burton (1989) cited the data of respiration rates for a batch of healthy and mature potatoes (cv. Arran Consul, King Edward and Majestic) one month after harvest.

Table 3. Respiration rate of potato tubers for the British cultivars Arran Consul, King Edward and Majestic.

Source: Burton, 1989

Temperature ℃	Release CO ₂ 10 ³ mg/kg s	Absorption O ₂ 10 ³ mg/kg s	Heat generation 10 ³ J/kg s
0	2.64	1.92	20.1
5	1.27	0.92	9.7
10	1.38	1.00	10.6
15	1.69	1.23	12.9
20	2.64	1.92	20.1
25	3.50	2.55	26.6

It was noted that the respiration rate is very high at the temperature of 0° C. Burton (1989) implied that in this case the high rate of respiration at temperatures below 5° C may be related to sucrose accumulation at the low temperatures.

Hunter (1985) observed the effect on the respiration rate of different storage temperatures (3.3° C, 7.2° C and 10.0° C). He concluded that the direct effect of temperature on respiration rate in potatoes is of relatively short duration (7 - 10 days). Generally, the decline and increase of the respiration rate are more rapid at higher storage temperatures during the falling rate period and the rising rate period after the end of dormancy, respectively. For a long storage period, the respiration is often minimized at 7.2° C. He further noted that the weight loss rate is closely related to the respiration rate, especially at high relative humidity and low vapor pressure deficit. Both respiration rate and weight loss rate can be expressed by the same type of exponential function with different coefficients: A[exp(-kt)]+C for the falling rate period, and A[exp(kt)-1]+C for the rising rate period.

The evaporation of water in an unventilated stock of potato will remove about half the metabolic heat production. Adequate ventilation to remove the heat buildup due to respiration and to maintain suitable levels of CO₂ and O₂ is still very important.

2.2.2.3 Sugar level

If potatoes are stored at a low temperature for a long time, a biological transformation will occur in the tuber. The starch will be gradually transformed into reducing sugars (glucose and fructose) and nonreducing sugar (sucrose). Burton (1982) observed the sugar contents of potato tubers (cv. Majestic) after 4 weeks of storage (17th Dec. to 14th Jan.) at various temperatures. He noted that sugar content increases very markedly when the temperature is below 10° C, as shown in Figure 1. Cash et al. (1986 and 1987) also noted that the sucrose, glucose and fructose contents of the Russet Burbanks and Atlantic potatoes increased during storage. The color of potato chips made from these potatoes became darker as the storage time increased.

Sowokinos and Preston (1988) developed the method of Chemical Maturity Monitoring (CMM) to analyze the sucrose and glucose contents within potato tubers during their growth period and storage period. Typical changes in sucrose concentration are shown in Figure 2. It is very clear that after several months of storage the sucrose level in potato tubers will gradually increase, especially during the senescent sweetening process. They suggested that for processing potatoes the maximum tolerable concentration levels of sucrose and glucose are a Sucrose Rating (SR) less than 1.0 (mg sucrose/g fresh tuber) and a glucose level less than 0.035 (mg glucose/g fresh tuber). They also thought that the ventilation stress after harvest may cause the sucrose values to increase to an SR of 2.0 or above. Therefore, storage management can be improved by monitoring the sucrose and glucose levels of the potato tubers.

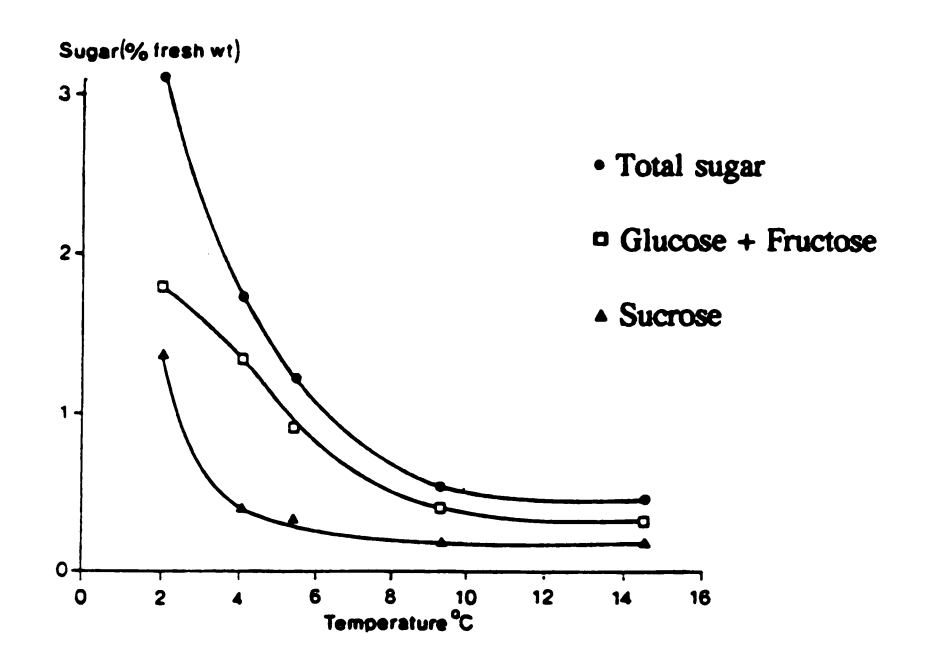


Figure 1. The relationship between storage temperature and sugar contents of potato tubers (cv. Majestic).

Source: Burton, 1982.

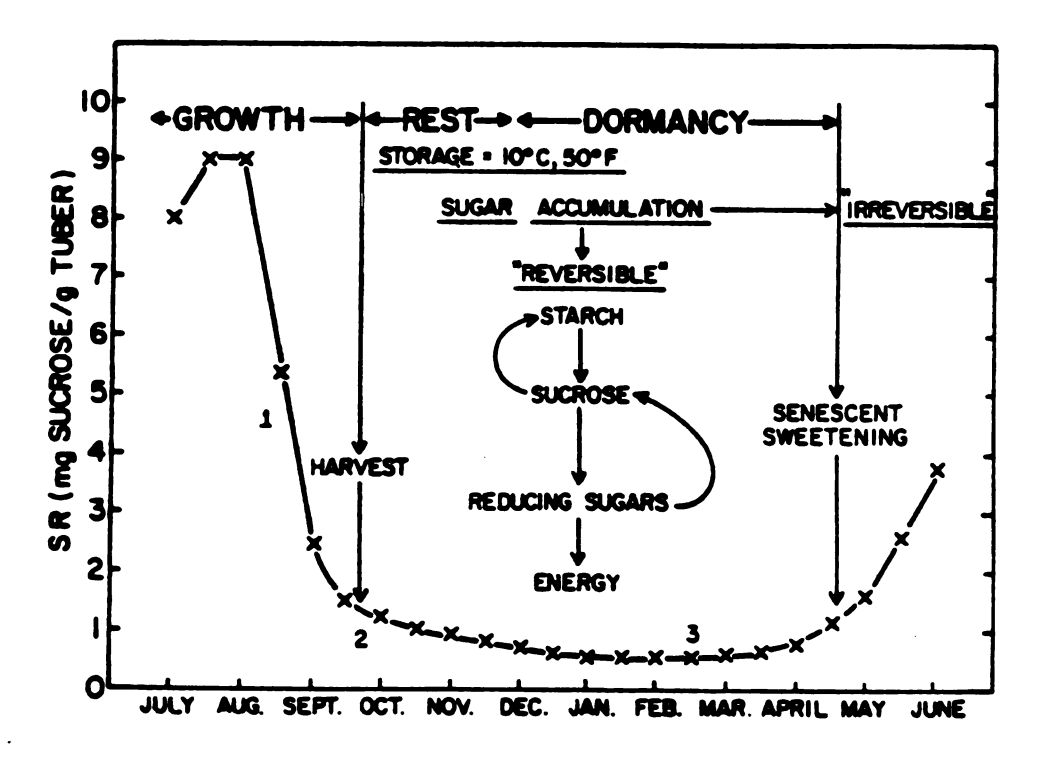


Figure 2. The typical changes in sucrose concentration during growth and storage of potato tubers. Source: Sowokinos and Preston, 1988

Cargill (1976) and Earl (1976) concluded that a high content of reducing sugars is undesirable in potatoes destined for potato chip, french fries and other dehydrated products, as the high concentration of sugars will result in dark-colored processed products. They suggested that the storage temperatures be between 7° and 10° C to prevent the transformation of starch to sugar.

2.2.2.4 Sprouting

Sprouting of stored potatoes should be prevented. Sprouting will increase water loss. Rastovski et al. (1987) noted that moisture loss through the epidermis of the potato sprouts is about 100 to 150 times as much as that through the intact periderm of a mature tuber. As the result of sprouting, potato tubers will shrivel and lose their market values. The sprouting of tubers in storage will also increase the resistance to air flow, thus increasing the pressure head losses.

Seelig (1972) stated that potatoes will not sprout until two to three months after harvest, even at temperatures of 10° to 15° C. But after two to three months, when the storage temperature rises above 4.4° C or when the temperature fluctuates, the dormancy of potatoes will be broken and sprouting will occur.

The dormancy period mainly depends on the cultivar of the potato. But as far as storage environment is concerned, maintenance of lower and stable temperature is preferable to help prevent sprouting. Cargill (1976) thought that the sprouting was minimized at temperatures below 4.4° C and almost nonexistent at temperatures around 2.2° C. Wilson (1967) reported that if sprout inhibitors are used the storage temperature

may be kept as high as 7.2° C; but without sprout inhibitors a temperature of 4.4° C will be necessary to prevent sprouting. He suggested that the actual storage temperature be a compromise between the temperature to prevent sprouting and the one to retard the conversion of starch to sugar.

Therefore, the philosophy of a potato storage is to retain water in the potato tuber, keep the respiration rate to a minimum, hold the reducing sugars to a low level and maintain the external appearance of the stored potatoes (Plissey, 1976).

2.2.3 Pathological problems

Hide and Lapwood (1978) reported that the potato is prone to more than one hundred diseases during its whole living period. Diseases that cause the deterioration of the stored potatoes are fungal diseases (such as late blight and silver scurf), bacterial diseases (such as bacterial soft rot, brown rot and ring rot), and storage pests (such as potato tuber moth and fruit flies).

Diseases require a suitable environment to survive and to develop. Among other factors, temperature and relative humidity in the storage are the most important factors that can be used to curb diseases. For instance, Rastovski et al. (1987) indicated that the prime requirement to control potato blight is for the tuber surface to be dry. Storage under warm dry condition for a few weeks is sufficient to help control blight. A storage temperature below 3° C and a relative humidity below 90 percent will prevent the spread of silver scurf. While the potato tuber moth is a dread parasite in tropical countries, it is well controlled at storage temperature below 10° C.

Campbell (1962) and Cargill (1976) also noticed that free water dripping from the ceiling onto potatoes or condensation of water on the cooler potatoes in the pile will cause wet potato tubers which may result in bacterial soft rot infection and subsequent wet breakdown. They emphasized that every precaution should be taken to eliminate free water on potatoes in storage.

2.3 Air ventilation systems for potato storage

2.3.1 Types of air ventilation system

There are two ways to aerate a potato storage: natural ventilation and forced ventilation. Natural ventilation by free convection is very slow, inefficient and uneven. It is most often used in small storages. In modern potato storages, forced ventilation is a common practice. It has the advantage of controlling the storage condition rapidly, easily and accurately. Wilson (1976) and Cloud (1976) thought that the forced ventilation system should blow the air up through the pile of potatoes while the air is maintained at the proper temperature and relative humidity. They believed that this type of ventilation system will give faster and more uniform cooling of the potatoes than a "shell" ventilation system where the air is moved around and above the stored potatoes.

Hunter and Yaeger (1972) proposed using a cross flow circulation system. But this type of ventilation system was not effective in maintaining uniform temperature and humidity. Also the storage width would be limited to about 3.0 to 5.0 m for efficiently controlling the air flow. This system has not been adopted commercially.

2.3.2 Structures of ventilation system

In order to ventilate a potato storage uniformly, duct systems are widely used as the air distribution system. Typical arrangements of the main plenum and lateral ducts are shown in Figure 3. The lateral ducts are placed either in-floor or on-floor. The in-floor duct system is permanent and is favored for ease of bin loading and unloading. The cross-section of this duct system is usually rectangular and the installation investment will be higher as compared with that of an on-floor duct system. The on-floor duct system is easy to place but it is not convenient for loading and unloading. The original investment for on-floor duct systems may be low, but the costs of repair and replacement of ducts will be significant. The cross-sections of this duct system may be triangular, circular, semicircular, or rectangular.

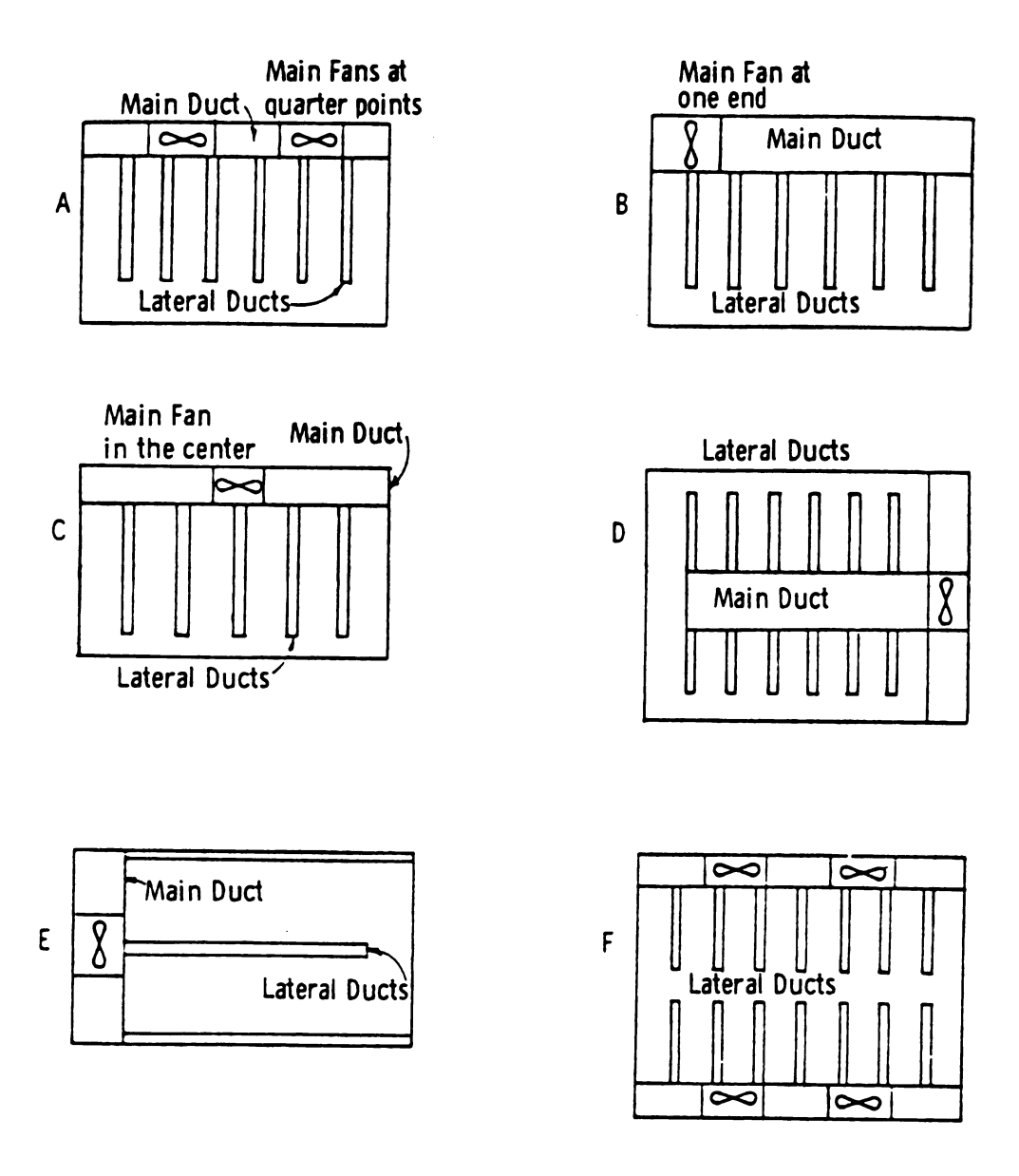


Figure 3. Typical arrangements of main plenum and lateral ducts for potato storage. Source: Cargill, 1976

2.3.3 Duct spacing and duct size

Cargill (1976) recommended that the spacing of the lateral ducts in a potato storage be 1.8 to 2.4 m between the centers of two adjacent ducts for in-floor ducts and 2.4 m for on-floor ducts.

Cloud and Morey (1980) analyzed the effect of equivalent duct diameter (four times cross-section area divided by perimeter) on the uniformity of air discharge. Under the conditions that the duct entrance velocity was 305 m/min, duct length was 24.4 m and the slot discharge area was equal to the duct cross-sectional area, they showed that ducts with equivalent diameter of 0.24 m have a relatively uniform air discharge along the duct length, and the air discharge near the duct entrance will increase as the equivalent diameter decreases (Figure 4).

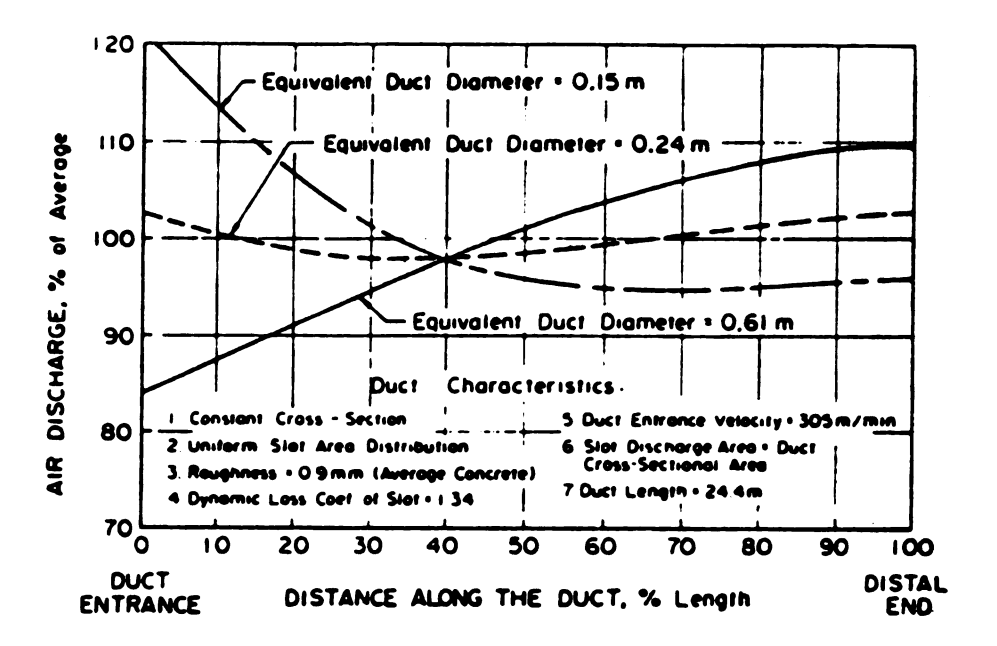


Figure 4. Effect of equivalent diameter on the uniformity of air discharge. Source: Cloud and Morey, 1980

2.3.4 Duct opening and its location

Wilson (1976) gave the lengths of 1.9 cm slot for in-floor rectangular duct corresponding to different potato bed depths as listed in Table 4. These data were calculated for a duct cross-sectional area of 0.25 m², a duct spacing of 3.1 m on center, an air flow of 0.5 m³/min per metric ton of potatoes, and a slot spacing of 30.5 cm along the duct.

The air discharge holes for a circular duct should be on each side near the floor and 90 degree apart. For a duct spacing of 2.4 m on center, air discharge holes with diameters of 2.5, 3.2 and 3.8 cm should be spaced according to the depth of the potatoes as shown in Table 5 (Wilson, 1976).

Cargill (1986) suggested that the effective slot area to the cross-section area of the lateral duct be 0.75 to 1.0, where the effective slot area is based on an air flow velocity of 305 m/min. For an in-floor rectangular duct, the potato will cover about 65 to 75 percent of the actual slot area. Therefore, the ratio of the actual slot area to the effective slot area should be 3.0 to 4.0.

Table 4. Potato bed depth vs the required length of 1.9 cm slot for in-floor rectangular duct in the Pacific Northwest. Source: Wilson, 1976.

Potato bed depth, meter	Length of 1.9 cm slot, cm	
3.1	7.3	
3.7	8.6	
4.3	10.2	
4.9	11.4	
5.5	12.7	
6.1	14.3	

Table 5. Potato bed depth vs spacing of discharge hole for circular duct in the Pacific Northwest.

Source: Wilson, 1976.

Potato bed depth, m	Spacing of 2.5 cm diameter hole, cm	Spacing of 3.2 cm diameter hole, cm	Spacing of 3.8 cm diameter hole, cm
3.1	22.9	35.9	51.6
3.7	19.1	29.9	43.2
4.3	16.5	25.7	36.8
4.9	14.0	22.5	32.4
5.5	12.7	20.0	28.9
6.1	11.4	17.8	26.0

Cloud and Morey (1980) also studied the effect of the ratio of discharge area to duct cross-sectional area on the uniformity of air discharge. Under the conditions that the duct entrance velocity was 305 m/min, duct length was 24.4 m and the equivalent duct diameter was 0.61 m, they found that an effective way to improve air discharge uniformity is to reduce the effective duct discharge area. This trend can be seen from Figure 5. But they noted that decreasing the effective duct discharge area would be at the expense of increased duct static pressure requirements.

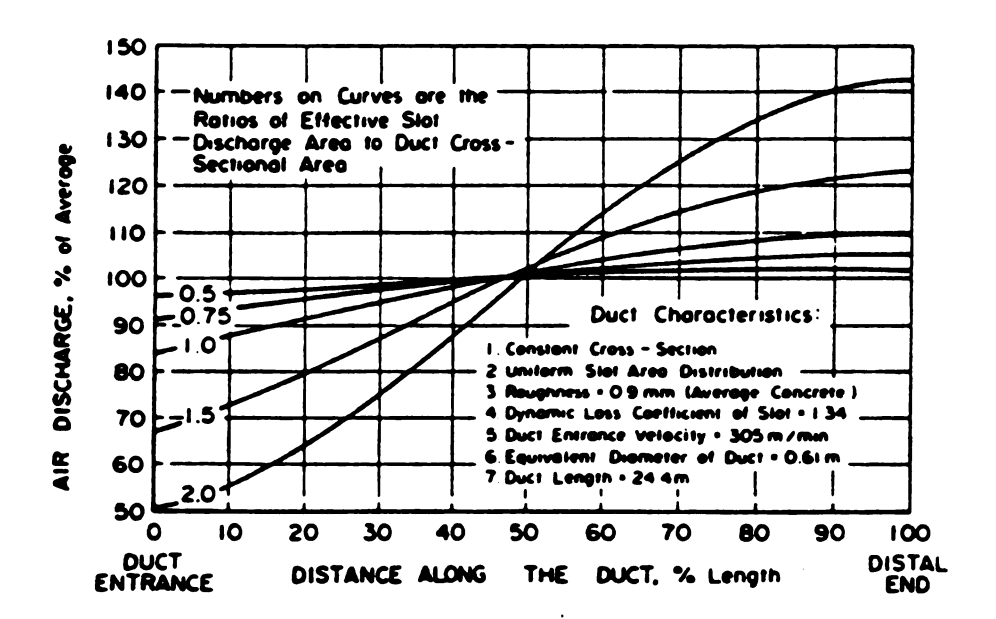


Figure 5. Effect of the ratio of discharge area to duct cross-sectional area on the uniformity of air discharge.

Source: Cloud and Morey, 1980

2.3.5 Ventilation rate for potato storage

Wilson (1967) proposed that, for wound healing and curing, a minimum ventilation rate of 0.53 m³/min per metric ton of potatoes be used to remove field heat and that the air be constantly circulated during this period. For the storage period, the rate of 0.25 to 0.31 m³/min per metric ton of potatoes will maintain the storage temperature, but the air circulation should be on an intermittent basis. Earl (1976) recommended a lower airflow of 0.31 m³/min per metric ton of potatoes be used during the wound healing period.

Wilkes (1976) believed that in a normal year a minimum air flow range of 0.2 to 0.6 m³/min per metric ton is sufficient, but during the problem years additional air flow in the range of 0.6 to 0.9 m³/min per metric ton should be used. Mitchell and Rogers (1976) thought that for table and seed potato storage the air flow should be 0.6 to 0.7 m³/min per metric ton, while for chipping potato storage the air flow should be 0.9 to 1.1 m³/min per metric ton.

Cargill (1976 and 1986) pointed out that a basic rule in potato storage is to use no more air than is required to maintain the storage temperature within 0.5° to 1.0° C of the desired temperature. In a storage with tuber temperatures of 7.2° to 10° C the heat of respiration will cause temperatures to increase 0.5° to 1.0° C in 24 hours. Therefore, during the storage period the fan should not be off longer than 24 hours at one time. He noted that a minimum ventilation rate of 0.93 m³/min per metric ton will be adequate.

Forbush and Brook (1989) observed the effect of ventilation rate on the temperature, moisture and quality responses of stored potatoes. In their experiment, ventilation rates

up to 1.9 m³/min per metric ton were used. They concluded that weight loss and temperature control were not directly correlated to ventilation rate, and higher ventilation rates were more effective at removing surface moisture from potatoes.

To effectively ventilate the potato storage, Cargill et al. (1989) and Brook (1991) suggested that the air velocity throughout the ventilation system should increase at each stage. For example, if the ratio of the total effective duct opening area to the cross-sectional area of the duct and the ratio of the total cross-sectional area of the ducts to the main plenum cross-sectional area are all equal to 0.75 to 1.0, then the air velocity should be 230 m/min in the main plenum, 260 m/min in the lateral ducts and 305 m/min at the outlet of the slots. These data were for potato storages in the Midwest USA. Waelti (1989) recommended a higher air flow velocities for storages in the Pacific Northwest USA. He thought the air velocity in the plenum should be 240 m/min, the air velocity at the entrance of the lateral duct should not exceed 300 m/min, and the velocity at the duct opening should be at least 381 m/min.

2.4 Equations of predicting the behavior of fluid flow through porous media

The characteristics of fluid flow through porous media have been studied extensively by researchers in various engineering areas. The research on this subject is very important to the storage of farm products, the usage of underground water, the control of reactions in chemical engineering and the exploration for petroleum. By conducting numerous experiments on different porous media under specific conditions, researchers have been able to generalize equations that best express their observations. They used these equations together with other equations, such as the continuity equation, to predict fluid flow patterns in porous media.

2.4.1 Darcy's equation

The earliest study on fluid flow through porous media was conducted by Darcy in 1856 (see Muskat, 1937 and Bear, 1972). Darcy investigated the flow phenomena of water in a vertical homogeneous sand filter. The experimental results lead to Darcy's law with the following form:

$$Q = \frac{KA(h_1 - h_2)}{H}$$
 [1]

Darcy's law is the fundamental equation governing fluid flow through porous media, but it is limited to a very low and narrow range of Reynolds number. For liquid flow, Bear (1972) reported that it is valid for Reynolds number from 1 to 10 for practically all

cases, as long as Reynolds number is based on the pore diameter. Greenkorn (1983) held that it is only valid in the creeping flow regime with Reynolds number, based on the effective particle diameter, less than 1. The difference of the valid ranges lies in the different definitions of the hydraulic diameter used in calculating Reynolds number.

Muskat (1937) proposed that in a general three-dimensional flow system the resultant velocity at any point is directly proportional to, in magnitude, and in the same direction as the resultant pressure gradient at that point. So the resultant velocity may be resolved into three component velocities parallel to the coordinate axes, each reacting to the pressure gradients independently of the others. Therefore, Darcy's law can be expressed for an isotropic porous medium as:

$$V_{x} = -\frac{k}{\mu} \frac{\partial P}{\partial x}$$

$$V_y = -\frac{k}{\mu} \frac{\partial P}{\partial y}$$

$$V_z = -\frac{k}{\mu} \frac{\partial P}{\partial z}$$
 [2]

where k is the permeability of the media and μ is the viscosity of the fluid.

From Equation [2] it is obvious that Darcy's law reveals the linear relationship between velocity and pressure gradient. However, there are flow regimes that deviate from linearity and display non-Darcian flows. Kutilek (see Scheidegger, 1974)

summarized various possibilities and presented twelve schematic flow curves for non-Darcian flows. Scheidegger (1974) discussed the physical causes of such deviation and analyzed a variety of correlation equations for nonlinear flow through porous media. He thought that the main cause of the nonlinear flow was the high flow velocity.

2.4.2 Muskat's equation

Muskat (1937) analyzed the behavior of fluid flow with high Reynolds number through porous media. He found that as the Reynolds number increases the pressure gradient begins to increase faster than the velocity. In this case, the pressure gradient will be proportional to the square of the velocity and will be independent of the viscosity of the fluid. For viscous flow with a low Reynolds number, the pressure gradient is directly proportional to the viscosity as stated by Darcy's law. He assumed that for the transition between viscous flow and turbulent flow the pressure gradient will be best described by the sum of terms of several powers of velocity, that will correspond to:

$$\frac{dP}{dn} = AV + BV^{C}$$
 [3]

where A and B are constants, and C is intermediate between 1.0 and 2.0.

Equations that have a form similar to that of Muskat's are widely used to represent experimental data. Ergun (1952) studied fluid flow through a packed column. He considered that the pressure losses are caused by both viscous energy loss and kinetic energy loss. Since viscous and kinetic energy losses are the functions of the first and

second order of velocity, respectively, he proposed the following equation for all types of flow:

$$\frac{dP}{dn}g = A\mu V + B\rho V^2$$
 [4]

In Equation [4], A and B are constants related to the properties of the fluid, the characteristics of the granular solid and the porosity of the packed column, ρ is the density of the fluid, and g is the acceleration of gravity. For a granular solid, constants $A = 150(1-\epsilon)^2/(\epsilon^3d^2)$ and $B = 1.75(1-\epsilon)/(\epsilon^3d)$, where ϵ is the porosity of the porous media and d is the effective diameter of the granular particle. If we let g be moved to the right side of the equation and be included inside the constants A and B, then

$$\frac{\mathrm{dP}}{\mathrm{dn}} = \mathrm{A}\mu \mathrm{V} + \mathrm{B}\rho \mathrm{V}^2 \tag{5}$$

which is equivalent to Muskat's equation.

Leva (1959) observed laminar and turbulent flows through beds packed with spherical and nonspherical particles. Assuming that the fluid flow will be influenced by the shape of the particle, the porosity of the media and the friction factor, he proposed that

$$\frac{dP}{dn} = Bf_L f_3^{C-3} V^2$$
 [6]

where f_L is the modified friction factor, f_s is the particle shape factor, B is the coefficient related to fluid properties and porosity of the porous media: $(B = 2\rho(1-\epsilon)^{3-c}/dg\epsilon^3)$, and

C is the state of flow factor that is also a function of Reynolds number. Leva's equation can be shown to be a special case of Muskat's equation.

An approach similar to Ergun's was proposed by Bakker-Arkema et al. (1969). They used cherry pits as the tested media and modified Ergun's equation with a constant K_R to fit their experimental data. Patterson (1969) determined the resistance to air flow of randomly packed beds of plastic sphere, cherry pits, shelled corn and navy beans for air flow rates in the range of 3.0 to 36.0 m³/min/m². A modified Ergun equation, the same as Bakker-Arkema's, was used for predicting air flow parameters. He reported that the modified equation fit the experimental data well for shelled corn and navy bean. Patterson et al. (1971) further simplified Ergun's equation for stored granular materials as follows:

$$\frac{dP}{dn} = K_B(AV + BV^2)$$
 [7]

where A and B are constants. This equation is similar to that of Muskat's.

Matthies and Peterson (1974) used several modified equations to relate pressure drop to velocity and to the characteristics of the granular materials. Among these equations

$$\frac{dP}{dn} = BV^{2-C}$$
 [8]

where B is the function of porosity and C is a constant. Gaffney and Baird (1977) evaluated the resistance of bell peppers to air flow, and formulated the following equation:

$$\frac{dP}{dn} = BV^{1.81}$$
 [9]

to express the straight lines in the log-log paper with B as a constant for discrete air flow ranges. Both Equation [8] and [9] are also special cases of Muskat's equation.

Bern and Charity (1975) modified Ergun's equation to relate pressure drop to air flow velocity and grain bulk density. Their equation

$$\frac{dP}{dn} = A + BV + CV^2$$
 [10]

is a second order polynomial function, where constants A, B and C are functions of air flow velocity range (m/min) and porosity.

In analyzing the air flow resistance of shelled corn in horizontal and vertical directions, Kay et al. (1989) used an equation like Equation [10] to represent the resistance data. They concluded that air flow resistance in the horizontal direction is 58 and 45 percent of that in the vertical direction with air velocity ranging from 6.0 to 28.6 and from 6.0 to 0.8 m³/min/m², respectively. They attributed these differences to the anisotropic characteristics of the shelled corn.

Considering that Ergun's equation is limited to spherical particles and Leva's equation requires two coefficients, friction factor and shape factor, to be determined, Chandra et al. (1981) modified Leva's equation to fit their data by using dimensionless analysis based on Buckingham's π theorem. Their equation has the following form:

$$\pi_1 = \pi_3^{-2.7} (185\pi_2 + 1.7\pi_2^2)$$
 [11]

where π_1 is the pressure drop number, π_2 is the Reynolds number and π_3 is the porosity number. They reported that the prediction equation correlates the experimental data with a mean deviation of 10 percent.

Haque et al. (1980) measured pressure in a bed of corn mixed with nonuniform distribution of fines and formulated a basic equation related pressure drop to air velocity and fine materials. Their equation also has the same form as that of Muskat's:

$$\frac{dP}{dn} = (A + Cf_m)V + BV^2$$
 [12]

where A, B and C are constants, and f_m is the percentage distribution of the fine materials depending on radial and axial coordinates in a cylindrical grain bed.

2.4.3 Shedd's equation

During the 1940's and 1950's, Shedd conducted a series of experiments to determine the resistances to air flow of various grains. The results were presented in the log-log scheme and these have been adopted as an ASAE standard since 1948 (ASAE Standards, 1988).

Shedd (1945) first attempted to use velocity V as a function of pressure P to represent his results for ear corn. After tests using other grains and seeds, he suggested that the

pressure gradient be used instead of pressure drop (Shedd, 1951 and 1953). In onedimensional space his equation takes the form of:

$$V = A \left(\frac{dP}{dn} \right)^{B}$$
 [13]

where A and B are constants related to the fluid properties and the characteristics of the media. When B = 1.0, this equation is similar to Equation [2] in one-dimensional space. Shedd (1953) also observed that the curves in the log-log scheme are convex upward. He indicated that the above formula may fit the curves for only a narrow range of velocity, beyond which the calculation according to Equation [13] may induce a considerable error.

Staley and Watson (1961) conducted a test on the resistance of potatoes to air flow. This was the first attempt for determining the air flow resistance with large farm products. The experimental data were plotted in a log-log scale and an equation like Shedd's with A = 345 and B = 0.562 in English units was suggested to describe the curves. Staley's data have been incorporated into the ASAE standard (ASAE Standards, 1988).

Wilhelm et al. (1978 and 1981) presented experimental data for snap beans, southern peas and lima beans in the same form as Shedd's chart. They stated that a dimensionless pressure parameter, $p = (\Delta P/\rho_b H)(g_c/g)$, used in an equation will produce a better correlation between the velocity and the pressure drop, where ΔP is the pressure drop, H is the depth of the bean in container, g_c is the gravitational constant and g is the gravity acceleration. Thus the following equation was put forward:

Actually this equation is a form of Shedd's equation in logarithmic form.

Calderwood (1973), Akritidis and Siatras (1979) and Farmer et al. (1981) performed tests on rough, brown and milled rice, pumpkin seeds and bluestem grass seeds, respectively. They also presented their data in the form of Shedd's chart, which fit the experimental data well.

Grama et al. (1984) studied the resistance to air flow of a mixture of shelled corn and fines. They observed the relationships between air flow velocity and pressure gradient under different levels of fines instead of different levels of grain bed depth. They found that air flow resistance of shelled corn increases when the fine material is added and the increase in air flow resistance becomes greater as the size of fines is decreased. Their results were given in a chart similar to Shedd's.

Jayas et al. (1987) employed Shedd's equation to match their data when rapeseeds and foreign materials were used as media. They noted a difference in the resistances between the horizontal and vertical directions. The resistance for horizontal air flow direction was 60 percent of that for vertical air flow direction according to their report.

2.4.4 Hukill's equation

Hukill and Ives (1955) recommended that pressure gradient be expressed as a logarithmic function of velocity. Their equation had the following form:

$$\frac{dP}{dn} = \frac{AV^2}{\ln(1+BV)}$$
 [15]

This equation fits Shedd's data very well with only small deviations for air velocities from 0.61 m/min to 12.2 m/min. But data for ear corn do not conform to this expression. Equation [15] was later adopted as an air flow resistance equation in ASAE Data: ASAE D272.7 (ASAE Standards, 1988), with constants A and B given for particular grains.

To determine the pressure drop in a grain bed, Spencer(1969) took Equation [15] as the mathematical model and suggested that two steps be taken. First, the velocity can be estimated by solving the linear Laplace equation through complex analytic function:

$$V = \frac{R_m}{2W} \frac{\sinh(2\pi x/W)}{\cosh(2\pi x/W) - 1}$$
 [16]

where W is the width of the bin, and R_m is the source strength related to mass flow rate. Secondly, the pressure gradient can be obtained by substituting V into Equation [15]. In this way, he reported that the calculated results give reasonable agreements with experimental data for a single duct arrangement in the tested system.

Haque et al. (1978) modified Hukill's equation based on their experimental data for air flow resistance of corn containing various levels of fines:

$$\frac{dP}{dn} = \frac{AV^2}{\ln(1+BV)}(1+f_mK_v)$$
 [17]

where K_v is a function of velocity and f_m has the same meaning as that in Equation [12]. This equation also has been adopted as an ASAE standard (ASAE Standards, 1988).

2.4.5 Sheldon's equation

Sheldon et al. (1960) investigated the resistance of shelled corn and wheat to air flow ranging from 0.003 to 0.3 m³/min/m². They found that the following equation correlating pressure drop P and air velocity V can be used to represent the straight lines in a log-log scale:

$$P = AV^{B}$$
 [18]

where $A = f_pH/D$ and B = 2.0. The friction factor f_p is also a function of velocity and porosity, while constants D and H are the equivalent diameter and height of the test bin, respectively.

Osborne (1961) determined the resistance to air flow of grains and other seeds that are commonly grown in Britain. He presented the data by using the static pressure as a dependent variable and the velocity as an independent variable. All the curves pass through the origin of the Cartesian coordinates, so the relationship between static pressure and velocity can be expressed as Equation [18].

Later, Lawton (1965) measured the resistance to air flow of some agricultural and horticultural seeds and employed Equation [18] to establish the relationship between static pressure and velocity. Husain and Ojha (1969) and Nellist and Rees (1969) also used an equation similar to Equation [18] to predict the resistance to air flow of three Indian varieties of paddy rices and soaked vegetable seeds, respectively.

Rabe and Currence (1975) developed an equation to include the effects of velocity, moisture content and bulk density of dry alfalfa on static pressure:

$$\ln P = -3.5896 + 0.0005 \text{m}_{,\rho_{h}} + 0.0149 \rho_{h} + 1.2351 (\ln V)$$
 [19]

where ρ_b is the dry matter bulk density and m_e the moisture content. If the first three items at the right side of the equation are merged into one coefficient and the logarithmic function is changed into exponential function, then the above equation can be simplified as Equation [18].

Neale and Messer (1976 and 1978) investigated the resistances to air flow of root and bulb vegetables and leafy vegetables, respectively. These vegetables have relatively large size compared with that of grains and seeds, yet the pressure drop and the velocity still follow the same relationship as given by Equation [18]. For potato, they gave B = 1.80 when the units for pressure were mm W.G. and the units for air velocity were m/s. Constant A was calculated for different P and V according to Equation [18].

2.4.6 Bear's equation

Bear (1972) reviewed various equations used to describe the nonlinear motion of fluid flow through porous media, except the equations that were used to predict the characteristics of air flow through farm product beds. He divided these equation into three groups according to the status of coefficients in the equations. In group 1, the coefficients were not related to any specific fluid and medium properties. Group 2 contained coefficients more or less related to fluid and medium properties and included unspecified numerical parameters. Group 3 was similar in nature to the group 2, but included the definite numerical parameters. For flow through isotropic porous media under steady state, most of the equations express the pressure gradient as a function of velocity and have the same form as that of Muskat's.

By combining Darcy's law and the continuity equation, Bear (1972) derived a partial differential equation for incompressible fluids (ρ = constant and μ = constant) and for inhomogeneous and anisotropic porous media:

$$\frac{\partial}{\partial x} \left(K_x \frac{\partial P}{\partial x} \right) + \frac{\partial}{\partial y} \left(K_y \frac{\partial P}{\partial y} \right) + \frac{\partial}{\partial z} \left(K_z \frac{\partial P}{\partial z} \right) = 0$$
 [20]

For inhomogeneous and isotropic porous media, the equation had the following form:

$$\frac{\partial}{\partial x} \left[K \frac{\partial P}{\partial x} \right] + \frac{\partial}{\partial y} \left[K \frac{\partial P}{\partial y} \right] + \frac{\partial}{\partial z} \left[K \frac{\partial P}{\partial z} \right] = 0$$
 [21]

For homogeneous and isotropic porous media, Equation [21] reduced to the Laplace

equation:

$$\frac{\partial^2 P}{\partial x^2} + \frac{\partial^2 P}{\partial y^2} + \frac{\partial^2 P}{\partial z^2} = 0$$
 [22]

In this case, the pressure distribution is purely related to the geometry of the field.

Bear (1972) stated that Equations [20], [21] and [22] can be applied to both steady flow and nonsteady flow of an incompressible fluid for particular boundary conditions. For example, under the nonsteady flow condition the variation in time may be introduced through time-dependent boundary conditions.

2.4.7 Brooker's equation

Based on the analysis of Shedd's data and on the consideration of the nonlinear characteristics of air flow patterns, Brooker (1961 and 1969) modified Shedd's curve by using several straight-line segments, each of which has its own values for the constants of A and B in Shedd's equation. This was a very important step taken towards the approximation of the curve and the application of Shedd's Equation (Equation [13]).

In a two dimensional space, Brooker (1961) decomposed the pressure gradient in the normal direction into that in the X and Y directions:

$$\left[\frac{\partial P}{\partial n}\right]^2 = \left(\frac{\partial P}{\partial x}\right)^2 + \left(\frac{\partial P}{\partial y}\right)^2$$
 [23]

He also related the velocity components in the X and Y directions to that in the normal

direction:

$$\frac{V_x}{V_z} = \frac{\partial P/\partial x}{\partial P/\partial n}$$

$$\frac{V_y}{V_z} = \frac{\partial P/\partial y}{\partial P/\partial n}$$
 [24]

The following partial differential equation (PDE) based on Shedd's equation and the theory of continuity for flow under steady state was developed:

$$\left[\left(\frac{\partial P}{\partial x}\right)^{2} + \left(\frac{\partial P}{\partial y}\right)^{2}\right] \frac{\partial^{2} P}{\partial x^{2}} + \frac{\partial^{2} P}{\partial y^{2}} - 2m \left[\left(\frac{\partial P}{\partial x}\right)^{2}\right] \frac{\partial^{2} P}{\partial x^{2}} + 2\frac{\partial P}{\partial x} \frac{\partial P}{\partial y} \frac{\partial^{2} P}{\partial x \partial y} + \left(\frac{\partial P}{\partial y}\right)^{2}\left(\frac{\partial^{2} P}{\partial y^{2}}\right) = 0$$
 [25]

where m = (B-1)/2.

2.4.8 Segerlind's equation

Segerlind (1982) suggested that Brooker's equations are not applicable to the analysis of the nonlinear air flow problem, since the variations of coefficients A and B were not taken into consideration in Equation [25]. Considering both coefficients A and B to be functions of the coordinates, he proposed the concept of granular permeability, K_G. Using Equations [13], [23] and [24] and the continuity equation, Segerlind (1982) developed, in the two-dimensional domain, the following equations:

$$\frac{\partial}{\partial x} \left[K_{G} \frac{\partial P}{\partial x} \right] + \frac{\partial}{\partial y} \left[K_{G} \frac{\partial P}{\partial y} \right] = 0$$
 [26]

where K_Q is also a function of the pressure gradient:

$$K_{G} = A \left[\left(\frac{\partial P}{\partial x} \right)^{2} + \left(\frac{\partial P}{\partial y} \right)^{2} \right]^{\frac{B-1}{2}}$$
 [27]

Equation [26] has the same form as Equation [20], but the coefficient K_0 in Equation [26] has a different physical meaning. It is closely related to the local pressure gradient and the coordinates. The numerical value of K_0 can only be determined by experimental methods.

Segerlind (1983) systematically analyzed the various forms of presenting experimental data on resistance to air flow. He suggested that Equation[13] be adopted for describing experimental data and all velocity-pressure gradient data be presented similar to the technique used by Brooker (1969). It means that to express Shedd's equation (Equation [13]) adequately, coefficients A and B must be assigned different values for various ranges of pressure gradient and air flow velocity. These suggestions together with Equations [26] and [27] not only point out a way of generalizing the experimental data, but also imply a method for describing air flow through granular particles.

2.4.9 Other equations

Grain storages have been used commercially since the 1930's. The first paper on the behavior of air flow through grain beds was published by Stirniman et al. (1931). They collected data on the resistance to air flow through rough rice in deep bins and presented the data on a log-log scale described by the following equation for static pressure in the range of 250 to 1,000 Pa:

$$V = KH^{c}$$
 [28]

where K and C in the equation are constants under specified pressure, and H is the depth of the grain bed. Hall (1955) developed a relationship between velocity and pressure for bed depths less than 0.3 m. He used Shedd's data (Shedd, 1951 and 1953) to do the analysis but employed an equation similar to Stirniman's to fit the data.

Kelly (1939) obtained air flow resistance data on wheat, expressed by velocity and pressure drop for the different wheat depths:

$$V = KP^{c}$$
 [29]

where K = 4005 and C = 0.5 in English units. Henderson (1943 and 1944) investigated the resistances of shelled corn, soybean and oats to air flow, and recommended a general equation, similar to Equation [29], be used to explain the relationship between air flow velocity and pressure drop in the tested beds. He defined K as a function of grain bed

depth. When conducting tests on soybeans and oats, he noted the curvature of the lines in the log-log scale.

Bunn and Hukill (1963) conducted an experiment for air flow through steel shot. By collecting the data for various porosities of the steel shot bed, they developed equations for both linear and non-linear flow. Under the linear flow condition, the equation was expressed in the exponential form:

$$\frac{\partial P}{\partial n} = A \left[exp \left(\frac{BV_n^2}{\partial P/\partial n} \right) - 1 \right]$$
 [30]

Obviously this equation can not be linearized with respect to the parameters A and B. So it is impossible for Equation [30] to be fit to experimental data by the standard least square method. For the non-linear flow condition, they also used the theory of continuity and decomposed pressure gradient and velocity in the same way as done by Brooker (1961) to formulate a partial differential equation. They believed that if the parameter A is first established by using Equation [30] then it is sufficient to use their PDE to predict air flow patterns in a nonlinear flow system.

2.5 Representing fluid flow through porous media

Fluid flow through porous media can be represented by iso-pressure lines, velocity distributions, streamlines, traverse time, volume flow rate, etc. These patterns are usually obtained by specifying in the coordinates of a confined space the corresponding data, such as pressure and velocity values, which may be obtained from experimental or calculated results.

Collins (1953) used experimental data from a grain dryer with an inverted U-shaped duct to develop the iso-therms, contour lines of equal moisture content, iso-pressure lines and streamlines as shown in Figure 6a, b, c and d, respectively. This was the first such attempt using pressure contour lines, streamlines, etc. to delineate the air flow patterns within a grain bed.

Hukill and Shedd (1955) introduced the concept of traverse time into the representation of air flow patterns. According to their definition, the traverse time is the length of time the air takes to pass through the grain. They suggested that the traverse time be used instead of cfm/bushel to express the effectiveness of ventilation. By using this concept, they were able to draw equal ventilation lines for nonlinear flow in an oat drying bin (Figure 7) and corn drying bin.

Hall (1955) proposed a graphical method for determining air flow at different locations in a grain bin. He also suggested that air flow rate per accumulated bushel of grain (cfm/acc bu) be used as an alternative measurement for air flow in a grain drying bin with a non-rectangular cross-section.

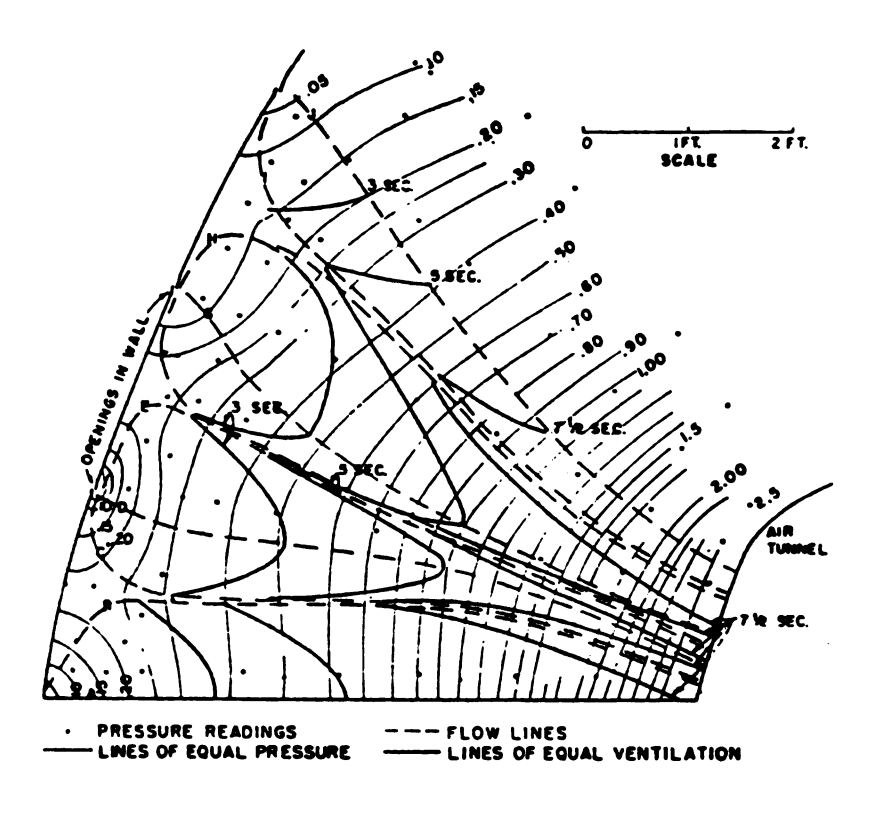
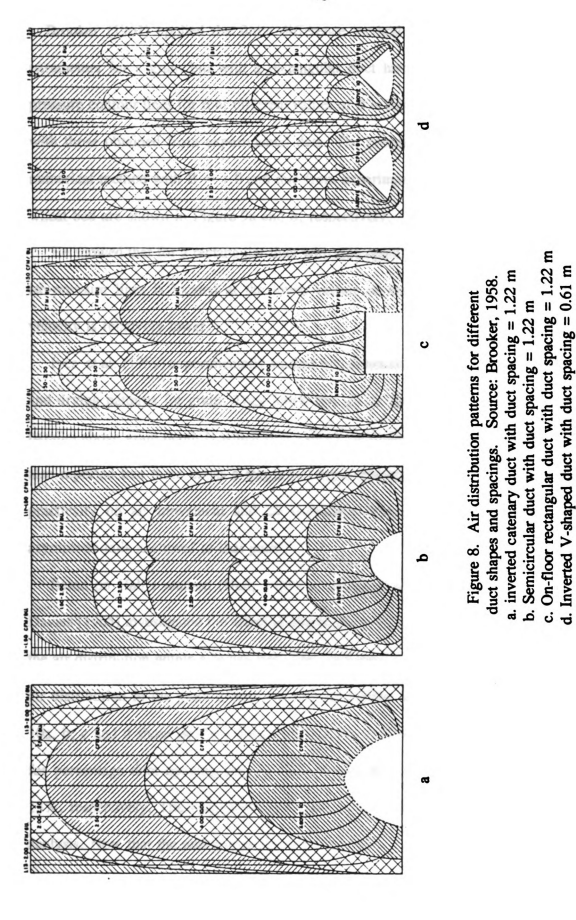


Figure 7. Air flow patterns in the section of an oat drying bin. Source: Hukill and Shedd, 1955.

Brooker (1958) analyzed lateral duct air flow patterns in grain drying bins. He revealed that air leaving a lateral duct will travel in various paths which are dependent on the structure of the bin and the duct. He used experimental data to plot the air distribution patterns for a grain bin with an inverted catenary duct, a semicircular duct, an on-floor rectangular duct having side openings and an inverted V-shaped duct having bottom openings as shown in Figure 8a, b, c and d, respectively. The duct spacings were 1.22 m on center for Figure 8a, b and c, and 0.61 m on center for Figure 8d.



Brooker (1961) applied the finite difference method to the calculation of air flow parameters for a grain bin with a rectangular duct having side openings. He plotted pressure contour lines for four different values of B in Equation [13] and compared them with those obtained from experimental data. The pressure patterns determined by the numerical method with B = 1.0 and that from experimental data for air flow through a wheat bed are shown in Figure 9a and b, respectively.

He showed that for a rectangular duct with side openings the largest spacing between iso-pressure lines is located at the lower corner of the bin cross-section, where the velocity is relatively lower.

Ives et al. (1959) experimentally studied two dimensional, nonlinear air flow patterns and drying patterns for grain. They found that all air flow streamlines are straight and parallel above grain depth H which is 0.5 times the distance L_d between the ducts. They also reported that there exists a stagnation point midway between ducts where there is practically no air movement and all ventilation fronts may be considered forming asymptotic tails anchored to that point.

Based on Hall's method (Hall, 1955) of analyzing non-parallel airflow, Boyce and Davies (1965) investigated the effect of lateral ducts with four different exhaust areas on the air distribution within a barley bed. They indicated there was a large variation in the air distribution in the grain around the duct depending on the air exhaust area. Figure 10a, b, c and d show iso-flow lines (left) and iso-pressure lines and streamlines (right) for percentage duct opening area to total duct surface area of 100%, 68%, 39% and 13%, respectively. The volumetric flow rate was 0.34 m³/min for all the ducts in their analysis. Note that the unit for iso-flow was ft³/min/ft².

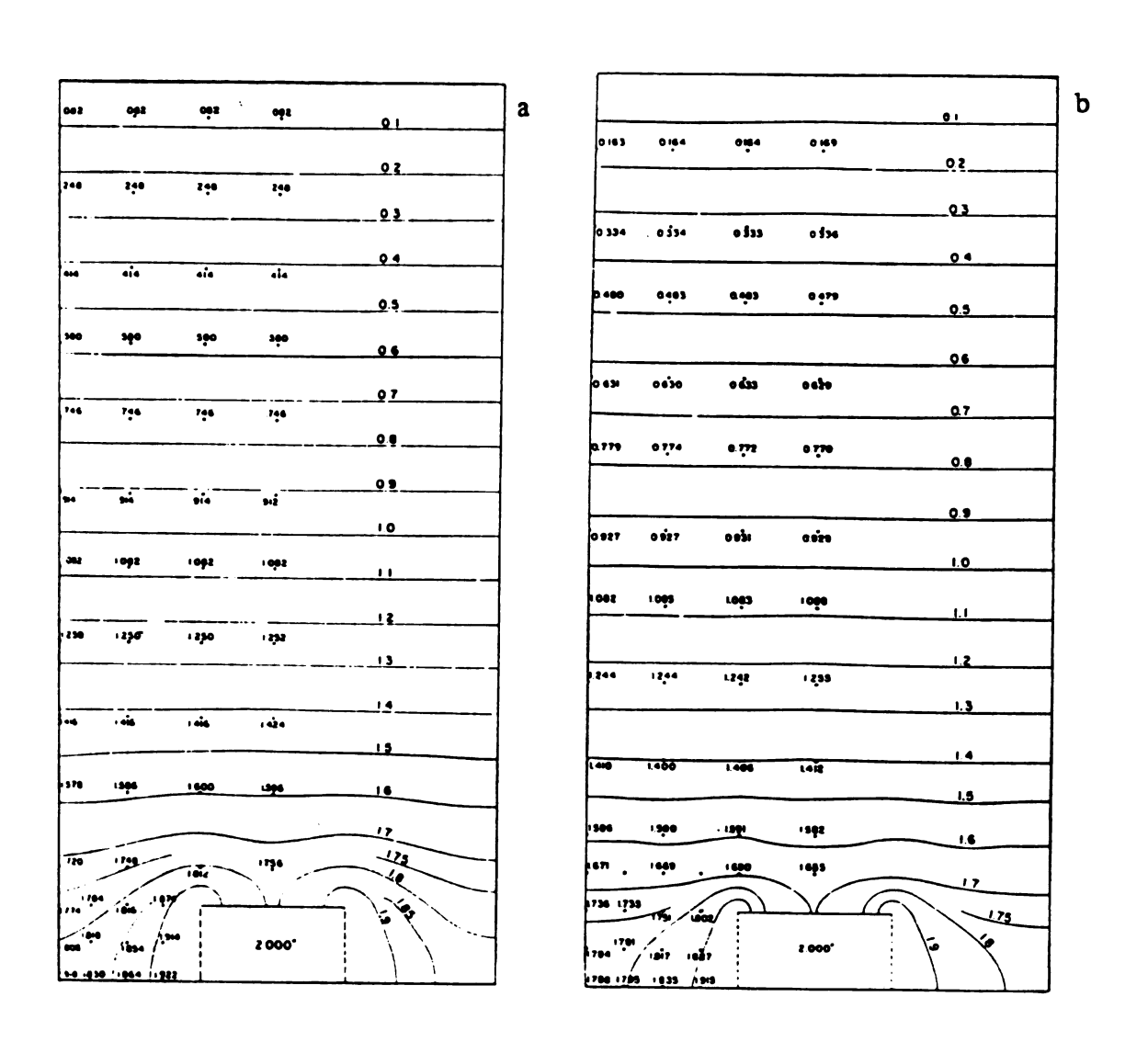
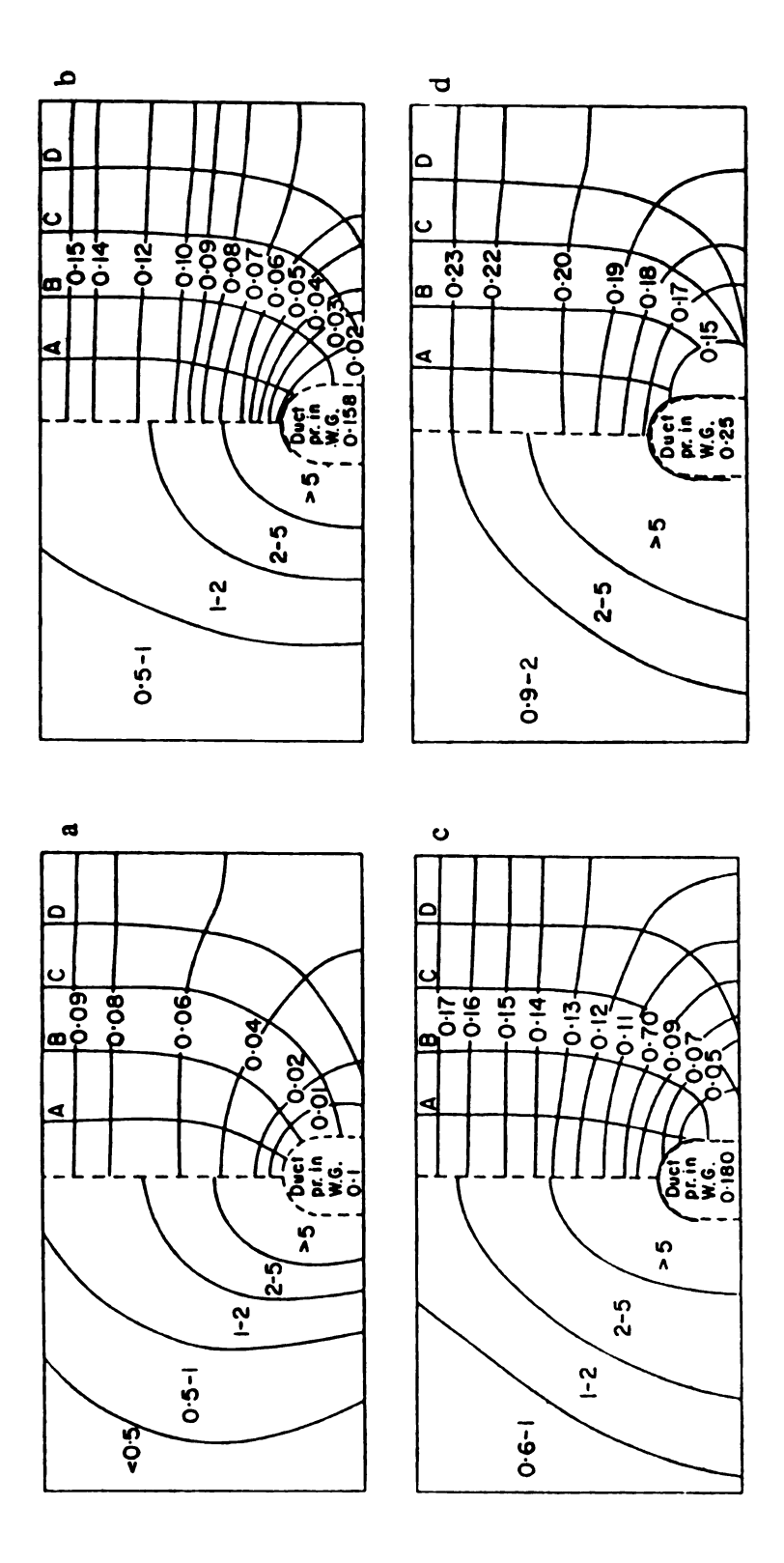


Figure 9. Pressure patterns established by numerical method and by experimental data. Source: Brooker, 1961.

a. By numerical method with B = 1.0 and $P_d = 500$ Pa

b. By experimental data with $P_d = 500$ Pa



Source: Boyce and Davies, 1965 Figure 10. Iso-flow lines, iso-pressure lines and streamlines for different duct openings.

- a. Percentage duct opening area to total duct surface area =100 %
- b. Percentage duct opening area to total duct surface area = 68 %
 c. Percentage duct opening area to total duct surface area = 39 %
 d. Percentage duct opening area to total duct surface area = 13 %

Barrowman and Boyce (1966) conducted experiments in a barley bed to determine the effects of duct spacing and opening, grain bed depth, and air flow rate on air distribution and pressure losses. These experiments are the continuation of work reported by Boyce and Davies (1965). For comparison, they employed the R ratio concept suggested by Rabe (1958) to express the duct opening area, in which R is defined as the ratio of open area of duct system to floor area served by duct system. For a perforated floor, R = 1.0. They found many duct systems have R values as low as 0.11 to 0.09. They recommended an R value of 0.25 and concluded:

- 1. Increasing the duct spacing will reduce the R ratio. In this case, duct pressure has to be increased to maintain the air velocity constant in the parallel flow region. This will in turn increase the duct entrance air velocity. Therefore, air distribution in the bed will be more uneven.
 - 2. Reducing the duct opening area only has a slight improvement in air distribution.
 - 3. Increasing the grain depth will improve air distribution in nonparallel flow region.
- 4. Air flow rate will affect the position of the iso-traverse time line, but will have only a slight affect on their shape.

Hohnor and Brooker (1965) used an analog method to predict the shapes and positions of the cooling front in a cylindrical grain bin with a cross-flow ventilation system. They noticed that the accuracy of this method depends on the deviations of the prototype system from a Laplace field. For the flow rate commonly used in grain ventilation systems, they believed the analog method to be quite accurate.

Brooker (1969) again used the finite difference method to predict air velocity distribution in a grain bin with a rectangular duct having side openings as shown in

Figure 11. He noted that the air velocity is uniform in the upper portion of the grain bin.

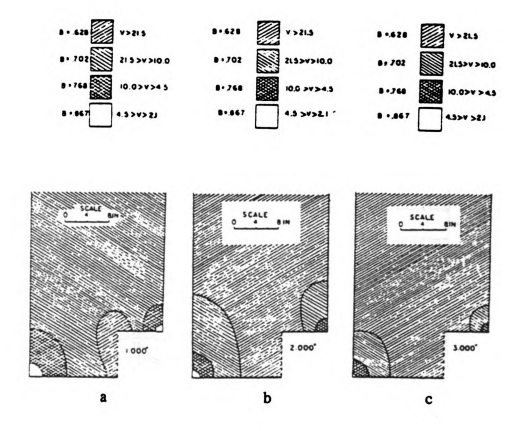


Figure 11. Velocity distribution in the lower portion of the bin for three duct pressures. Source: Brooker, 1969.
a. Duct pressure equals to 250 Pa, and unit of V is fpm b. Duct pressure equals to 500 Pa, and unit of V is fpm c. Duct pressure equals to 750 Pa, and unit of V is fpm

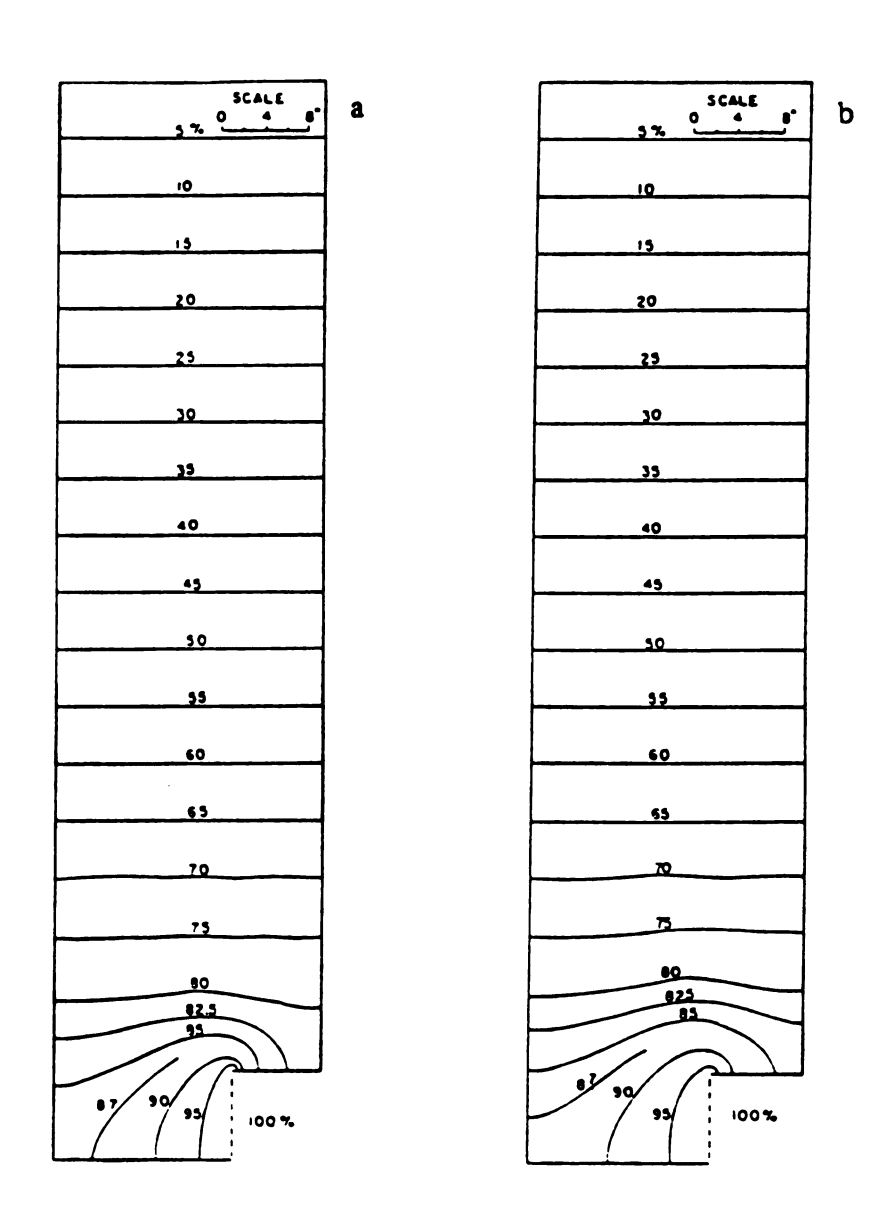


Figure 12. Calculated pressure patterns expressed as percentage of duct pressure. Source: Brooker, 1969.

a. Duct pressures: 250, 500 and 750 Pa, B = 0.628 to 0.768

b. Duct pressure: 500 Pa, B = 1.0

Brooker (1969) also claimed that when the iso-pressure lines from the numerically calculated values are plotted as percentages of the duct pressure, the geometries of the iso-pressure lines remain the same if B in Equation [13] is unchanged. Figure 12a is the calculated pressure patterns expressed as the percentage of duct pressure for three duct pressures of 1.0, 2.0 and 3.0 inch water (250, 500 and 750 Pa) with B = 0.628 to 0.768. Figure 12b is the calculated pressure pattern for a duct pressure of 2.0 inch water (500 Pa) with B = 1.0. From Shedd's data, the B value will approach 1.0 when air velocity is low. In this case, he recommended the use of Laplace equation as the governing equation in the calculation.

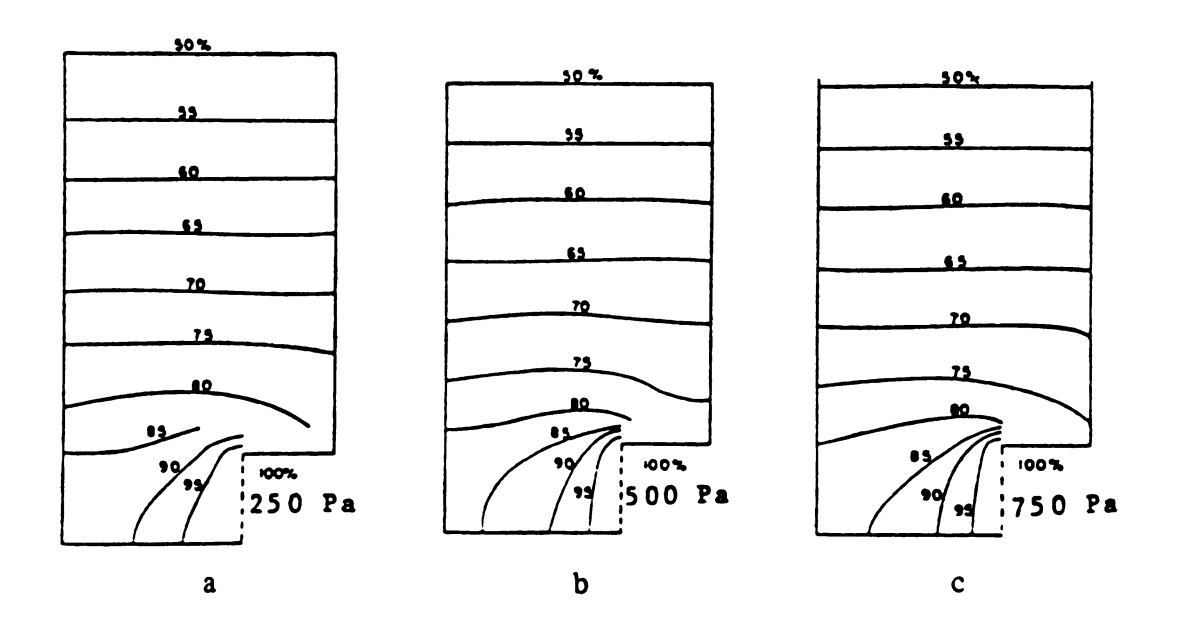


Figure 13. Pressure patterns obtained from experimental data for different duct pressures. Source: Brooker, 1969.

However, Brooker (1969) also found that the pressure patterns obtained from experimental data are different for duct pressures of 250, 500 and 700 Pa as shown in Figure 13a, b and c, respectively. This is contrary to the result obtained from the numerical calculation as stated above.

Jindal and Thompson (1972) used the same equation and method as that used by Brooker (1961 and 1969) to analyze two-dimensional air flow patterns for long triangular shaped piles of grain sorghum with a rectangular lateral duct through the center of the pile. The top and two sides of the duct were perforated. They developed a numerical procedure to find the flow streamlines, which together with iso-pressure lines are shown in Figure 14a, b and c for grain repose angles of 25°, 35° and 45°, respectively.

They concluded that the duct size greatly affected the total air flow rate for a given pile configuration, but the repose angle seemed not to affect the total air flow rate. They also pointed out that increasing the base width of the grain pile decreased the total air flow rate.

Pierce and Thompson (1975) extended the work done by Jindal and Thompson (1972). They intended to predict air flow patterns for a conical shaped grain pile with a rectangular duct through the center. The effects of the duct size, repose angle and pile diameter on air flow rate were the same as that mentioned by Jindal and Thompson (1972). The air flow patterns from their calculated data is shown in Figure 15. The shaded area represents the region near ground, where the spoilage of grain is most likely to occur. The air flow rate for the lower shaded area, which accounts for 37 percent of the pile volume, is less than 50 percent of the average air flow rate for the whole pile.

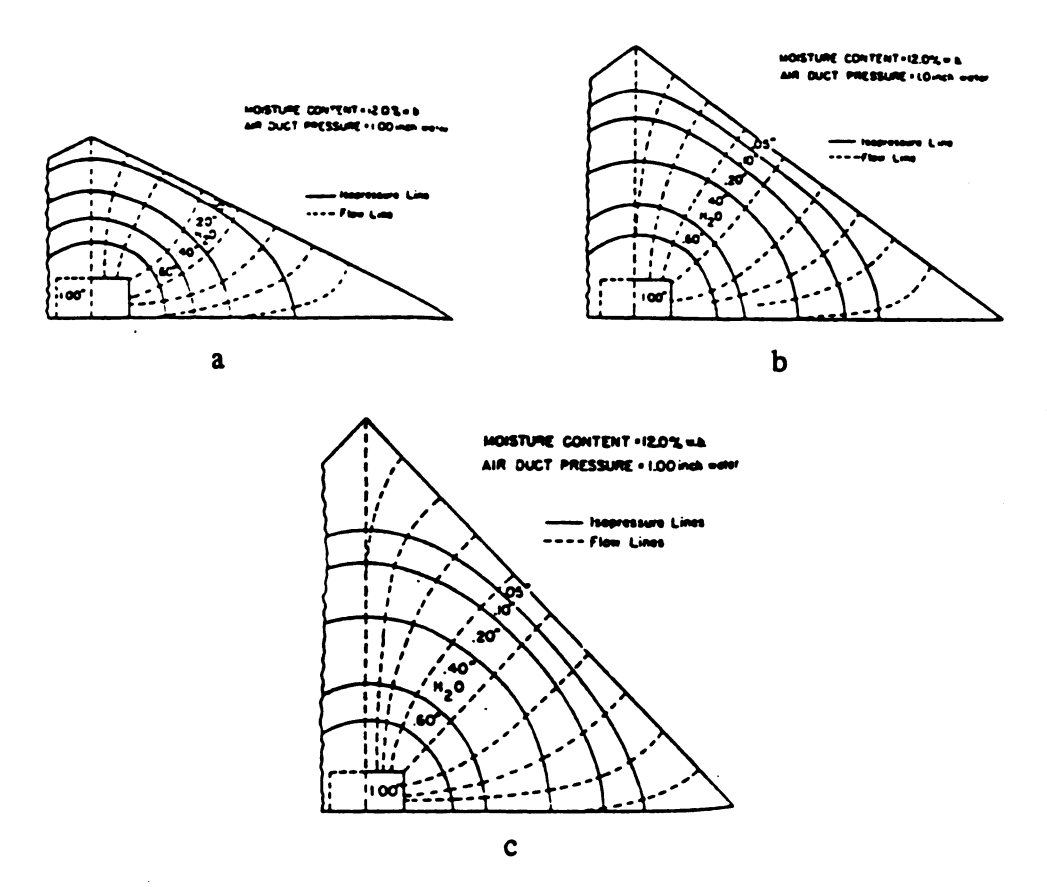


Figure 14. Air pressure and flow path patterns for different grain repose angles. Source: Jindal and Thompson, 1972.

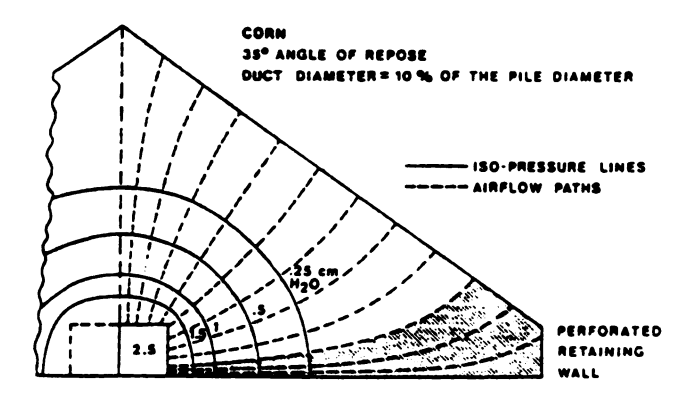


Figure 15. Air pressure and flow path patterns for a section of a conical shaped pile. Source: Pierce and Thompson, 1975.

Based on Brooker's nonlinear partial differential equation (Equation [25]), Marchant (1976a) first applied the successive over relaxation numerical method to the solution of this equation to estimate air flow patterns within rectangular and cylindrical hay bales. Late, realizing the disadvantages of the finite difference method in solving the partial differential equation, Marchant (1976b) employed the finite element method to solve the following equation in two dimensional space:

$$\frac{\partial}{\partial x}(\frac{1}{K}\frac{\partial P}{\partial x}) + \frac{\partial}{\partial y}(\frac{1}{K}\frac{\partial P}{\partial y}) = 0$$
 [31]

in which K is a function of velocity. He found that the calculated values were very close to the experimental data for linear air flow. He concluded that the finite element method can cope with any geometrical shape and any correlation of pressure gradient with velocity. He plotted iso-pressure lines for a rectangular grain bin with lateral ducts having different shapes and openings. He compared these figures with Brooker's experimental data (Brooker, 1958) as shown in Figure 16a, and with Barrowman and Boyce's experimental data (Barrowman and Boyce, 1966) as shown in Figure 16b and c (the dotted lines represented the elements). He noted that the calculated pressure contour lines overlapped those obtained from experimental results.

Using Equation [12], [23] and [24] and the continuity equation, Haque et al. (1980) developed a partial differential equation and used the finite element method to calculate pressure and velocity values and to determine the direction of air flow movement for any point in a conical-top cylindrical grain bed with a perforated floor. They claimed the pressures calculated numerically agreed well with the observed data.

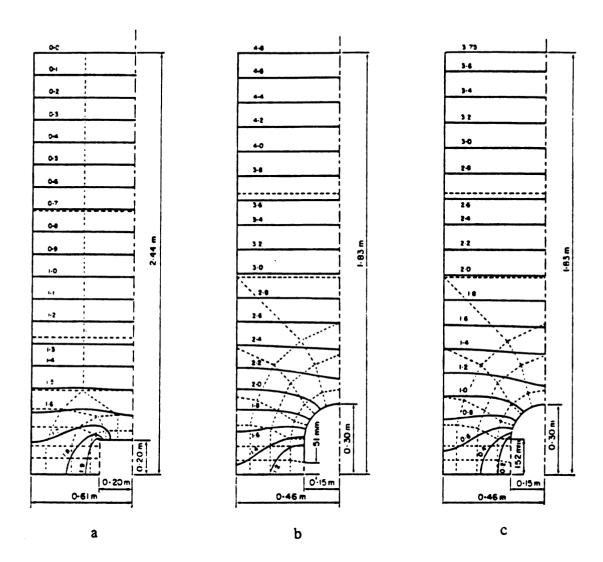


Figure 16. Calculated iso-pressure lines in a grain drying bin with different duct shapes and openings. Source: Marchant, 1976b.

a. Calculated iso-pressure lines overlapped those obtained from Brooker's experimental data. Duct opening = 0.2 m.

b. Calculated iso-pressure lines overlapped those obtained from Barrowman and Boyce's experimental data. Duct opening = 0.051 m.

c. Calculated iso-pressure lines overlapped those obtained from Barrowman and Boyce's experimental data. Duct opening = 0.152 m.

Lai (1980) modified Ergun's equation (Equation [4]) and used the method of lines to convert a nonlinear partial differential equation into a system of ordinary differential equations to solve three-dimensional air flow problems in a cylindrical bed with two different porosity distributions. He found that the pressure distribution showed significant variations at the air entrance because of the nonuniform entrance velocity. He also observed that a bed with nonuniform porosity will generally display a lower pressure drop than will a bed with uniform porosity, even if the average void fractions are equal in both beds.

Segerlind (1982) used the finite element method to solve Equations [26] and [27] for a rectangular bin filled with shelled corn. His computed results both for linear flow and nonlinear flow were very close to those given by Brooker's calculated results (Brooker, 1961) and experimental results (Brooker, 1969), respectively. The pressure contour lines in the entrance region with a duct pressure of 3.0 inch water (750 Pa) are shown in Figure 17. The values of the upper and low corner nodes were incorporated into the impermeable boundary conditions in his calculation.

Khompos (1983) and Khompos et al. (1984) applied Segerlind's equations to air flow problems in a three-dimensional domain and also employed the finite element method to analyze air flow patterns for cylindrical grain bins with different duct shapes and locations. The typical pressure and velocity distributions for a Y-shaped duct with a grain depth of 9 m are shown in Figure 18 and 19, respectively.

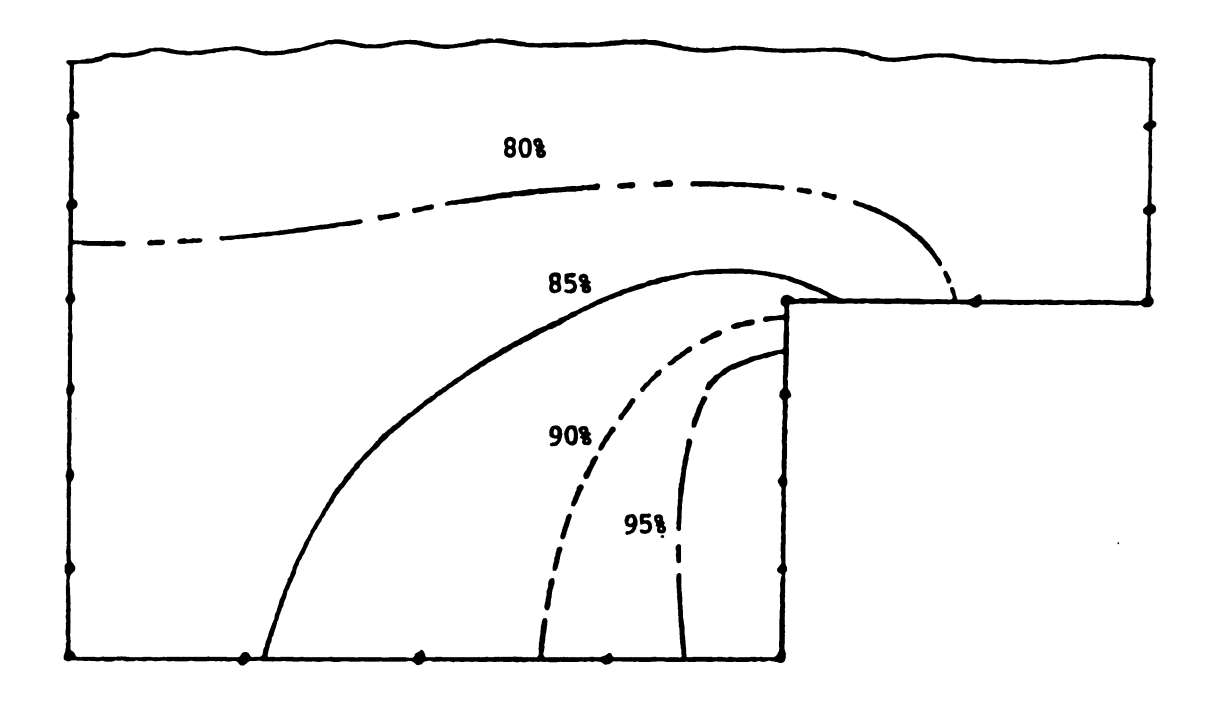


Figure 17. Pressure contour lines in the entrance region. Source: Segerlind, 1982.

Smith (1982) used the finite element method together with a frontal solution technique to solve Equation [31] for hay and grain beds in three-dimensional space. He thought that K can be taken as a constant for linear flow with low air velocity. For nonlinear flow, he held that Equation [13] can still be used if K is expressed as a function of velocity. He believed that his method can be used to obtain the solution for air flow problems with reasonable accuracy. But he also found that the calculated air velocity is less accurate than the pressure value and most of the errors arise in regions with high air velocities.

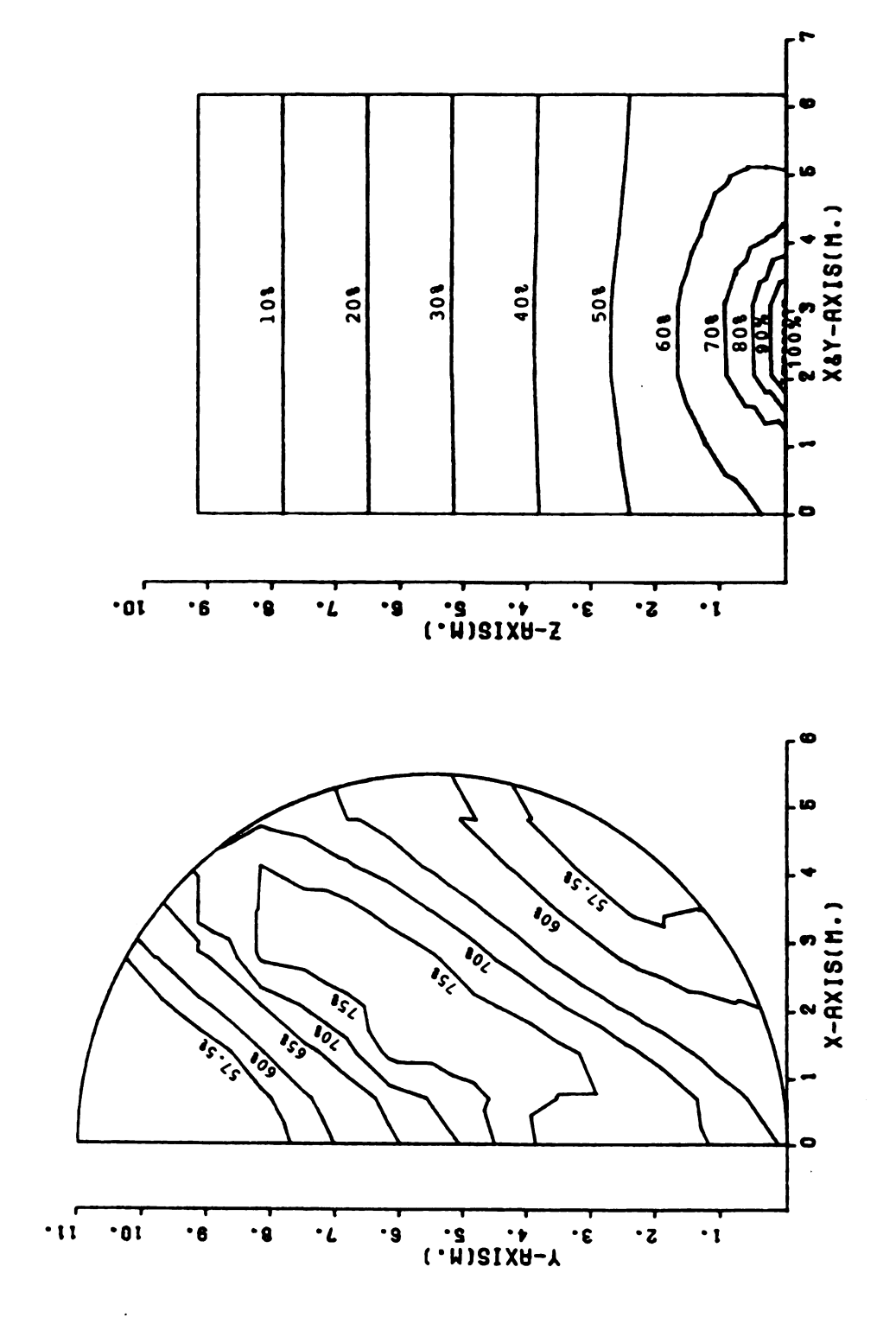


Figure 18. Pressure distribution for Y-shaped duct. Source: Khompos, 1983.

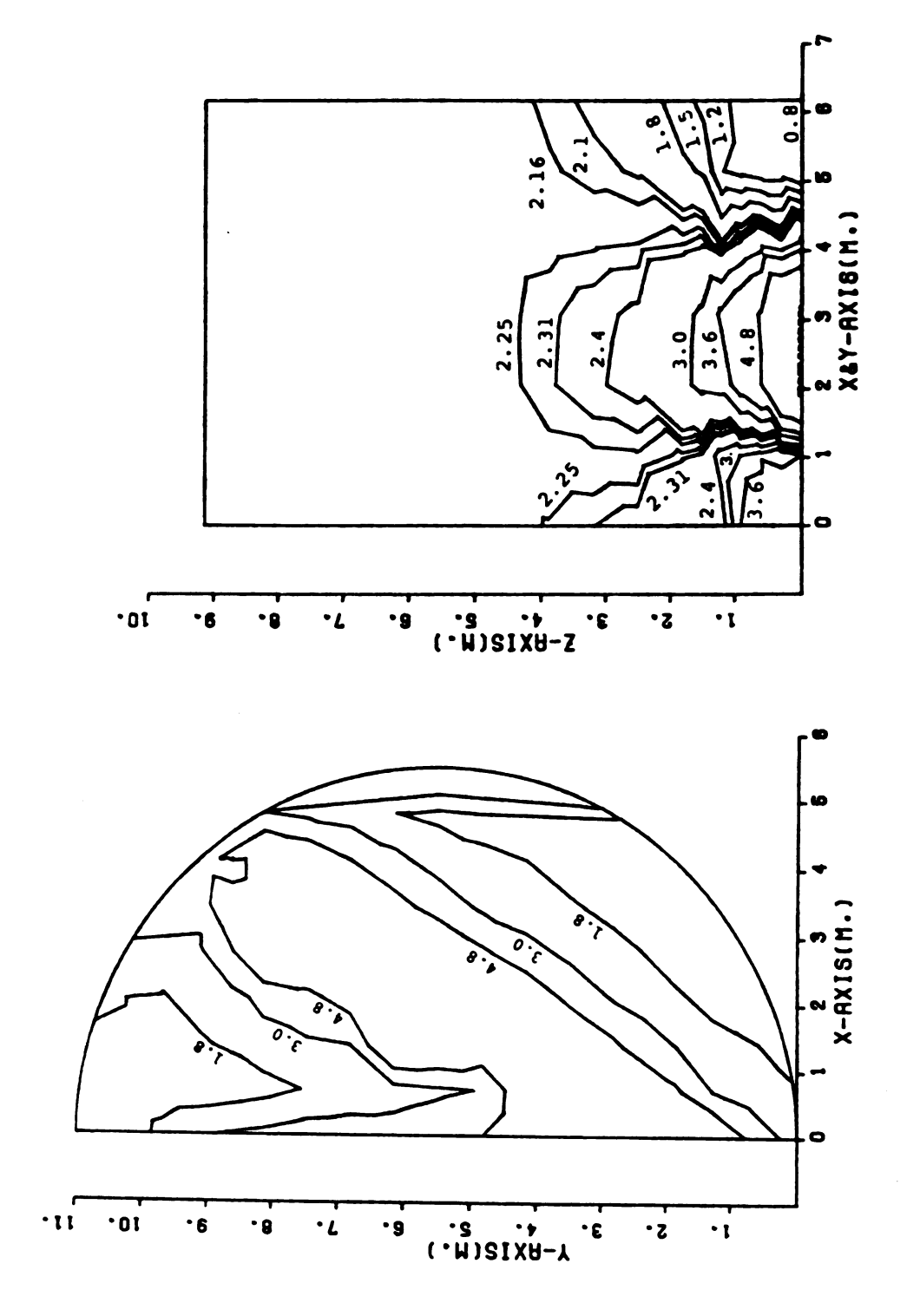


Figure 19. Velocity distribution for Y-shaped duct. Source: Khompos, 1983.

Miketinac and Sokhansanj (1985) employed an equation similar to Equation [31] as the governing equation and used the finite element method to calculate the pressure distribution for the grain bed as outlined by Brooker (1969). To deal with the difficulty of obtaining accurate numerical solutions for the entrance corners of the rectangular duct, they proposed that a refined mesh be used near the air duct. The resulting pressure patterns for air flow in a Laplace field are very close to those calculated by Brooker (1969). The calculated pressure patterns for nonlinear flow are shown in Figure 20a, b and c for duct pressures of 250, 500 and 750 Pa, respectively. The values of constants A and B in Equation [13] were taken from Segerlind (1982). Comparing Figure 20 with Figure 13 they found that differences existed, which they attributed to the inaccuracy of the experimental data.

Later Miketinac et al. (1986) used the same technique as Miketinac and Sokhansanj (1985) to analyze the air flow patterns for several bins and floor configurations. The typical velocity vector for bins with semicircular and rectangular ducts are shown in Figure 21a and b, respectively.

Chapman et al. (1989) applied the finite element method to the solution of Segerlind's equations (Segerlind, 1982) for the analysis of air flow patterns in a grain storage with different duct distributions. They thought that the pressure pattern alone is not the best way for describing nonlinear air flow behavior, but that the isotraverse time lines as introduced by Hukill and Shedd (1955) can reflect the actual shape of the temperature front when it moves through the grain bed. The pressure contour lines, the streamlines and the iso-traverse time lines for flat grain storage with three circular ducts are shown in Figure 22a, b and c, respectively.

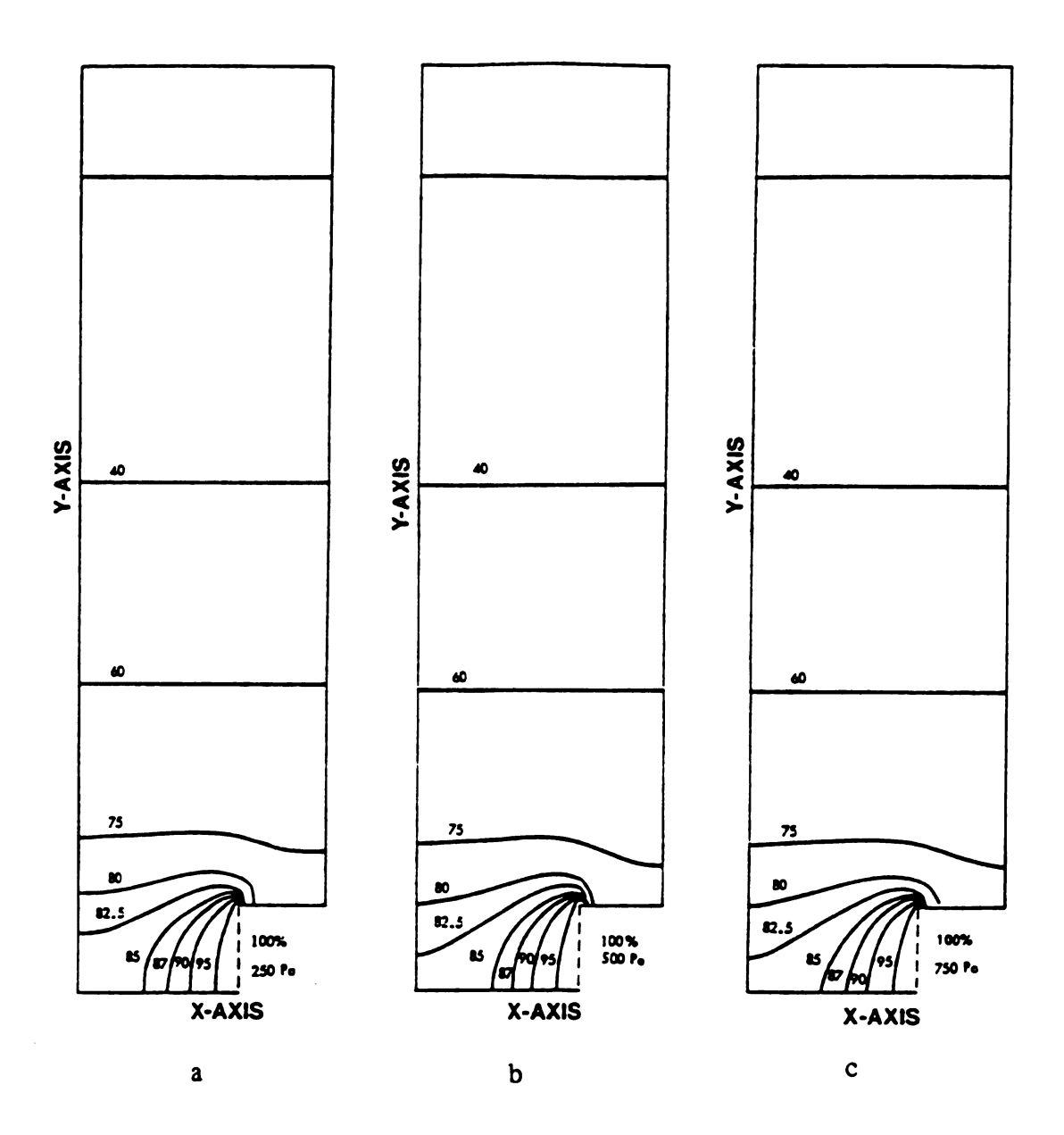


Figure 20. Pressure contour lines for grain bed with different duct pressures. Source: Miketinac and Sokhansanj, 1985.

- a. Duct pressure equals to 250 Pa
- b. Duct pressure equals to 500 Pa
- c. Duct pressure equals to 750 Pa

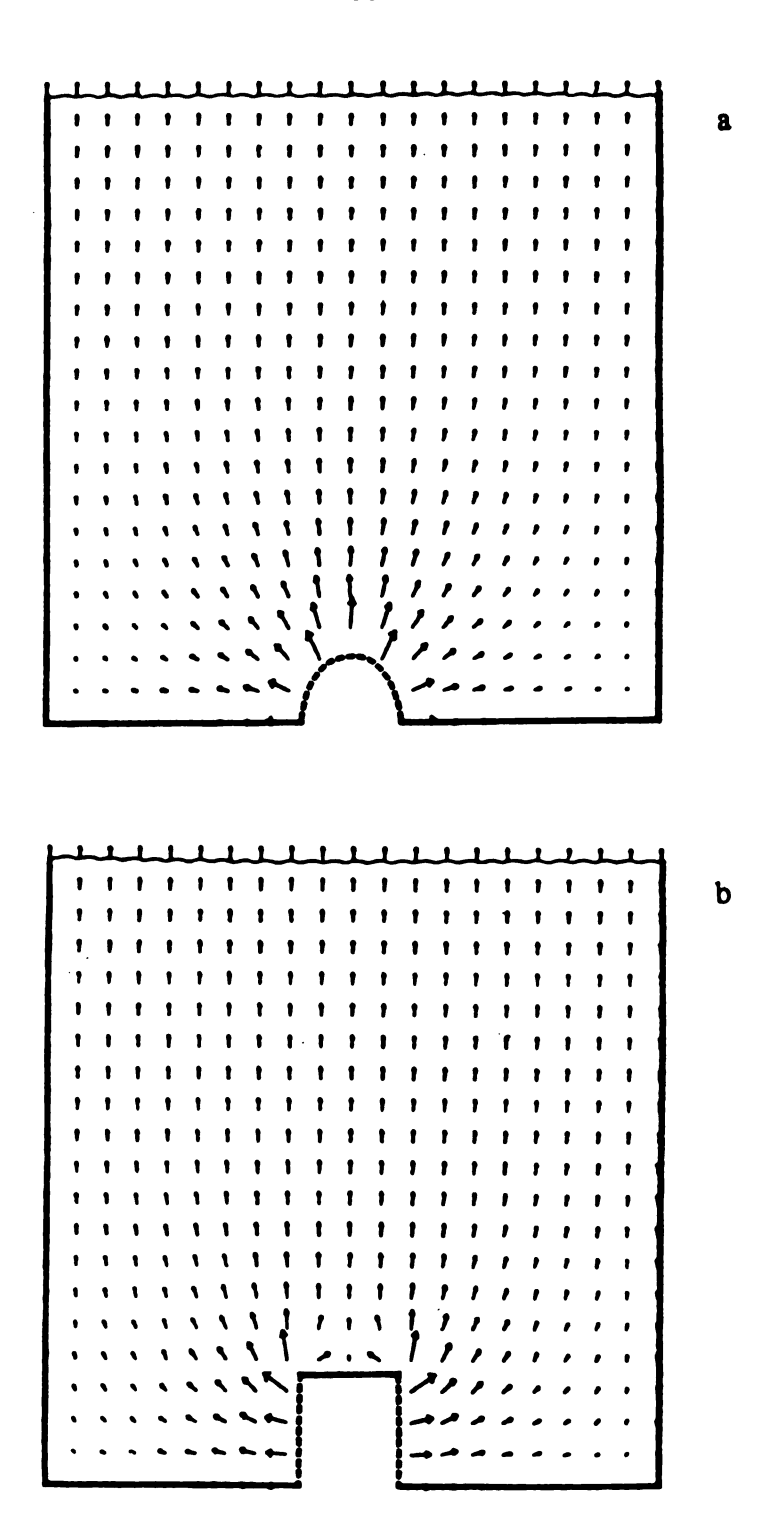


Figure 21. Velocity vector fields for bins with semicircular and rectangular ducts. Source: Miketinac et al. 1986.

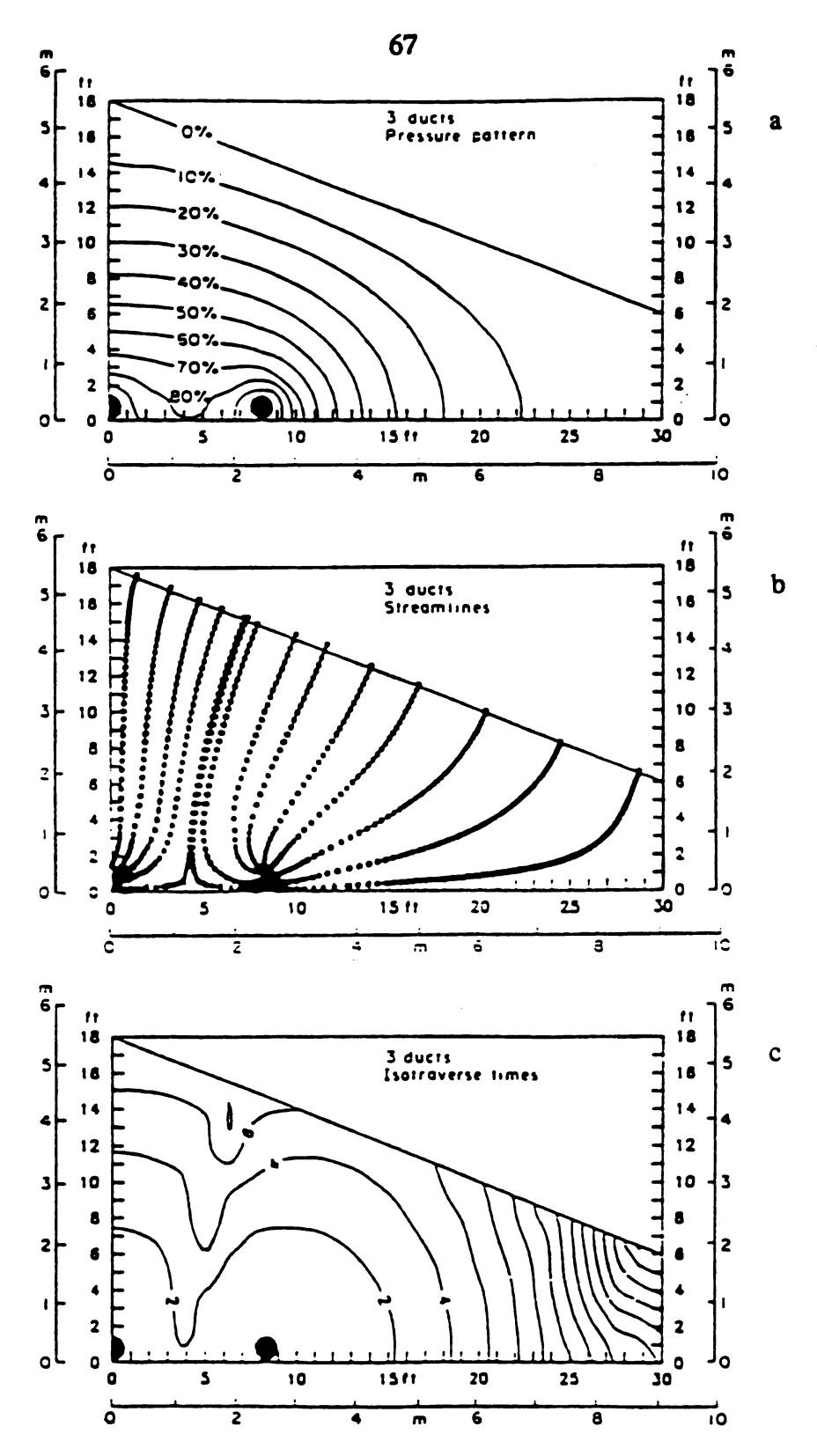


Figure 22. Air flow patterns for flat grain storage with three circular ducts. Source: Chapman et al. 1989.

CHAPTER 3

ANALYSIS METHODS

3.1 Establishment of mathematical models

3.1.1 Models of pressure and velocity distributions

The equations governing air flow through the potato storage are derived from the basic physical principle of conservation of mass and from equations developed through the analysis of experimental data.

The principle of conservation of mass defines that, when fluid flow passes through a confined space the net out flow of mass from a volume should be equal to the inflow minus the decrease of mass within the volume. Following Eulerian description, Incropera and DeWitt (1985) and Sabersky et al. (1989) used the concept of a differential control volume to derive the continuity equation in three-dimensional Cartesian coordinates:

$$\frac{\partial \rho}{\partial t} + \frac{\partial}{\partial x} (\rho V_x) + \frac{\partial}{\partial y} (\rho V_y) + \frac{\partial}{\partial z} (\rho V_z) = 0$$
 [32]

Suppose the fluid under study (air) is incompressible, $\rho = \text{constant}$, then

$$\frac{\partial V_x}{\partial x} + \frac{\partial V_y}{\partial y} + \frac{\partial V_z}{\partial z} = 0$$
 [33]

Equation [33] is the reduced form of Equation [32], or simply, divV = 0.

The relationship between the air velocity and the pressure gradient for air flow through the potato storage can be expressed by Equation [13] (Staley and watson, 1961).

In a three-dimensional domain, the pressure gradients in x, y and z directions can be related to that in the normal direction in the same way as in Equation [23]:

$$\left[\frac{\partial P}{\partial n}\right]^2 = \left(\frac{\partial P}{\partial x}\right)^2 + \left(\frac{\partial P}{\partial y}\right)^2 + \left(\frac{\partial P}{\partial z}\right)^2$$
 [34]

The velocity components in x, y and z directions also can be related to that in the normal direction in the same way as indicated in Equation [24]:

$$\frac{V_x}{V_z} = \frac{\partial P/\partial x}{\partial P/\partial n}$$

$$\frac{V_y}{V} = \frac{\partial P/\partial y}{\partial P/\partial n}$$

$$\frac{V_z}{V_z} = \frac{\partial P/\partial z}{\partial P/\partial n}$$
 [35]

From Equations [13], [33], [34] and [35], a partial differential equation can be developed:

$$\frac{\partial}{\partial x} \left[K_{\alpha} \frac{\partial P}{\partial x} \right] + \frac{\partial}{\partial y} \left[K_{\alpha} \frac{\partial P}{\partial y} \right] + \frac{\partial}{\partial z} \left[K_{\alpha} \frac{\partial P}{\partial z} \right] = 0$$
 [36]

where the granular permeability

$$K_{G} = A \left[\left(\frac{\partial P}{\partial x} \right)^{2} + \left(\frac{\partial P}{\partial y} \right)^{2} + \left(\frac{\partial P}{\partial z} \right)^{2} \right]^{\frac{B-1}{2}}$$
 [37]

Equations [36] and [37] are actually the representations of Segerlind's equations (Equations [26] and [27]) in three-dimensional space.

Equations [36] and [37] can be used for inhomogeneous and isotropic porous media, because the coefficient K_0 is a function of the coordinates, but not a function of the orientations of the media. These two equations have been successfully used to analyze air flow patterns in a grain storage (Segerlind, 1982, Khompos, 1983 and Chapman et al. 1989). They will be used as the basic equations in the present study for the calculation of the pressure distribution within the potato storage.

After obtaining the pressure distribution, the velocity in the normal direction and the velocity components in x, y and z directions can be determined from Equations [13] and [35], respectively.

3.1.2 Models of streamlines and flow rates

To describe fluid motion in a space, an imaginary streamline curve is introduced. It is defined as a curve everywhere parallel to the local velocity vector (Greenkorn, 1983 and Sabersky et al. 1989). By this definition, the relationship of the increment of the curve, dx and dy, and the velocity components, V_x and V_y , can be expressed by the following equation:

$$\frac{dx}{dy} = \frac{V_x}{V_y}$$
 [38]

or

$$-V_{v}dx+V_{x}dy = 0 ag{39}$$

In two-dimensional space the continuity equation (Equation [33]) has the form of

$$\frac{\partial V_x}{\partial x} + \frac{\partial V_y}{\partial y} = 0$$
 [40]

By introducing the stream function Ψ and defining that

$$V_{x} = \frac{\partial \Psi}{\partial y}$$

E

a

u

li

an

$$V_{y} = -\frac{\partial \Psi}{\partial x}$$
 [41]

Equation [39] is equivalent to

$$\frac{\partial \Psi}{\partial x} dx + \frac{\partial \Psi}{\partial y} dy = 0$$
 [42]

and the continuity equation (Equation[40]) remains satisfied.

Because Ψ is a function of x and y, $d\Psi$ can be expanded as

$$d\Psi = \frac{\partial \Psi}{\partial x} dx + \frac{\partial \Psi}{\partial y} dy$$
 [43]

When Ψ is constant, i.e. $d\Psi = 0$, Equation [43] is the same as Equation [42]. Therefore, lines of constant Ψ also represent streamlines (Sabersky et al. 1989).

From Equation [24]

$$\frac{V_x}{V_y} = \frac{\partial P/\partial x}{\partial P/\partial y}$$
 [44]

and from Equation [41]

$$\frac{V_x}{V_y} = -\frac{\partial \Psi/\partial y}{\partial \Psi/\partial x}$$
 [45]

it follows that

$$\frac{\partial P}{\partial x} \frac{\partial \Psi}{\partial x} + \frac{\partial P}{\partial y} \frac{\partial \Psi}{\partial y} = 0$$
 [46]

Equation [46] means that the velocity potential (pressure, gravity or their sum) and the stream function are mutually orthogonal because their inner product is equal to zero. That is to say the streamline is always perpendicular to the iso-pressure line. Therefore, if the pressure distribution is known, then the streamline can be obtained from the orthogonal relationship of Equation [46].

As mentioned above, the streamline takes the direction of the local velocity vector, there is no flow across the streamline. The boundaries of the stationary solid surfaces and the symmetric surfaces are always the streamlines. According to these concepts the rate of fluid flow in the area between two streamlines will be constant.

3.2 Application of finite element method

The finite element method has been used for solving problems of solid mechanics for a long time. During the past decade, the finite element method has found increased use and wider acceptance for the solutions of the equations governing fluid mechanics and heat transfer. The main idea of the finite element method is to change the continuous problem into a discrete problem which is represented by a system of algebraic equations. When a governing equation for a field problem can not be solved analytically, the finite element method may be the best alternative to solve it numerically. Generally the

solutions of Equations [36] and [37] can not be found by classical analytical methods, except when K_0 in Equation [37] is equal to one. In the latter case, Equation [36] is reduced to the Laplace equation (Equation [22]) which together with certain boundary conditions can be solved analytically (Churchill and Brown, 1987). In most cases, the only way to solve Equations [36] and [37] is to resort to numerical methods (Hariharan and Houlden, 1986) - at present, the finite element method. The procedures of applying the finite element method are outlined in the following sections.

3.2.1 Applying the Galerkin method

The Galerkin method is a member of the larger class of weighted residual methods. It makes the residual of an equation for a certain solution orthogonal to the interpolation function of each element. Thus the inner product of the residual and the interpolation function equals zero (Fletcher, 1984 and Ortega, 1987). In the Galerkin method, the elements are isoparametric because the interpolation function (also known as shape function or weight function) used to describe the coordinate transformation is chosen from the same family of the trial function which is used to represent the dependent variables. In this case, the convergence to the exact solution can be secured as the node number tends to infinity (Fletcher, 1984). The objective of applying the Galerkin method to Equation [36] is to reduce the partial differential equation to a system of algebraic equations. According to the inner product law, the weighted residual integral equation has the following form (Segerlind, 1984):

$$\{R^{(0)}\} = \int_{V} [N]^{T} \left[\frac{\partial}{\partial x} \left(K_{\sigma} \frac{\partial P}{\partial x} \right) + \frac{\partial}{\partial y} \left(K_{\sigma} \frac{\partial P}{\partial y} \right) + \frac{\partial}{\partial z} \left(K_{\sigma} \frac{\partial P}{\partial z} \right) \right] dV \qquad [47]$$

where [N] is the row vector of the shape function in Cartesian coordinates. For the above nonlinear formulation, it is reasonable to choose a twenty-node three-dimensional solid element. The row vector of the shape function for this element is given by

$$[N] = [N_1 \ N_2 \ N_3 \dots N_{2n}]$$
 [48]

The finite element approximations are

$$X = [N]\{x\}$$

 $Y = [N]\{y\}$
 $Z = [N]\{z\}$
 $P^{(e)} = [N]\{P^{(e)}\}$ [49]

3.2.2 Applying the Green-Gauss theorem

The general form of the Green-Gauss theorem (Sneddon, 1976 and Pearson, 1983) is

$$\int_{V} \left[\frac{\partial Q}{\partial x} + \frac{\partial R}{\partial y} + \frac{\partial T}{\partial z} \right] dxdydz = \int_{S} (Q\cos\alpha + R\cos\beta + T\cos\gamma)dS$$
 [50]

where $\cos\alpha$, $\cos\beta$ and $\cos\gamma$ are the direction cosines of the curved surface S.

By using the chain rule and applying the Green-Gauss theorem to Equation [47], this second order integral can be changed into a first order integral and surface integrals.

Note that by using $\{R^{(a)}\}=\{0\}$ and the homogeneous boundary conditions (Churchill and Brown, 1987), Equation [47] will be reduced to

$$[K^{(0)}]\{P^{(0)}\} = \{0\}$$
 [51]

where [K^(e)] is an element stiffness matrix,

$$[K^{(e)}] = \int_{V} [B]^{T}[D][B]dV$$
 [52]

The row vector [B] contains the first order derivatives of [N] with respect to the coordinates of x, y and z. It has the form of

$$[B] = \begin{bmatrix} \frac{\partial N_1}{\partial x} & \frac{\partial N_2}{\partial x} & \frac{\partial N_3}{\partial x} & \dots & \frac{\partial N_{20}}{\partial x} \\ \frac{\partial N_1}{\partial y} & \frac{\partial N_2}{\partial y} & \frac{\partial N_3}{\partial y} & \dots & \frac{\partial N_{20}}{\partial y} \\ \frac{\partial N_1}{\partial z} & \frac{\partial N_2}{\partial z} & \frac{\partial N_3}{\partial z} & \dots & \frac{\partial N_{20}}{\partial z} \end{bmatrix}$$
[53]

The matrix [D] is a diagonal one with the K_G values defined in the diagonal. The coefficient K_G is a constant value for a particular step in the calculation, but must be updated at each iteration step.

3.2.3 Jacobian transformation

Before Equation [52] can be solved, the physical coordinates (x, y and z) related to all the variables should be mapped into the natural coordinates $(\xi, \eta \text{ and } \zeta)$.

For the twenty-node solid element (Figure 23), the shape functions for these nodes in the natural coordinates are as follows (Kardestuncer and Norrie, 1987):

$$N_{i} = \frac{1}{8}(1+\xi_{o})(1+\eta_{o})(1+\zeta_{o})(\xi_{o}+\eta_{o}+\zeta_{o}-2)$$

$$i=1,3,5,7,13,15,17,19$$

$$N_{i} = \frac{1}{4}(1-\xi^{2})(1+\eta_{o})(1+\zeta_{o})$$

$$i=2,6,14,18$$

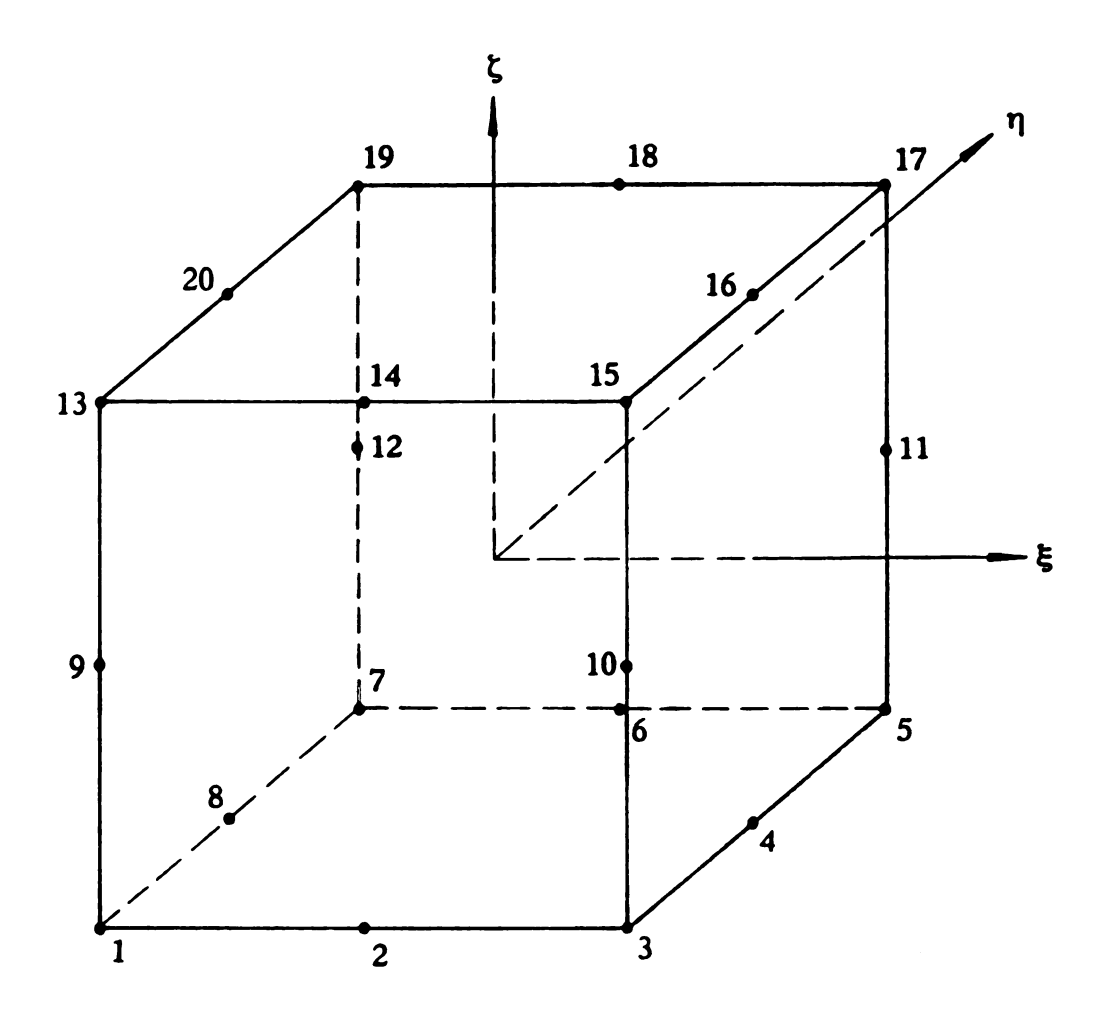
$$N_{i} = \frac{1}{4}(1-\eta^{2})(1+\xi_{o})(1+\zeta_{o})$$

$$i=4,8,16,20$$

$$N_{i} = \frac{1}{4}(1-\zeta^{2})(1+\xi_{o})(1+\eta_{o})$$

$$i=9,10,11,12$$
[54]

where $\xi_o = \xi_i \xi$, $\eta_o = \eta_i \eta$ and $\zeta_o = \zeta_i \zeta$ for node i.



Firgure 23. Sketch of twenty-node solid element with natural coordinates

By using the chain rule, the partial differential forms of the shape functions with respect to natural coordinates can be expressed as

$$\frac{\partial N_i(\xi,\eta,\zeta)}{\partial \xi} = \frac{\partial N_i}{\partial x} \frac{\partial x}{\partial \xi} + \frac{\partial N_i}{\partial y} \frac{\partial y}{\partial \xi} + \frac{\partial N_i}{\partial z} \frac{\partial z}{\partial \xi}$$

$$\frac{\partial N_i(\xi,\eta,\zeta)}{\partial \eta} = \frac{\partial N_i}{\partial x} \frac{\partial x}{\partial \eta} + \frac{\partial N_i}{\partial y} \frac{\partial y}{\partial \eta} + \frac{\partial N_i}{\partial z} \frac{\partial z}{\partial \eta}$$

$$\frac{\partial N_i(\xi,\eta,\zeta)}{\partial \zeta} = \frac{\partial N_i}{\partial x} \frac{\partial x}{\partial \zeta} + \frac{\partial N_i}{\partial y} \frac{\partial y}{\partial \zeta} + \frac{\partial N_i}{\partial z} \frac{\partial z}{\partial \zeta}$$
 [55]

Equation [55] can be represented in the following matrix form:

$$\begin{bmatrix} \frac{\partial N_{i}(\xi,\eta,\zeta)}{\partial \xi} \\ \frac{\partial N_{i}(\xi,\eta,\zeta)}{\partial \eta} \\ \frac{\partial N_{i}(\xi,\eta,\zeta)}{\partial \zeta} \end{bmatrix} = \begin{bmatrix} J \end{bmatrix} \begin{bmatrix} \frac{\partial N_{i}}{\partial x} \\ \frac{\partial N_{i}}{\partial y} \\ \frac{\partial N_{i}}{\partial z} \end{bmatrix}$$
[56]

where Jacobian matrix [J] is given by

$$[J] = \begin{bmatrix} \frac{\partial x}{\partial \xi} & \frac{\partial y}{\partial \xi} & \frac{\partial z}{\partial \xi} \\ \frac{\partial x}{\partial \eta} & \frac{\partial y}{\partial \eta} & \frac{\partial z}{\partial \eta} \\ \frac{\partial x}{\partial \zeta} & \frac{\partial y}{\partial \zeta} & \frac{\partial z}{\partial \zeta} \end{bmatrix}$$
[57]

Thus the matrix [B] in the natural coordinates becomes

$$[B(\xi,\eta,\zeta)] = [J]^{-1} \begin{bmatrix} \frac{\partial N_i(\xi,\eta,\zeta)}{\partial \xi} \\ \frac{\partial N_i(\xi,\eta,\zeta)}{\partial \eta} \\ \frac{\partial N_i(\xi,\eta,\zeta)}{\partial \zeta} \end{bmatrix}$$
[58]

where [J]-1 is the inverse of [J],

$$[J]^{-1} = \frac{\operatorname{adj}[J]}{|\det[J]|}$$
 [59]

The differential volume of the element, dV, is given by

$$dV = dxdydz = |det[J]|d\xi d\eta d\zeta$$
 [60]

After Jacobian transformation, the element stiffness matrix [K^(e)] becomes the integrals in the natural coordinates (Segerlind, 1984),

$$[K^{(\omega)}] = \int_{-1}^{-1} \int_{-1}^{-1} \int_{-1}^{+1} [B(\xi, \eta, \zeta)]^{\mathsf{T}} [D] [B(\xi, \eta, \zeta)] |\det[J] |d\xi d\eta d\zeta$$
 [61]

3.2.4 Gauss-Legendre quadrature

Because of the presence of Jacobian matrix [J], the exact solution of Equation [61] is still very difficult. To evaluate integral Equation [61] numerically, Gauss-Legendre quadrature is introduced. The sampling points, n, can be estimated from the formula:

(2n-1) = N, where N is the degree of the polynomials (Segerlind, 1984).

For the present problem, the highest power of ξ , η and ζ within Equation [61] is equal to 6. Therefore, the choice of 3 sampling points for each of the variables is suitable. The locations of the sampling points and the weighting coefficients can be obtained from the related reference books (Segerlind, 1984, Reddy, 1984, and Kardestuncer and Norrie, 1987). For three sampling points

$$\xi_i = 0.0$$
 $w_i = 8/9$ $\xi_i = \pm 0.774597$ $w_i = 5/9$

The integral Equation [61] thus becomes a numerical summation:

$$[K^{(e)}] = \sum_{i=1}^{3} \sum_{j=1}^{3} \sum_{k=1}^{3} [f(\xi_i, \eta_j, \zeta_k) w_{ijk}]$$
 [62]

where

$$f(\xi_{:},\eta_{:},\zeta_{k}) = [B(\xi,\eta,\zeta)]^{T}[D][B(\xi,\eta,\zeta)] |\det[J]|$$
 [63]

3.2.5 Applying the direct stiffness method

A single finite element is continuous in nature. But the continuity requirement for the discrete representation of the entire region can be satisfied only by assembling the individual element matrix $[K^{(o)}]$ into a global matrix [K]. This process is the direct stiffness method. For the present problem, the global matrix [K] is a symmetric, banded and positive definite matrix.

At this stage, the partial differential equation (Equation [36]) is finally changed into a system of homogeneous algebraic equations which are represented by a matrix form:

$$[K]{P} = {0}$$
 [64]

The nodal pressure values can be obtained by solving Equation [64] along with the prescribed boundary conditions.

3.2.6 Applying the Newton-Raphson method

In determining the pressure and velocity distributions at any point, say $A(x_A, y_A, z_A)$, of a cross-section of the potato storage, three sets of data are required: the element

number where point A is located and the coordinates of the nodes of this element, the nodal pressure values of this element, and the natural coordinates of point A. The Cartesian coordinates and the natural coordinates are related through Equation [49] of the finite element approximations which can be rewritten as

$$F_1(\xi,\eta,\zeta) = [N]\{x\} - x_A = 0$$

$$F_2(\xi,\eta,\zeta) = [N]\{y\} - y_A = 0$$

$$F_1(\xi,\eta,\zeta) = [N]\{z\} - z_A = 0$$
 [65]

Thus F_1 , F_2 and F_3 form a set of nonlinear algebraic equations. To obtain ξ_A , η_A and ζ_A corresponding to x_A , y_A and z_A from Equation [65], both the successive substitution method and the Newton-Raphson method are available. Because the Newton-Raphson method converges quadratically, it takes only two iterations to reduce an error of 10^2 to an error of 10^4 (Finlayson, 1980, and Chapra and Canale, 1988), this method is chosen to solve Equation [65].

By expanding Equation [65] in a Taylor series about the kth iteration and neglecting the second and higher order of the derivatives, the following equations are obtained:

$$F_{i}(\xi_{k+1},\eta_{k+1},\zeta_{k+1}) = F_{i}(\xi_{k},\eta_{k},\zeta_{k}) + \frac{\partial F_{i}(\xi_{k},\eta_{k},\zeta_{k})}{\partial \xi}(\xi_{k+1} - \xi_{k})$$

$$+\frac{\partial F_{i}(\xi_{k},\eta_{k},\zeta_{k})}{\partial \eta}(\eta_{k+1}-\eta_{k})+\frac{\partial F_{i}(\xi_{k},\eta_{k},\zeta_{k})}{\partial \zeta}(\zeta_{k+1}-\zeta_{k})$$
 [66]

where i=1, 2, 3. Because ξ_{k+1} , η_{k+1} and ζ_{k+1} are expected to be the solutions of Equation [65], let $F_i(\xi_{k+1}, \eta_{k+1}, \zeta_{k+1}) = 0$. Equation [66] can be written in matrix form:

$$\begin{bmatrix} \mathbf{A} \end{bmatrix}_{\mathbf{k}} \begin{bmatrix} \boldsymbol{\xi}_{\mathbf{k}+1} - \boldsymbol{\xi}_{\mathbf{k}} \\ \boldsymbol{\eta}_{\mathbf{k}+1} - \boldsymbol{\eta}_{\mathbf{k}} \\ \boldsymbol{\zeta}_{\mathbf{k}+1} - \boldsymbol{\zeta}_{\mathbf{k}} \end{bmatrix} = - \begin{bmatrix} \mathbf{F}_{1} \\ \mathbf{F}_{2} \\ \mathbf{F}_{3} \end{bmatrix}_{\mathbf{k}}$$
 [67]

where the Jacobian matrix [A] is given by

$$[A]_{k} = \begin{bmatrix} \frac{\partial F_{1}}{\partial \xi} & \frac{\partial F_{1}}{\partial \eta} & \frac{\partial F_{1}}{\partial \zeta} \\ \frac{\partial F_{2}}{\partial \xi} & \frac{\partial F_{2}}{\partial \eta} & \frac{\partial F_{2}}{\partial \zeta} \\ \frac{\partial F_{3}}{\partial \xi} & \frac{\partial F_{3}}{\partial \eta} & \frac{\partial F_{3}}{\partial \zeta} \end{bmatrix}_{k}$$
[68]

The subscript k means that the related variables are evaluated in the kth iteration. Since values of ξ , η and ζ are between -1 and +1, the selection of zeros for ξ_o , η_o and ζ_o is reasonable.

3.3 Compilation of computer programs

The computer programs are designed mainly for establishing within the potato storage the pressure distributions, velocity distributions, streamlines or air flow path and flow rates. All the required information about the air flow patterns can be obtained from the analysis of these data. The computer programs were written in FORTRAN and run on the IBM Mainframe 3090 in the Computer Laboratory, Michigan State University.

3.3.1 Calculation of nodal pressure values

The program uses the procedures outlined in Section 3.2 to find the pressure distribution in three-dimensional space. The input data of the incidence matrices, including element number and nodal number, and nodal coordinates can be produced by automatic mesh generation programs (Ansys, Manual, 1987 and FIDAP Manual, 1989). The incidence matrices and nodal coordinates are different for different duct configurations, different duct spacings and different depths of the potato pile. The band width can be obtained from the information contained in the incidence matrices. During the process of calculation, K_0 was assigned a value of 1.0 at the first step, but was updated in the subsequent iteration steps. Detailed processes are shown in the flow chart in Figure 24. The output of this program was used as the main input data for the calculation of iso-pressure lines, velocity profiles, and streamlines and air flow rates in the selected cross-sections.

BEGIN

INPUT

of incidence matrices, nodal coordinates, band width, coeff. of A and B, and boundary conditions

INITIALIZATION

of nodal value vector {P}
and force vector {F}
with zero

CALCULATION

of matrix [B] and [B]^T,
Jacobian [J] and |det [J]|
normal pressure gradient $\partial P/\partial n$, and granular
permeability K_G
(K_G=1.0 at first step)

FORMATION

of element matrix [K^(e)] according to Equation [62] and Equation [63]

SUMMATION

of global matrix [K] by using direct stiffness method

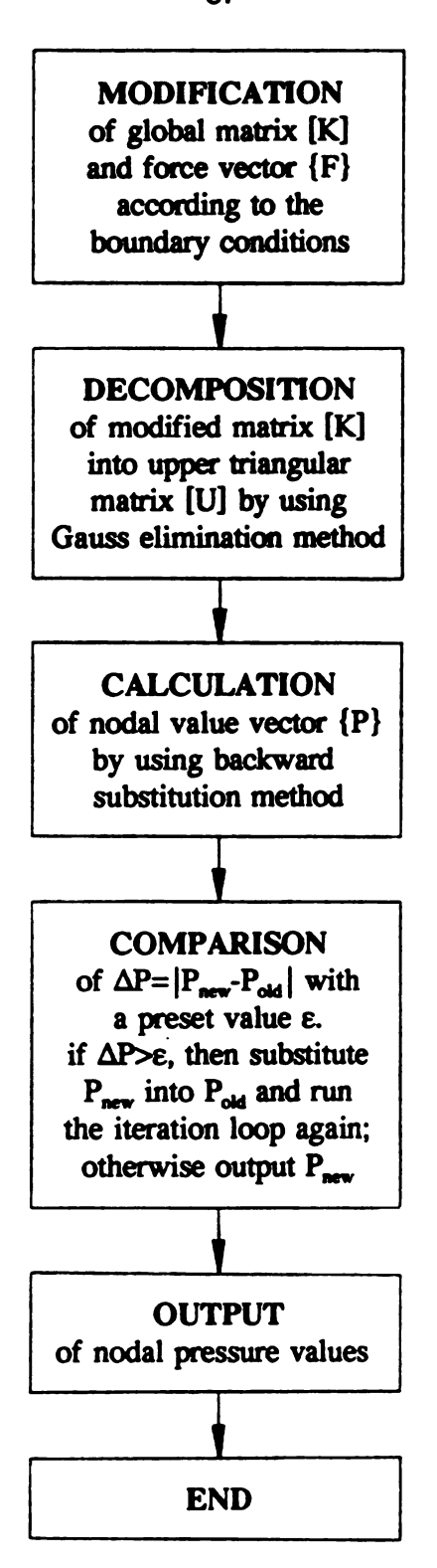
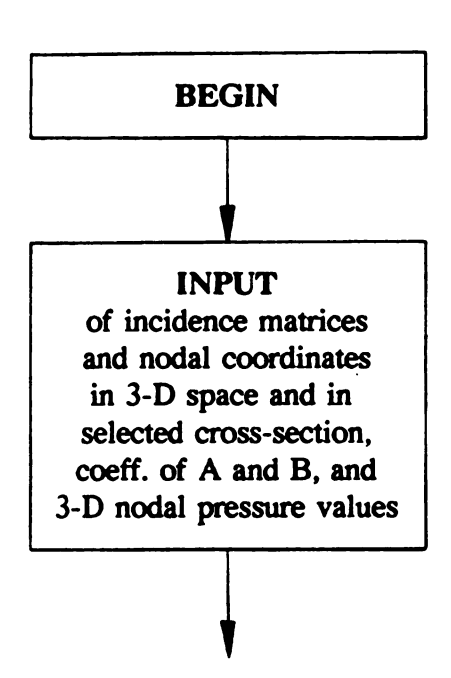


Figure 24. The flow chart of the computer program for the calculation of nodal pressure values in 3-D space

3.3.2 Calculation of pressure and velocity for the selected cross-section

The main purpose of this program is to calculate the pressure distribution and velocity profile for selected cross-sections which are perpendicular to the center line of the lateral duct. The input data are 3-D nodal pressure values, the incidence matrices and nodal coordinates in 3-D space and in the 2-D cross-section, and the coefficients A and B. The transformation of the coordinate systems plays an important role in the investigation of the pressure and velocity variations in the selected cross-section. The output of this program will be used for plotting pressure contour lines and velocity profiles. For the continuity of the whole procedure, the plotting process was included as a part of this program. The flow diagram is shown in Figure 25.



DETERMINATION of the element number in 3-D space in which the node of the selected cross-section is located, and the nodal coordinates and the nodal pressure values related to this element **TRANSFORMATION** of Cartesian coord. into natural coord. for the node in the selected cross-section by Newton-Raphson method **CALCULATION** of the nodal pressure values and normal velocity and its components for the node in the selected cross-section **OUTPUT** of the calculated pressure and velocity values **PLOT** the pressure contour lines and the velocity profiles for the selected cross-section **END**

Figure 25. The flow chart of the computer program for the calculation of pressure and velocity in 2-D space

3.3.3 Calculation of streamlines and flow rate for the selected cross-section

Streamlines for the selected cross-section can be determined through its definitions or through its properties. The calculation of flow rate is based on the fact that the flow rate will remain constant between two streamlines. This program also needs the incidence matrices and nodal pressure values in 3-D space as its input data. The output of this program will be used to draw streamlines in two-dimensional space, to obtain regression equations for the streamlines, and to calculate the flow rates. The flow chart of this program is shown in Figure 26.

BEGIN

INPUT

of incidence matrices and nodal coordinates in 3-D space, coeff. A and B, and 3-D nodal pressure values

SELECTION

of any point on the top free surface or in the duct opening of the selected cross-section to start the process for determining the streamline

DETERMINATION

of the element number in 3-D space in which the node of the selected cross-section is located, and the nodal coordinates and nodal pressure values related to this element

TRANSFORMATION

of Cartesian coord. into natural coord. for the node in the selected cross-section by Newton-Raphson method

CALCULATION

of normal velocity and its components for the node in the selected cross-section

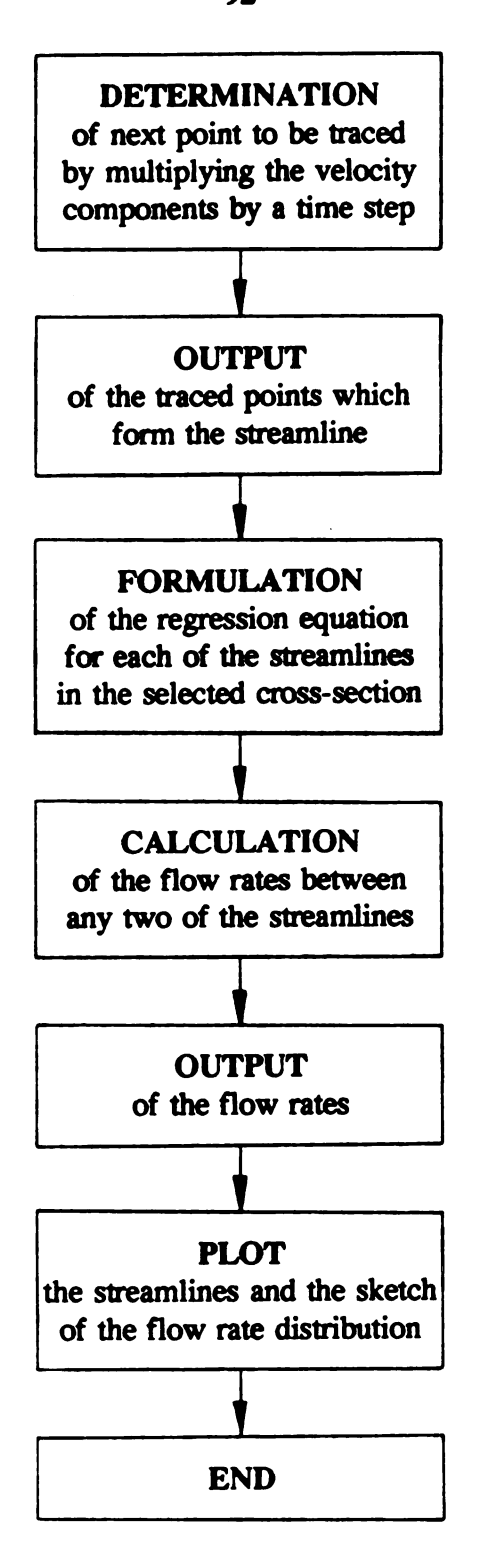


Figure 26. The flow chart of the computer program for the calculation of streamline and flow rate in 2-D space

CHAPTER 4

ANALYSIS OF AIR FLOW PATTERNS

4.1 Preparation of basic data

To run the computer programs, the variables affecting air flow patterns and their levels were decided, the parameters, such as the dimension and configuration of duct system and potato storage, the properties of air and the characteristics of potato tubers, were prepared, and the mesh schemes were generated.

Under present study, it was assumed that the air flow was inviscid, the air temperature was 10° C and the relative humidity was 95 %.

4.1.1 Basic data of duct system and potato storage

The basic data for a duct system and potato storage were as follows.

Storage dimension: $L \times W \times H = 19.5 \text{ m} \times 9.1 \text{ m} \times 5.3 \text{ m}$

Specific gravity of potato: $g = 641.3 \text{ kg/m}^3$

Storage capacity: $C_1 = L \times W \times H_P \times g/1,000 = 489.0$ metric ton

Requirement of air flow rate per metric ton: $q = 0.94 \text{ m}^3/\text{min}/(\text{metric ton})$

Total air flow rate required: $Q = C_1 \times q = 460.0 \text{ m}^3$

Air flow velocity in the main plenum: $V_p = 198.0 \text{ m/min}$

Cross-sectional area of the main plenum: $A_p = Q/V_p = 2.3 \text{ m}^2$

Air flow velocity in the lateral duct: $V_1 = 259.0 \text{ m/min}$

Air flow velocity exiting duct: $V_e = 305.0$ m/min

4.1.2 Selection of variables and their levels

To evaluate the effects on the pressure and velocity distributions of the variables, such as duct size, duct spacing, lateral duct pressure, depth of potato pile, and the distance from a selected cross-section to the duct entrance, three levels for each of the variables and four duct shapes (triangular duct, circular duct, semicircular duct and rectangular duct) were selected as listed in Table 6.

Table 6. Selected variables and their levels as used in the computer programs

Variables	Level 1	Level 2	Level 3
Lateral duct pressure P _d (Pa)	125	250	375
Duct spacing L _d (m)	1.8	2.4	3.1
Depth of potato pile H_P (m)	3.1	4.3	5.5
Triangular duct size $h_t \times a_t (m \times m)$	0.59 × 0.34	0.64 × 0.36	0.67 × 0.39
Circular duct size d _e (m)	0.51	0.54	0.58
Semicircular duct r _s (m)	0.36	0.38	0.41
Rectangular duct size $a_r \times b_r (m \times m)$	0.32 × 0.32	0.34 × 0.34	0.36 × 0.36
Distance from selected cross-section to duct entrance (m)	2.0	6.0	10.0

4.1.3 Coefficients in Shedd's equation

The granular permeability K_0 is a function of coefficients A and B, which can only be determined experimentally. Staley and Watson (1961) reported A = 345 and B = 0.562 in English units for a range of pressure gradients (0.001 - 0.02 inch water/ft) and air flow velocities (6.0 - 50 ft³/min/ft²). Because the regression line of the experimental data in the log-log scale is usually not a straight line, A and B values are not constant in a wide range of pressure gradients. Therefore, it is reasonable to use several segments of straight line instead of one single straight line to approach the test data as suggested by Segerlind (1983).

To obtain coefficients A and B for a potato storage, Equation [15] and values of a and b in ASAE Data Standard D272.2 (ASAE Standard, 1988) were first used to calculate the pressure gradient for a given air flow. Then, using a nonlinear regression method, various values of A and B (Table 7) were produced for the corresponding range of velocity and pressure gradient according to Equation [13].

Table 7. Coefficients A and B of Equation [13] for air flow through potato storage.

Range of air flow (m ³ /s/m ²)	Range of pressure gradient (Pa/m)	Coefficient of A	Coefficient of B
>0.05 - 0.10	>1.5 - 5.0	0.0404	0.568
>0.10 - 0.20	>5.0 - 17.0	0.0411	0.558
>0.20 - 0.50	>17.0 - 90.0	0.0422	0.549
>0.50 - 1.00	>90.0 - 324.0	0.0435	0.542
>1.00 - 2.00	>324.0 - 1165.0	0.0446	0.538

4.1.4 Defining boundary conditions

A sketch of the boundary conditions for a potato storage with triangular ducts is shown in Figure 27. Boundary conditions of the first type, Dirichlet conditions, are defined at the nodes on the surface of GHIJ with P = 0, and on a part of surface of ABCD with $P = P_d$. Boundary conditions of the second type, Neumann conditions, are defined at the nodes on the solid boundaries, AEHGB and DFIJC, on the symmetric boundaries, BGJC and EHIF, and on a part of surface of ABCD with $\partial P/\partial n = 0$.

The boundary conditions for potato storage with circular ducts, semicircular ducts or in-floor rectangular ducts are similar to those with triangular ducts. The locations of the boundary nodes with $P = P_d$ for the above four duct shapes are also shown in Figure 27.

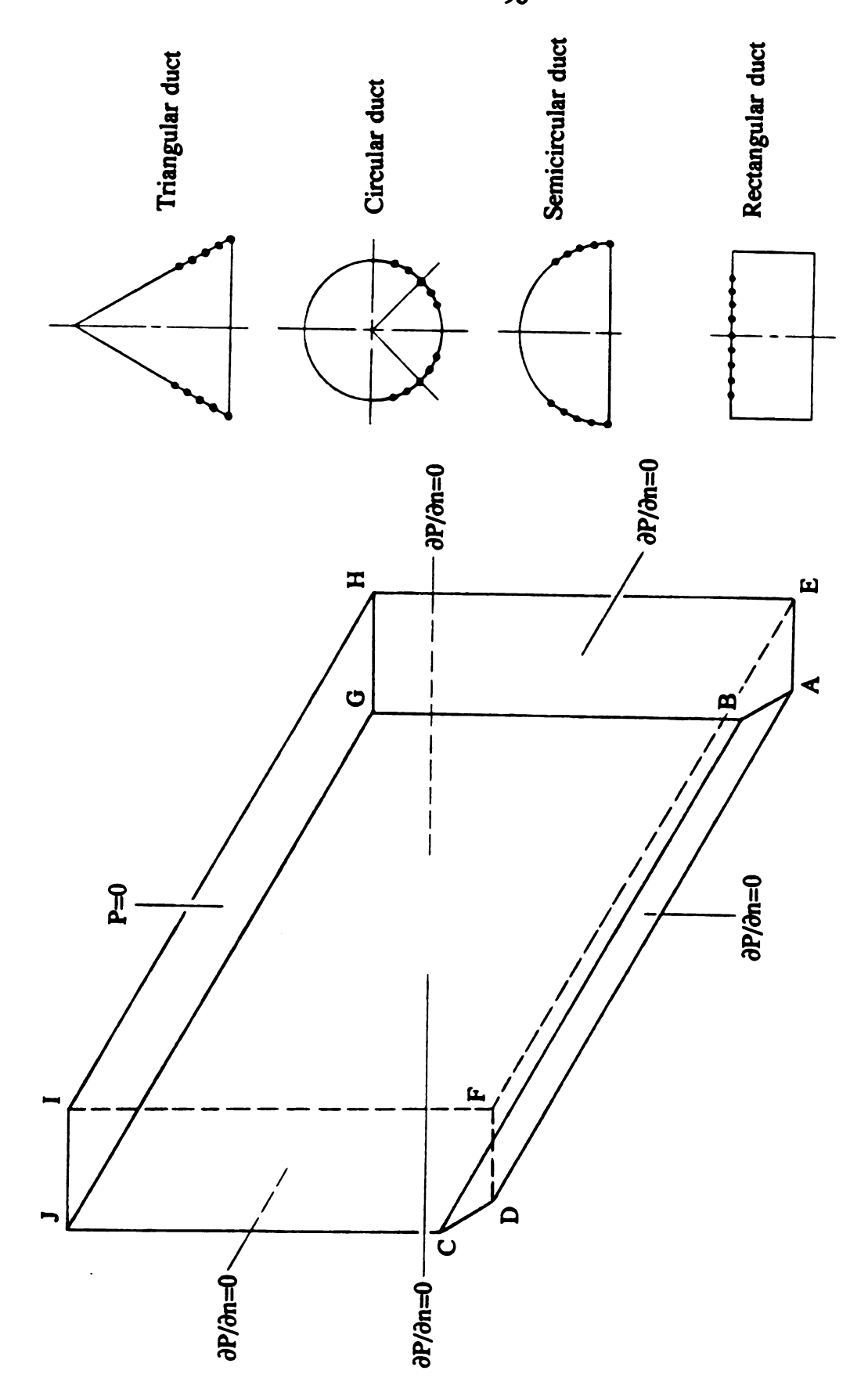


Figure 27. Sketch of boundary conditions for potato storage

4.1.5 Calculation of duct pressures

When air flows through a duct system, the pressure and velocity will change along the longitudinal dimension of the duct. The magnitude of the change depends on the cross-sectional area of duct, duct shape, roughness of duct interior surface, size and location of the duct openings, and the flow rate delivered by the duct.

The pressure and the velocity changes for a duct can be obtained from the Bernoulli equation (Sabersky et al. 1989):

$$\frac{V_2^2}{2g} + \frac{P_2}{\rho g} + y_2 = \frac{V_1^2}{2g} + \frac{P_1}{\rho g} + y_1 + M - h_f$$
 [69]

where variables upstream and downstream are assigned by subscript 1 and 2, respectively. Each term in Equation [69] represents the energy per unit weight and has the dimension of length. The elevation heads, y_1 and y_2 , are measured at the center lines of the duct upstream and downstream, respectively. In the present problem they are equal. The function of pump work, M, is to increase the total head of the flow. While the friction loss, h_f , is usually obtained from the friction factor:

$$f = \frac{h_f}{\left[\frac{1}{d}\right] \left[\frac{V^2}{2g}\right]}$$
 [70]

which is a function of Reynolds number and the relative roughness ratio, ε_s/d , of the duct. The Reynolds number is defined as:

$$Re_{D} = \frac{\rho V_{m} d}{\mu}$$
 [71]

where V_m is the mean fluid velocity over the duct cross-section. Incropera and DeWitt, (1985) and Sabersky et al. (1989) cited the Moody diagram, as shown in Figure 28, to find friction factors for a wide range of Reynolds numbers.

For fully developed laminar flow, the friction factor also can be calculated from the following formula (Incropera and Dewitt, 1985):

$$f = \frac{64}{Re_{D}}$$
 [72]

The Moody diagram (Figure 28) is designed for round ducts only. For noncircular ducts, such as triangular ducts, rectangular ducts and semicircular ducts, the friction factor also can be estimated from the Moody diagram by assigning the hydraulic diameter D_h instead of d in the calculation of Reynolds number with

$$D_{h} = \frac{4A_{c}}{P_{m}}$$
 [73]

where A_c and P_w are the flow cross-sectional area and the wetted perimeter, respectively (Incropera and DeWitt, 1985, and Sabersky et al. 1989).

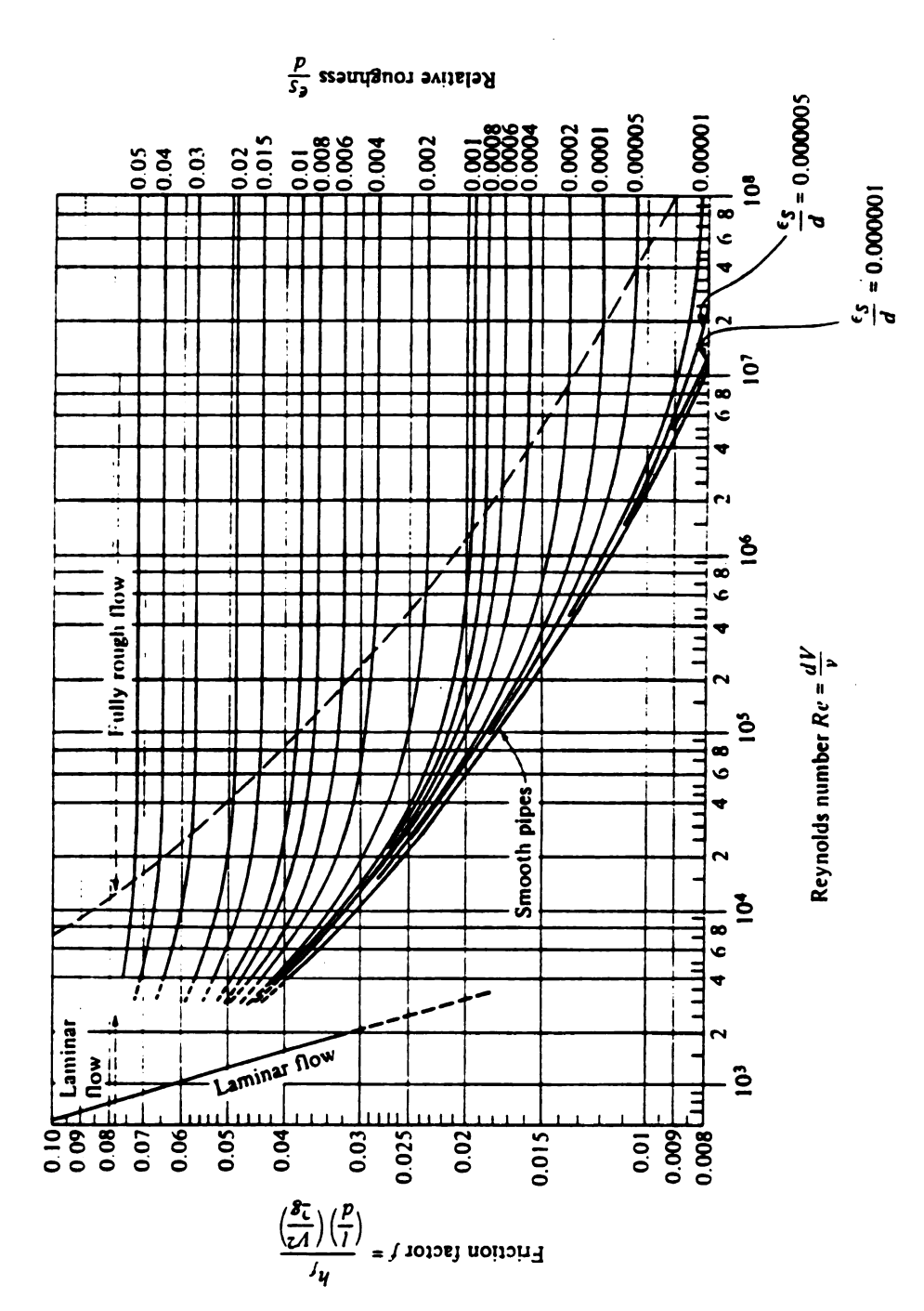


Figure 28. Friction coefficient as a function of Reynolds number for round pipes of various relative roughness ratio e_/d.

Source: Sabersky et al. 1989

4.1.6 Mesh generation

Mesh generation is a major step in using the finite element method to discretize twodimensional and three-dimensional domains. The accuracy and the cost of the solution processes of the finite element method depend largely on the mesh scheme employed. As mentioned above, a solid element with 20 nodes has been chosen for the threedimensional problem. For the regions where the pressure or velocity may be expected to change dramatically, smaller elements should be used, otherwise larger elements were used.

The generation of elements and nodes, if done by hand, is time consuming. There are automatic mesh generation programs (Segerlind, 1984) and some commercial software packages available to generate two- and three-dimensional elements and nodes (ANSYS Manual, 1987 and FIDAP Manual, 1989). The meshes generated by using FIDAP for a potato storage are shown in the Figure 29, 30, 31 and 32 for triangular duct, circular duct, semicircular duct and in-floor rectangular duct, respectively.

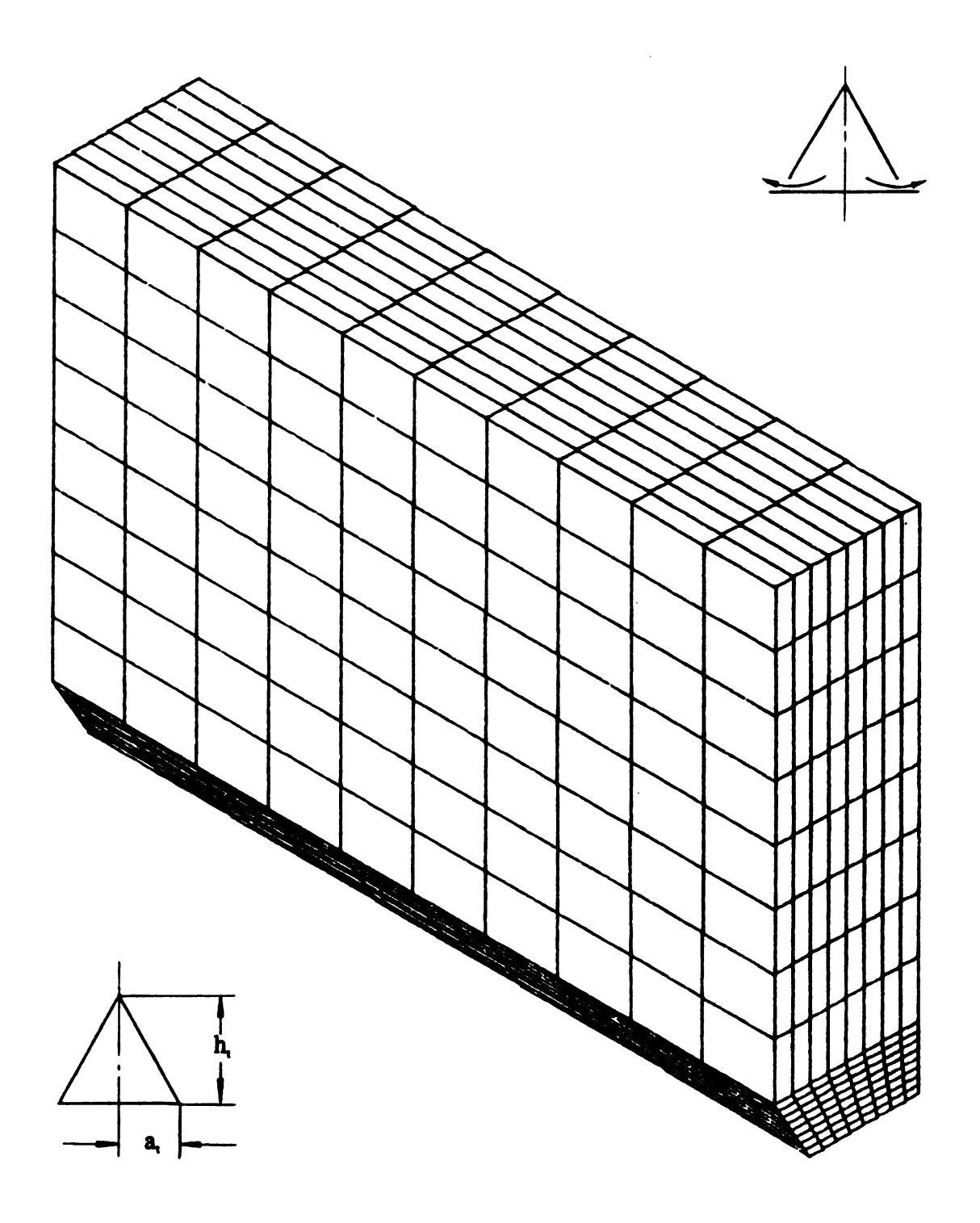


Figure 29. Mesh generation for potato storage with triangular duct

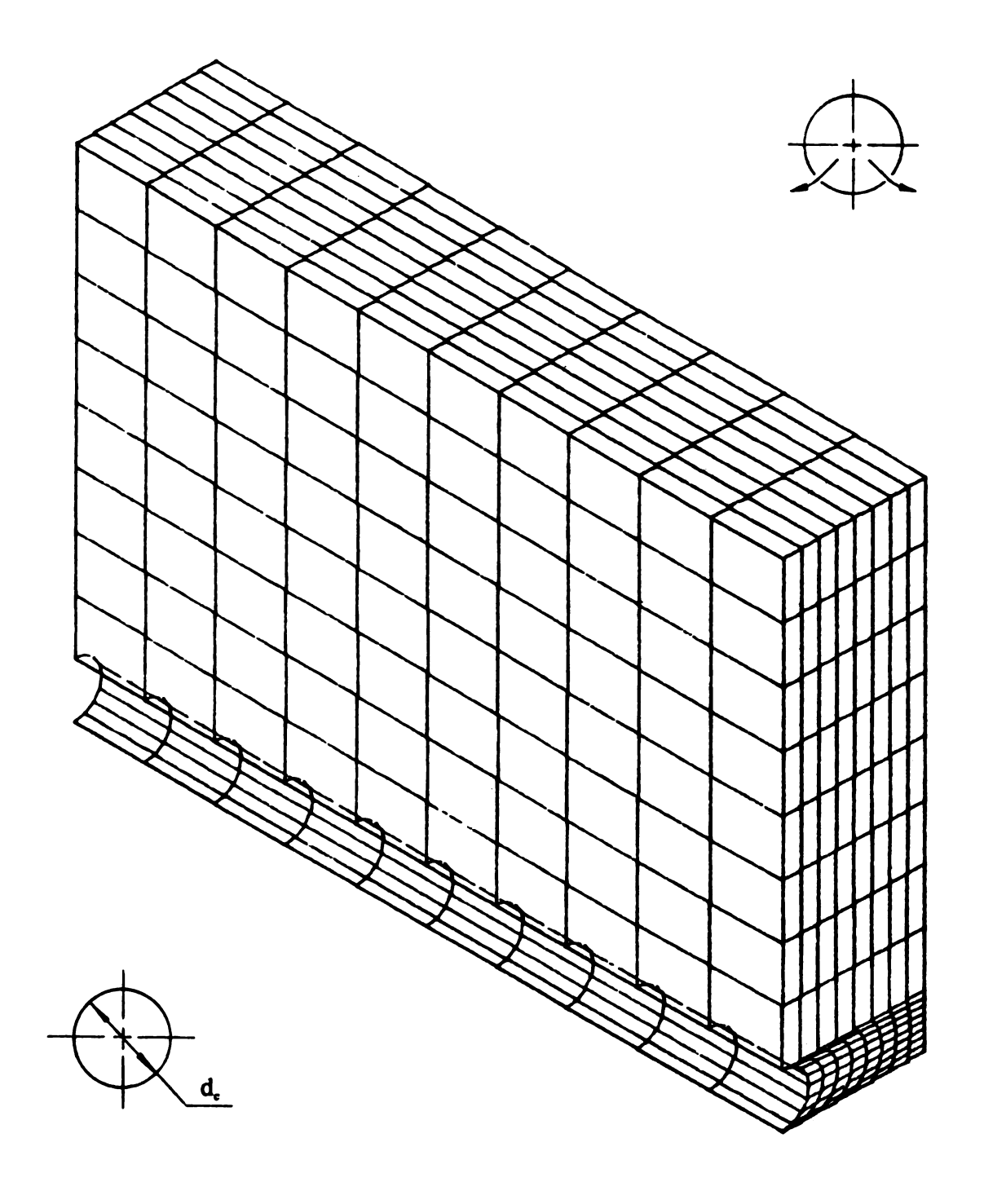


Figure 30. Mesh generation for potato storage with circular duct

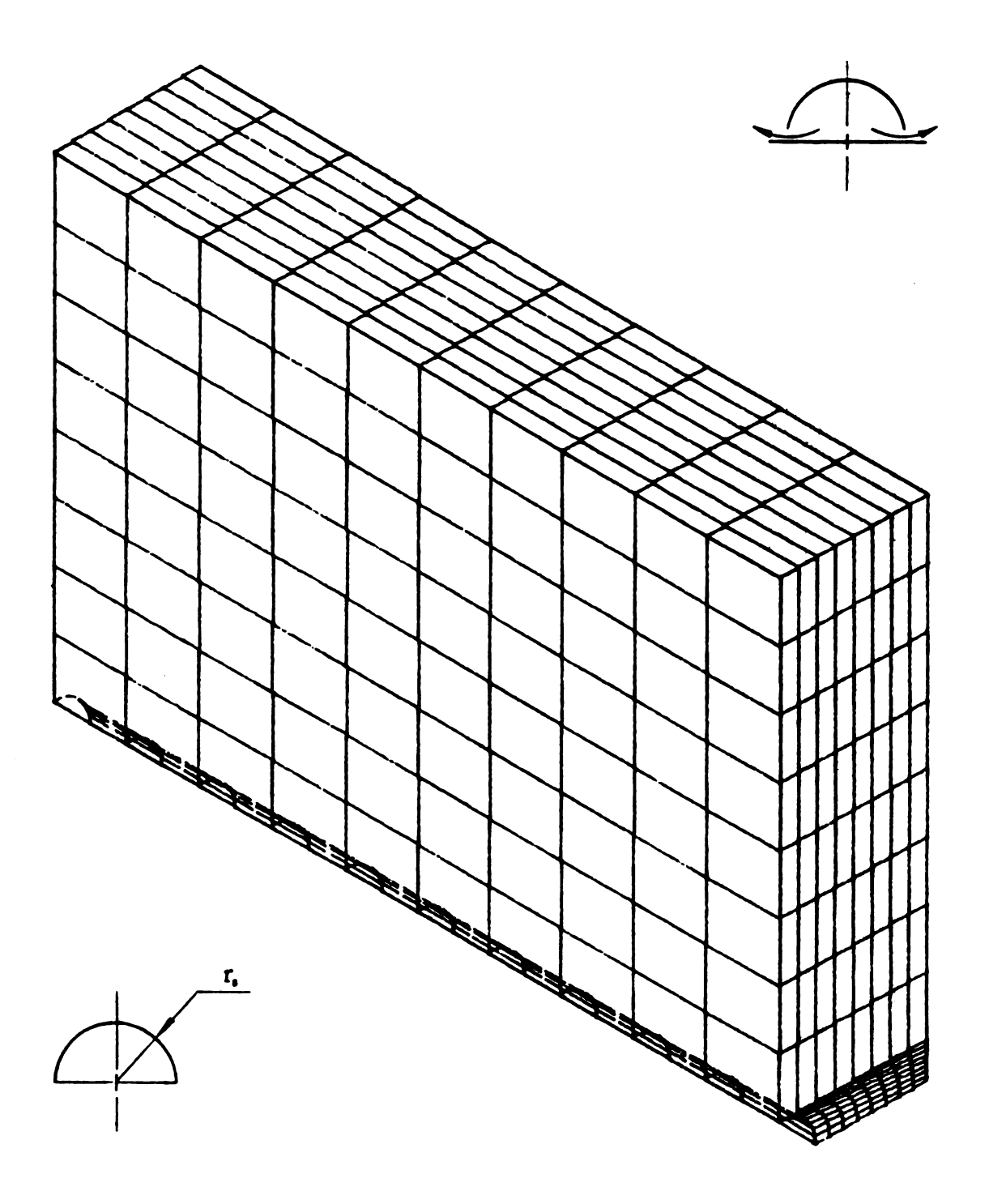


Figure 31. Mesh generation for potato storage with semicircular duct

4.2 The effect on air flow patterns of variables under study

In the present study, it was found that for any selected cross-section, which is perpendicular to the center line of the lateral duct, the streamlines are parallel and the air flow is uniform in the upper region of the potato pile when the depth of the potato pile is equal to or greater than the spacing between two adjacent ducts, i.e. $H_P \geq L_d$. Nonlinear air flow usually dominates in the lower region of the potato storage where the effects of the variables under study become very distinct. Therefore, analysis of air flow patterns for the lower part of potato storage appears more attractive than that for the upper part. In the following sections, all air flow patterns are shown only for the region that is under the depth of 2.1 m for the selected cross-section, and because of the symmetry, only half of the cross-section are displayed.

It was also noted that in the lower part of the potato storage, the areas near the floor and in the middle between two adjacent ducts are usually ventilated poorly. To highlight these areas, they were defined by a streamline, the symmetric line and the floor, and were shaded. Generally, in any given cross-section a lot of air streamlines can be drawn. But for the purpose of clarity and ease of comparison, the streamlines were chosen to be 0.24 m apart starting from the symmetric line at the top free surface of the potato pile and were progressing from the top free surface to the lateral duct. Since the velocity in the vicinity of the duct opening is larger than in other parts of the potato pile, the time step was set in a decreasing pattern to produce an accurate streamline.

In all Figures contained in section 4.2, the iso-pressure lines were represented by the percentage duct pressure and the velocity profiles were symbolized by their magnitude

in m/min. The volumetric air flow rate (L^3t^{-1}), the air flow rate per metric ton of potatoes ($L^3t^{-1}M^{-1}$) or mass air flow rate (Mt^{-1}) usually refers to air flow rate in a three-dimensional space. While in a two-dimensional space the air flow rate per unit thickness (L^2t^{-1}) was used.

4.2.1 The effect of duct spacing on air flow patterns

To compare the effect of different duct spacings on air flow patterns, three duct spacings of 1.8 m, 2.4 m and 3.1 m were chosen. The related data and Figure numbers are listed in Table 8. Other variables and their levels were as follows: the duct pressure was 125 Pa, the depth of the potato pile was 4.3 m, and the dimension for the triangular duct was $h_t \times a_t = 0.59$ m $\times 0.34$ m, for the circular duct was $d_c = 0.51$ m, for the semicircular duct was $r_s = 0.36$ m and for the in-floor rectangular duct was $a_t \times b_t = 0.32$ m $\times 0.32$ m.

The iso-pressure lines and streamlines for the triangular duct with duct spacings of 1.8 m, 2.4 m and 3.1 m are shown in Figures 33, 34 and 35, respectively. It is very clear from these Figures that there is a larger space between two iso-pressure lines in the lower right region than in the other parts of the cross-section. This means that the lower right region has a lower pressure gradient than in the other parts whether the duct spacing is large or small. In the region directly above the duct, the pressure distributions were fairly uniform for all three duct spacings. Comparing Figures 33, 34 and 35, it appears that the pressure value in the lower right region for Figure 33 is larger than in Figure 34, which in turn is larger than in Figure 35.

In the present study the flow is assumed to be steady state. Thus the air flow path will follow the streamline exactly. From Figures 33, 34 and 35 it can be observed that the streamlines in the lower region of potato pile are not parallel, so the air flow is nonlinear. The path line directly above the duct is the shortest, while the path line near the symmetric line between two adjacent ducts is the longest. As a result of the unequal air flow path, it will take longer for the ventilation to bring the entire potato pile to the same temperature. It can also be seen that the streamline forming the shaded area in Figure 33 is shorter than in Figure 34, which in turn is shorter than in Figure 35. This shows that the air flow condition is dependent on the duct spacing. Potato storages with smaller duct spacing have more uniform air distribution than those with larger duct spacing.

Suppose the air flow rates per metric ton of potatoes are the same for these three duct spacings, and consider the fact that in the two-dimensional domain the air flow rates in the area between two streamlines are constant, then the air flow per unit thickness in the shaded area can be obtained. The shaded area in Figures 33, 34 and 35 accounts for 32.4%, 27.0% and 24.2% of the total cross-sectional area, but only receive 26.7%, 20% and 16 % of the total flow rate per unit thickness, respectively. This indicates that the air ventilation is uneven through the selected cross-section with the shaded area poorly ventilated.

The velocity profiles corresponding to the three different duct spacings are also shown in Figures 33, 34 and 35, respectively. They closely follow the relevant pressure distribution patterns. The velocities in the upper region of the cross-section are very uniform, while those in the region near the lower right corners are the lowest.

Theoretically, these corners are the stagnant points where there is no air movement at all because of the zero velocity. Decreasing the duct spacing is favorable for improving the aeration situation in the lower right part, which can be seen by comparing velocity profiles in Figures 33, 34 and 35.

The discussion above is for triangular ducts. A similar tendency was observed for circular, semicircular and in-floor rectangular ducts with the three duct spacings. The isopressure lines, streamlines and velocity profiles for these ducts are plotted in Figures 36, 37 and 38 for circular ducts, in Figures 39, 40 and 41 for semicircular ducts, and in Figures 42, 43 and 44 for in-floor rectangular ducts. The percentage shaded area over the total cross-sectional area and the percentage air flow rate per unit thickness of the shaded area for these three duct shapes with three duct spacings have been given in Table 8.

Table 8. The effect of duct spacing on air flow patterns: related data and Figure numbers

			_	
Duct shapes	Duct spacing (m)	Shaded area over total area (%)	Flow rate for shaded area (%)	Figure No. referring to iso-pressure lines, streamlines and velocity profiles
Triangular duct	1.8	32.4	26.7	Fig. 33
Triangular duct	2.4	27.0	20.0	Fig. 34
Triangular duct	3.1	24.2	16.0	Fig. 35
Circular duct	1.8	33.1	26.7	Fig. 36
Circular duct	2.4	27.0	20.0	Fig. 37
Circular duct	3.1	24.0	16.0	Fig. 38
Semicircular duct	1.8	33.3	26.7	Fig. 39
Semicircular duct	2.4	27.0	20.0	Fig. 40
Semicircular duct	3.1	24.0	16.0	Fig. 41
Rectangular duct	1.8	31.5	26.7	Fig. 42
Rectangular duct	2.4	27.0	20.0	Fig. 43
Rectangular duct	3.1	24.3	16.0	Fig. 44

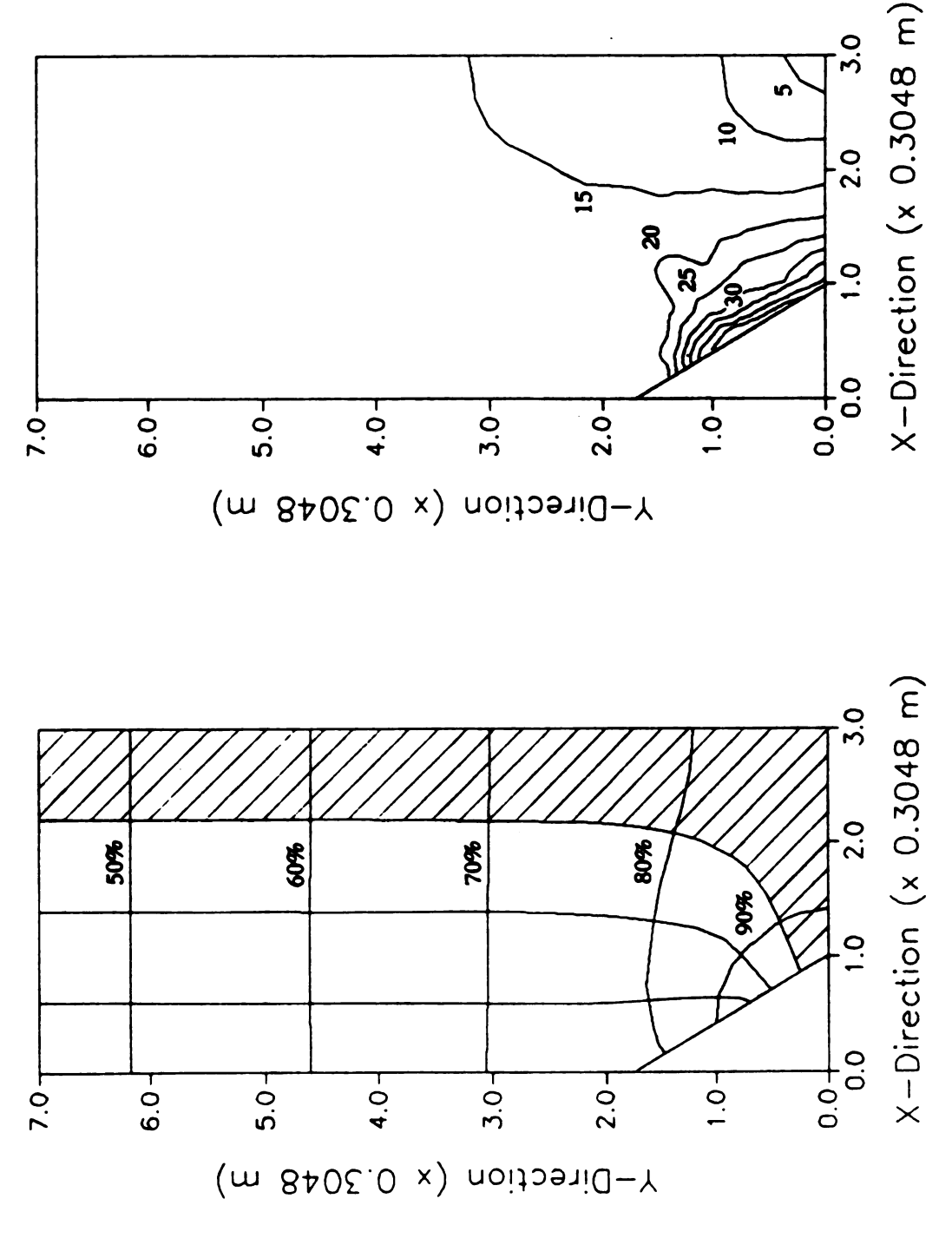
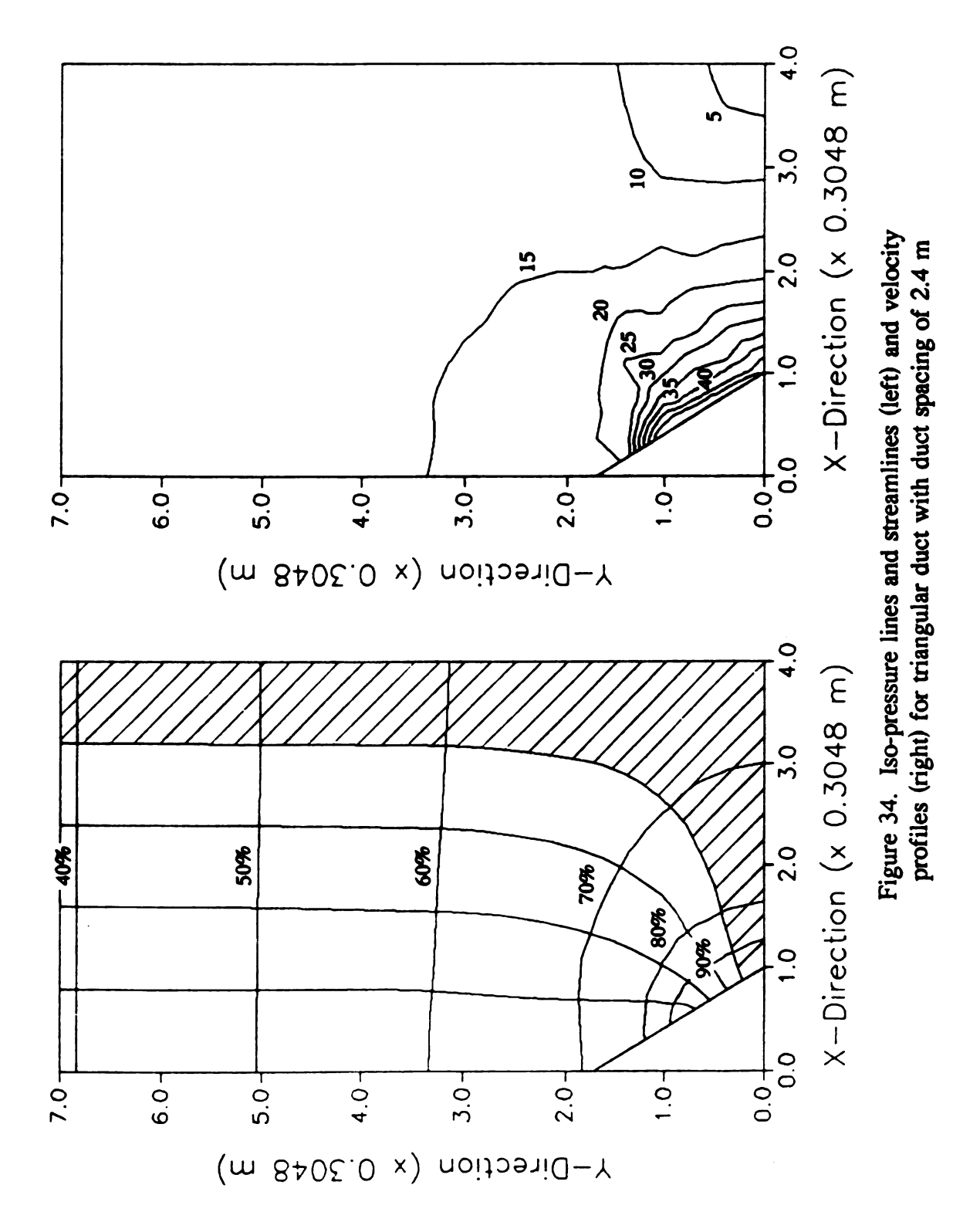


Figure 33. Iso-pressure lines and streamlines (left) and velocity profiles (right) for triangular duct with duct spacing of 1.8 m



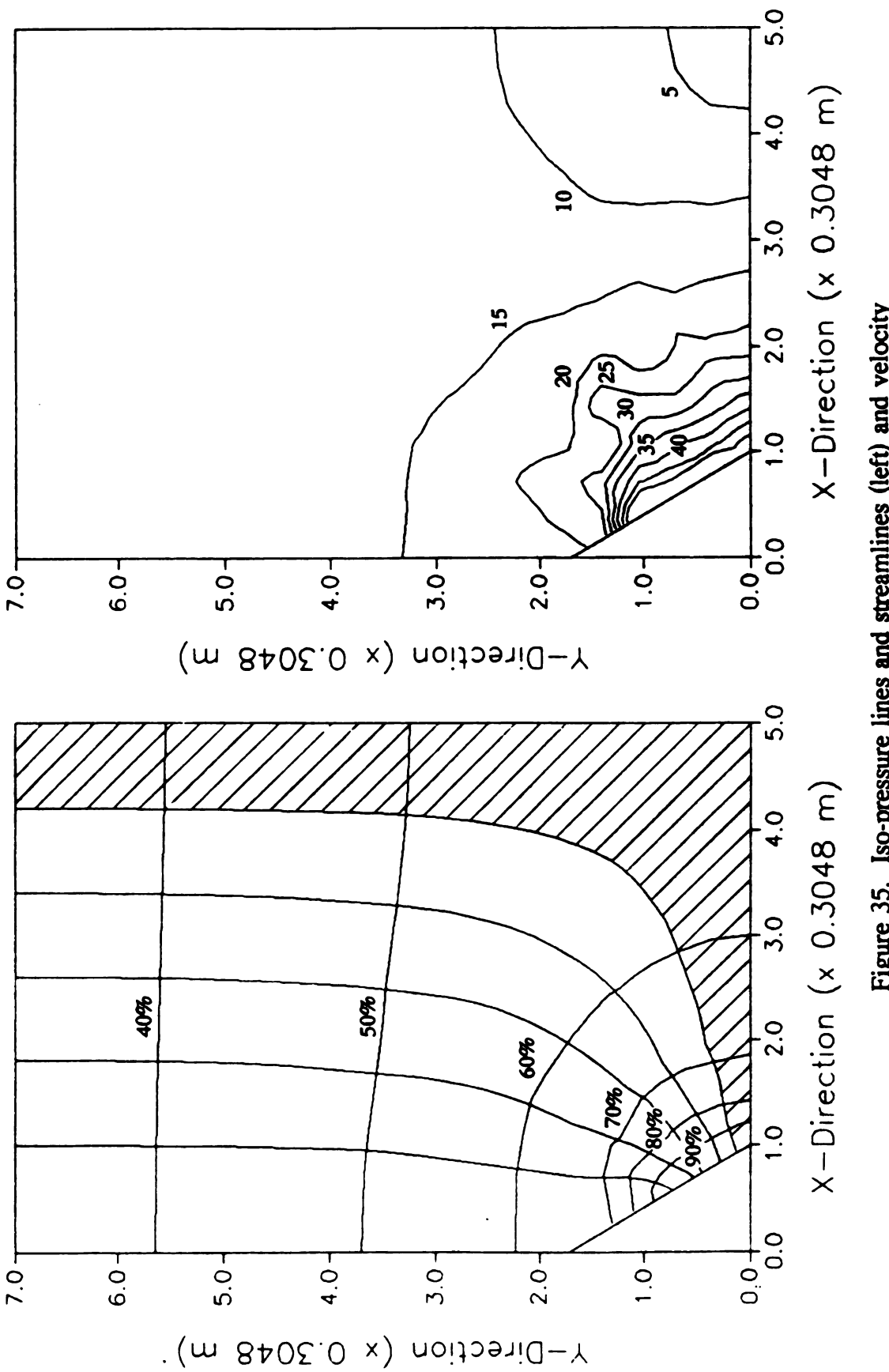
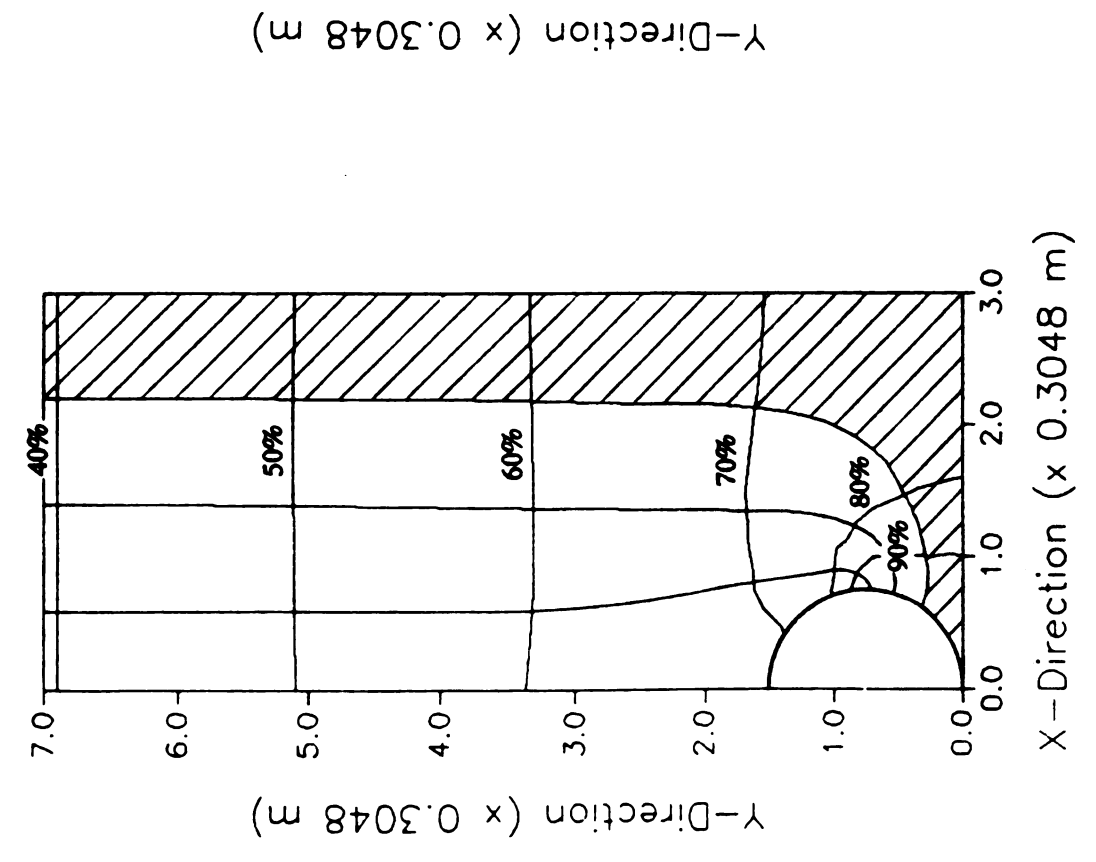


Figure 35. Iso-pressure lines and streamlines (left) and velocity profiles (right) for triangular duct with duct spacing of 3.1 m



3.0-

2.0-

7.07

6.0-

5.0-

4.0-

Figure 36. Iso-pressure lines and streamlines (left) and velocity profiles (right) for circular duct with duct spacing of 1.8 m

X-Direction (x 0.3048 m)

2.0

0.0+0.0

1.0-

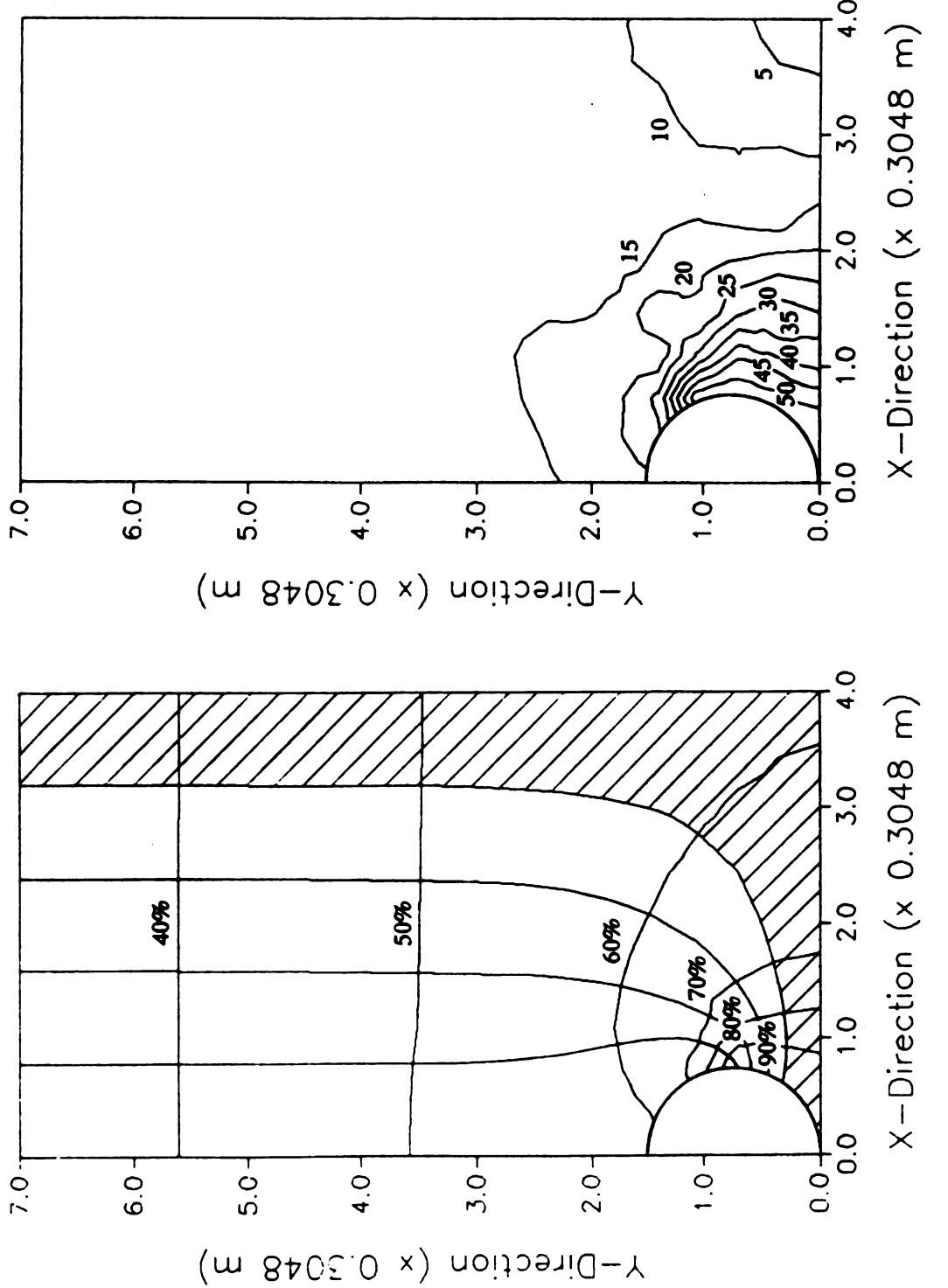


Figure 37. Iso-pressure lines and streamlines (left) and velocity profiles (right) for circular duct with duct spacing of 2.4 m

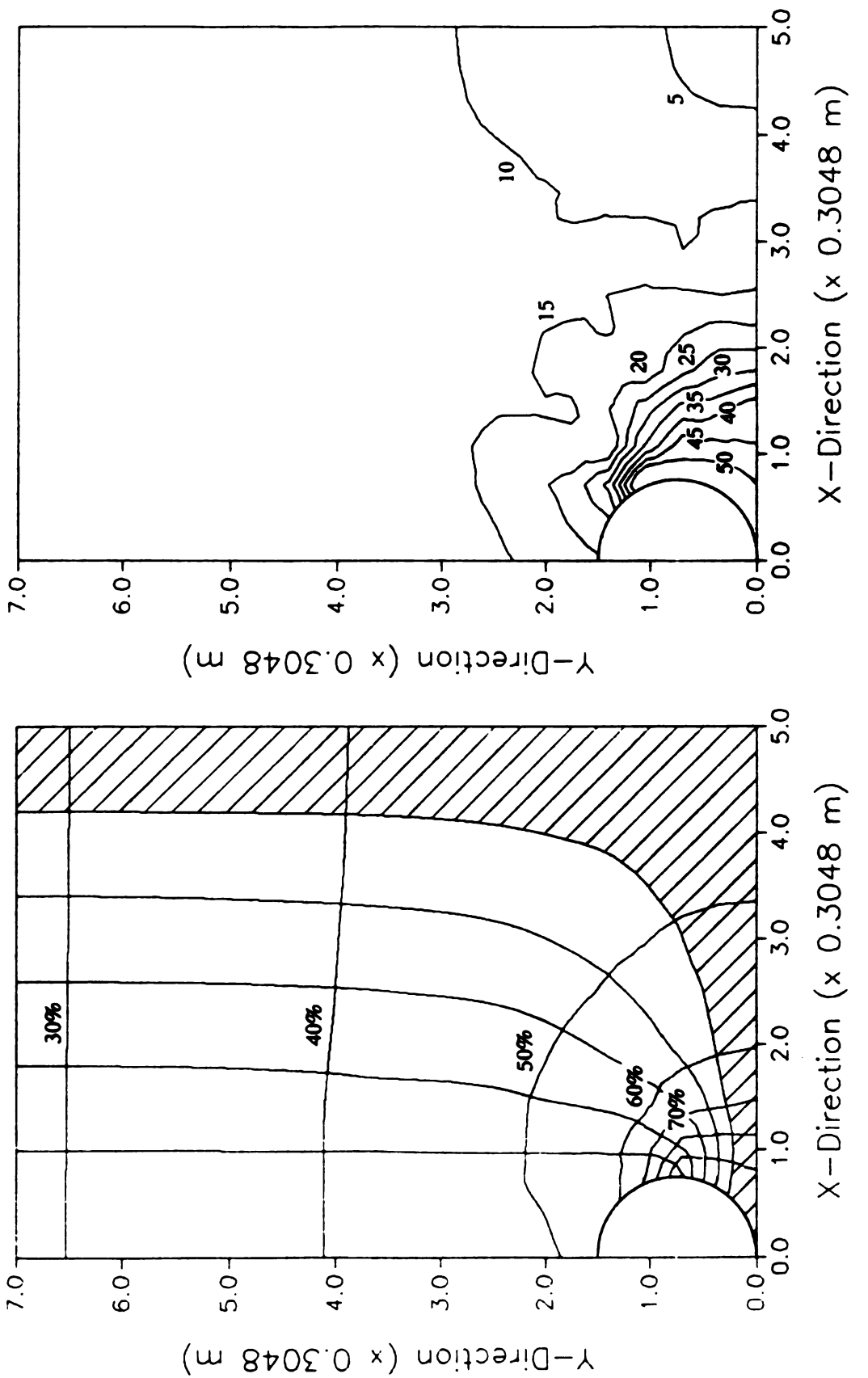


Figure 38. Iso-pressure lines and streamlines (left) and velocity profiles (right) for circular duct with duct spacing of 3.1 m

8

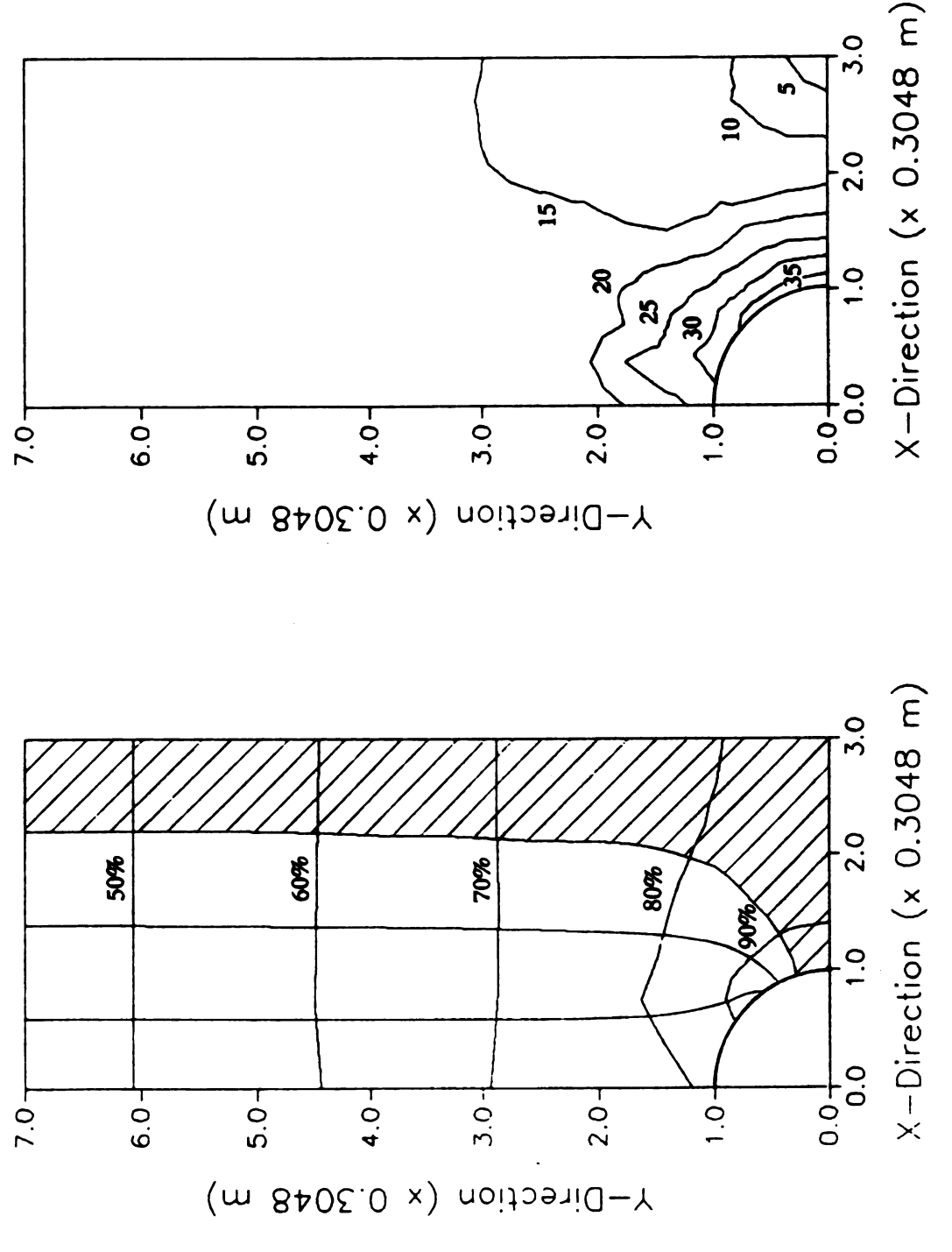


Figure 39. Iso-pressure lines and streamlines (left) and velocity profiles (right) for semicircular duct with duct spacing of 1.8 m

2.0

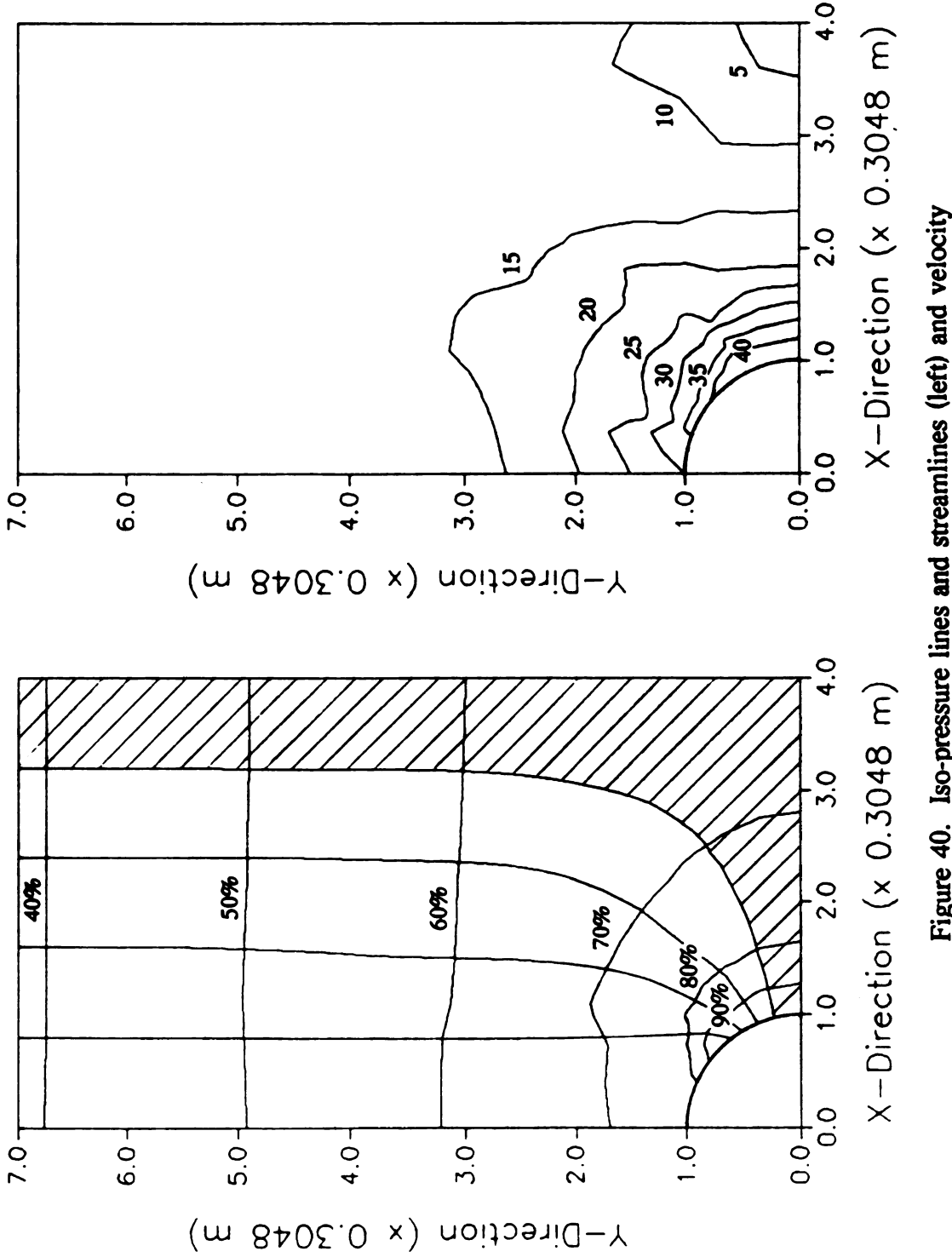


Figure 40. Iso-pressure lines and streamlines (left) and velocity profiles (right) for semicircular duct with duct spacing of 2.4 m

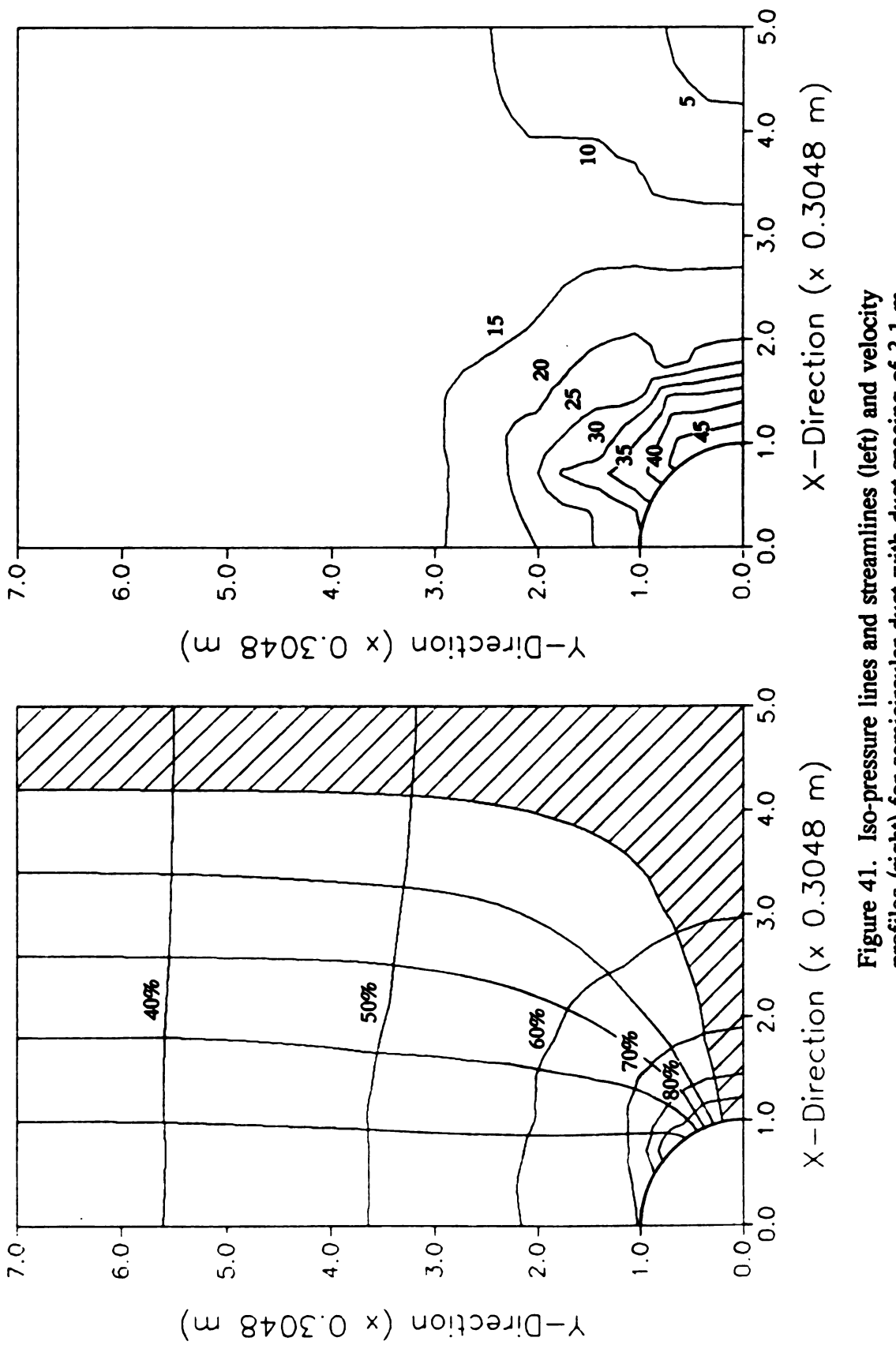


Figure 41. Iso-pressure lines and streamlines (left) and velocity profiles (right) for semicircular duct with duct spacing of 3.1 m

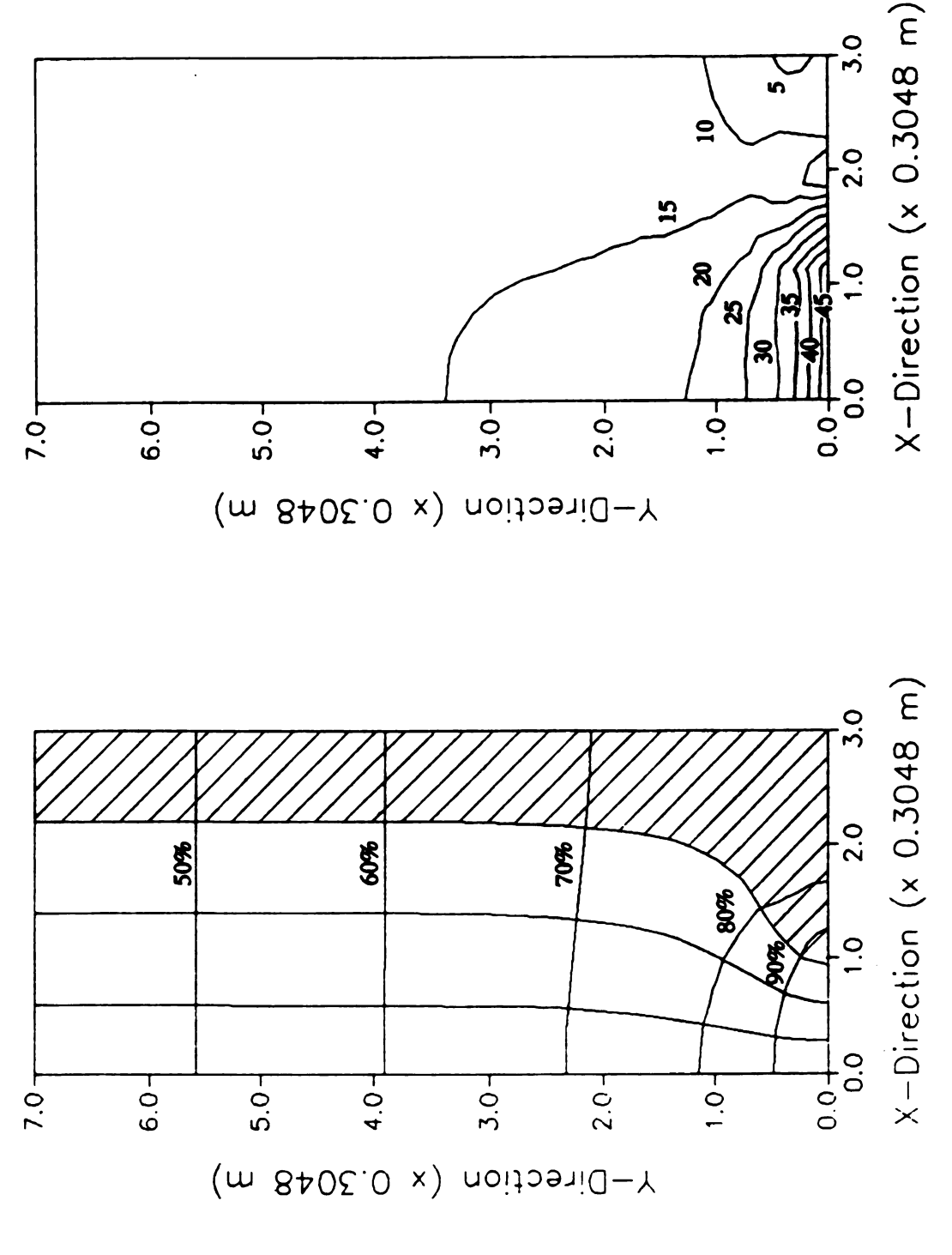


Figure 42. Iso-pressure lines and streamlines (left) and velocity profiles (right) for rectangular duct with duct spacing of 1.8 m

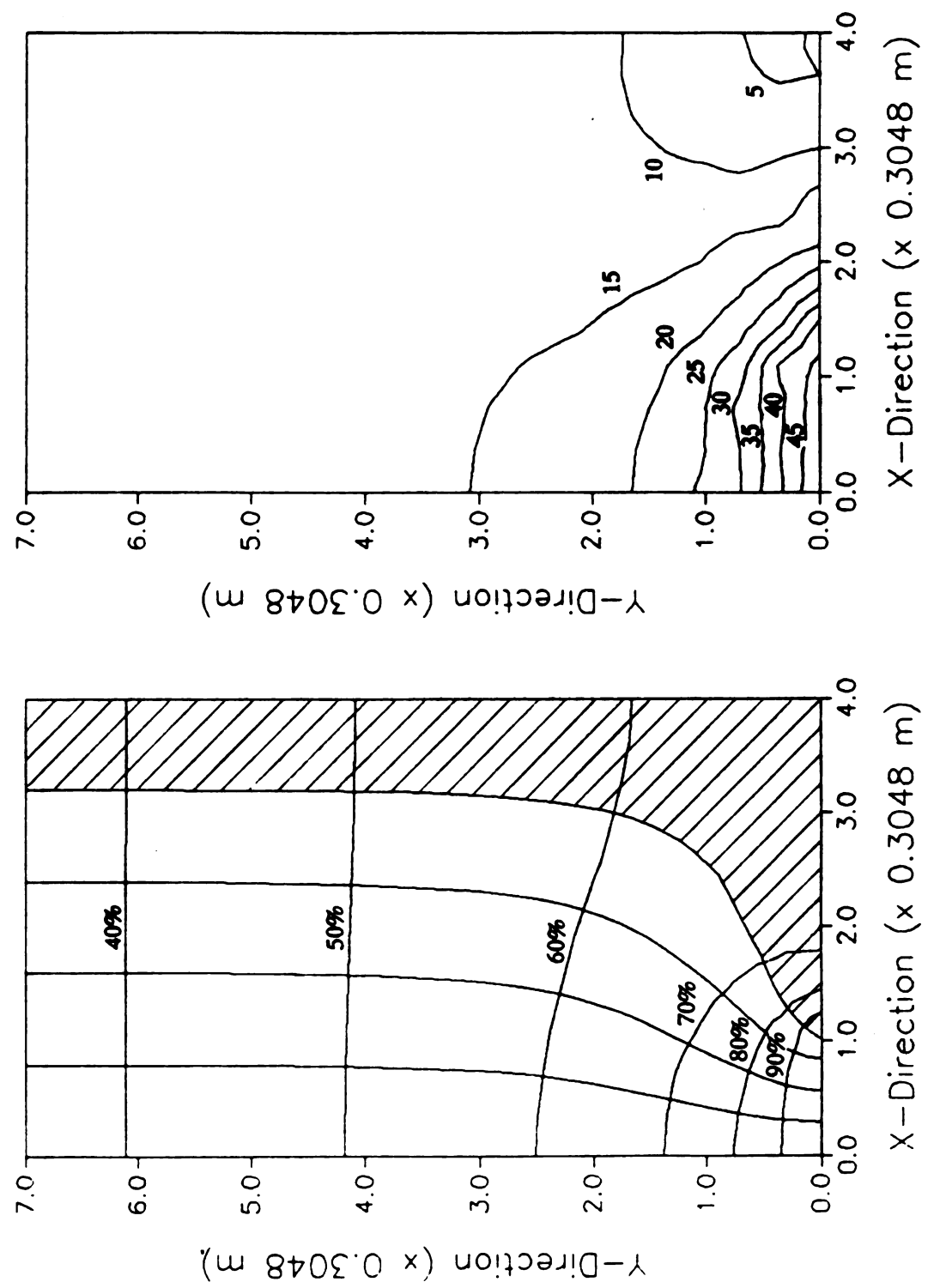
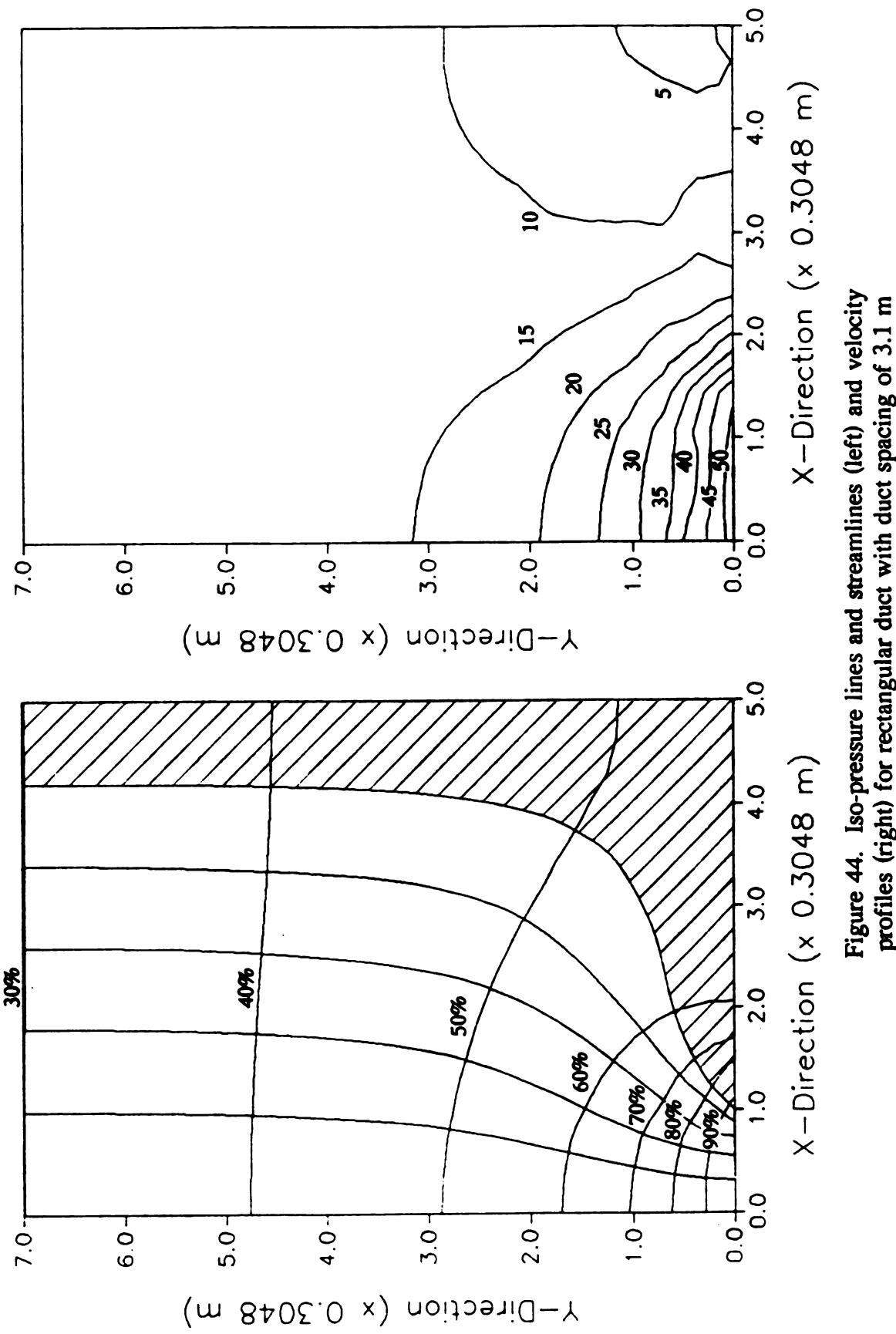


Figure 43. Iso-pressure lines and streamlines (left) and velocity profiles (right) for rectangular duct with duct spacing of 2.4 m



profiles (right) for rectangular duct with duct spacing of 3.1 m

4.2.2 The effect of duct size on air flow patterns

To evaluate the effect of duct size on air flow patterns, three levels of duct size for four duct shapes were chosen. The related data and Figure numbers are given in Table 9. The duct spacing was 2.4 m, the duct pressure was 125 Pa, and the depth of the potato pile was 4.3 m.

In general, the effect of duct size on air flow patterns is very similar to that of duct spacing. Let us take the triangular duct for example. The iso-pressure lines and streamlines for duct sizes of 0.59 m × 0.34 m, 0.64 m × 0.36 m and 0.67 m × 0.39 m are drawn in Figures 34, 45 and 46, respectively. It can be seen that the pressure patterns above or near the duct consist of higher pressure than those in the lower right region where the pressure gradient is also very low for all duct dimensions. Along with the increase of the duct size, the iso-pressure line with the same percentage of duct pressure in the lower right part will move upward and toward the middle between two adjacent

ducts. Therefore, increasing duct size had the same effect as decreasing duct spacing. By comparing Figures 34, 45 and 46, the effect of duct size on pressure distribution becomes very obvious. As also can be seen from Table 9, the air flow rates per unit thickness in the shaded area for three duct sizes are the same. But the shaded areas in Figure 34, 45 and 46 cover 27.0%, 26.2% and 25.0% of the total cross-sectional areas, respectively. Therefore, each unit volume of potato pile within the shaded area will receive less air flow than the other part in the same cross-section, and the shaded area for a larger duct size will be better ventilated than for a smaller duct size.

The velocity profiles for a triangular duct presented in Figures 34, 45 and 46 are in accordance with the pressure and air flow distributions for the relevant duct sizes. Increasing duct size obviously will improve the air flow situation in the middle lower region between two adjacent ducts.

The above analysis is for triangular ducts with different duct sizes. The general tendency of the effect of duct size on air flow patterns for circular duct, semicircular duct and in-floor rectangular duct is the same. The related data and Figure numbers can be obtained from Table 9.

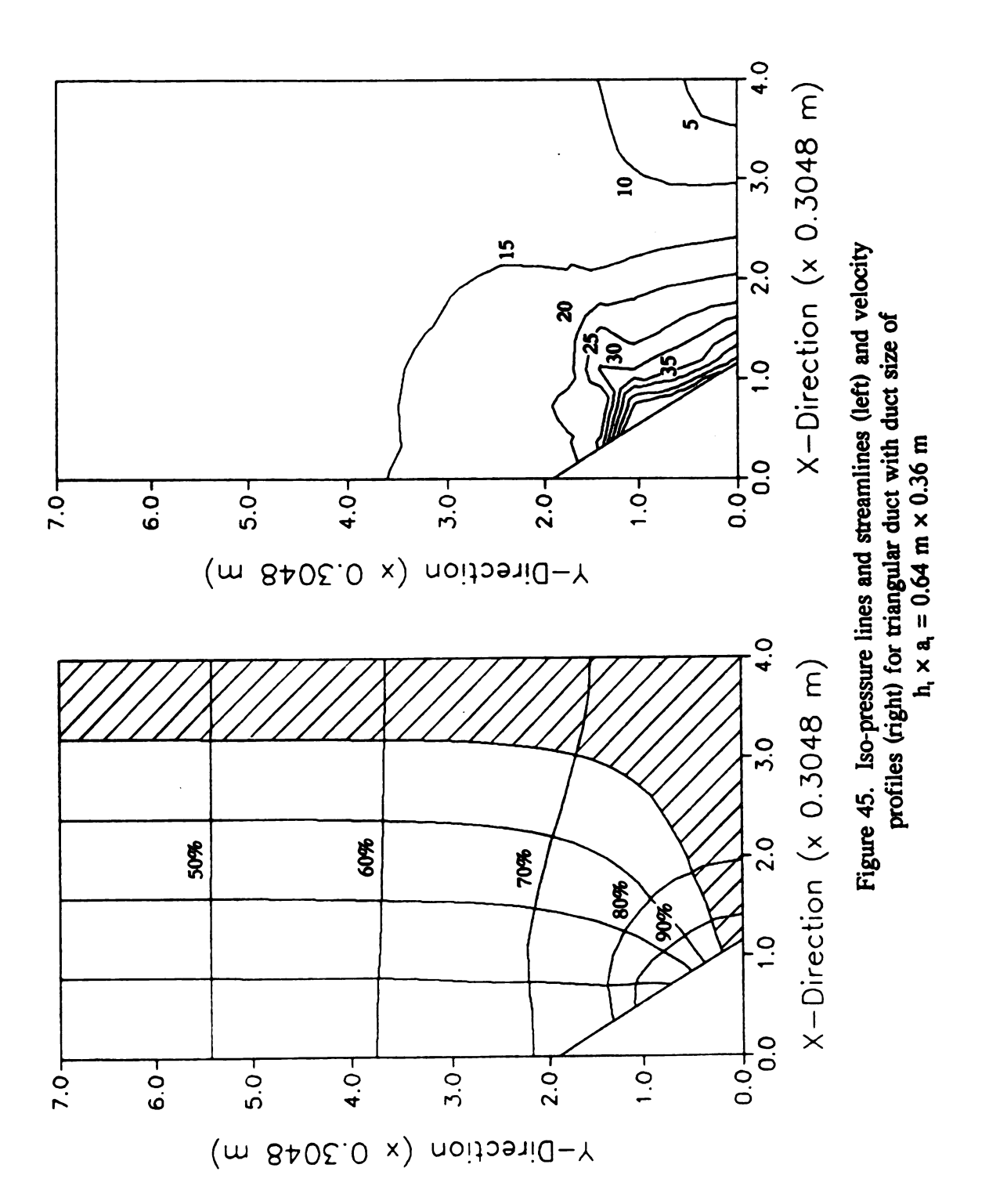
A little larger duct may not increase the cost significantly, but will improve air flow conditions both in the duct system and in the storage. A small duct is usually unfavorable. Suppose two ducts with different sizes must deliver air at the same flow rate, then the smaller duct will have a higher air velocity than the larger one. High air velocity will cause turbulence and nonuniform air flow in the duct system. It will also increase the pressure head loss and energy consumption. According to Equation [69] and [70], the pressure head loss is directly proportional to the square of velocity. If the cross-sectional area of a duct is reduced to half, the air velocity will be doubled under the same flow rate and the pressure head loss will be quadrupled. Usually the air flow velocity in the lateral duct is designed at 240 to 300 m/min (Cargill, 1976 and Rastovski et al. 1987), exceeding this limit by reducing duct size will increase pressure head loss markedly.

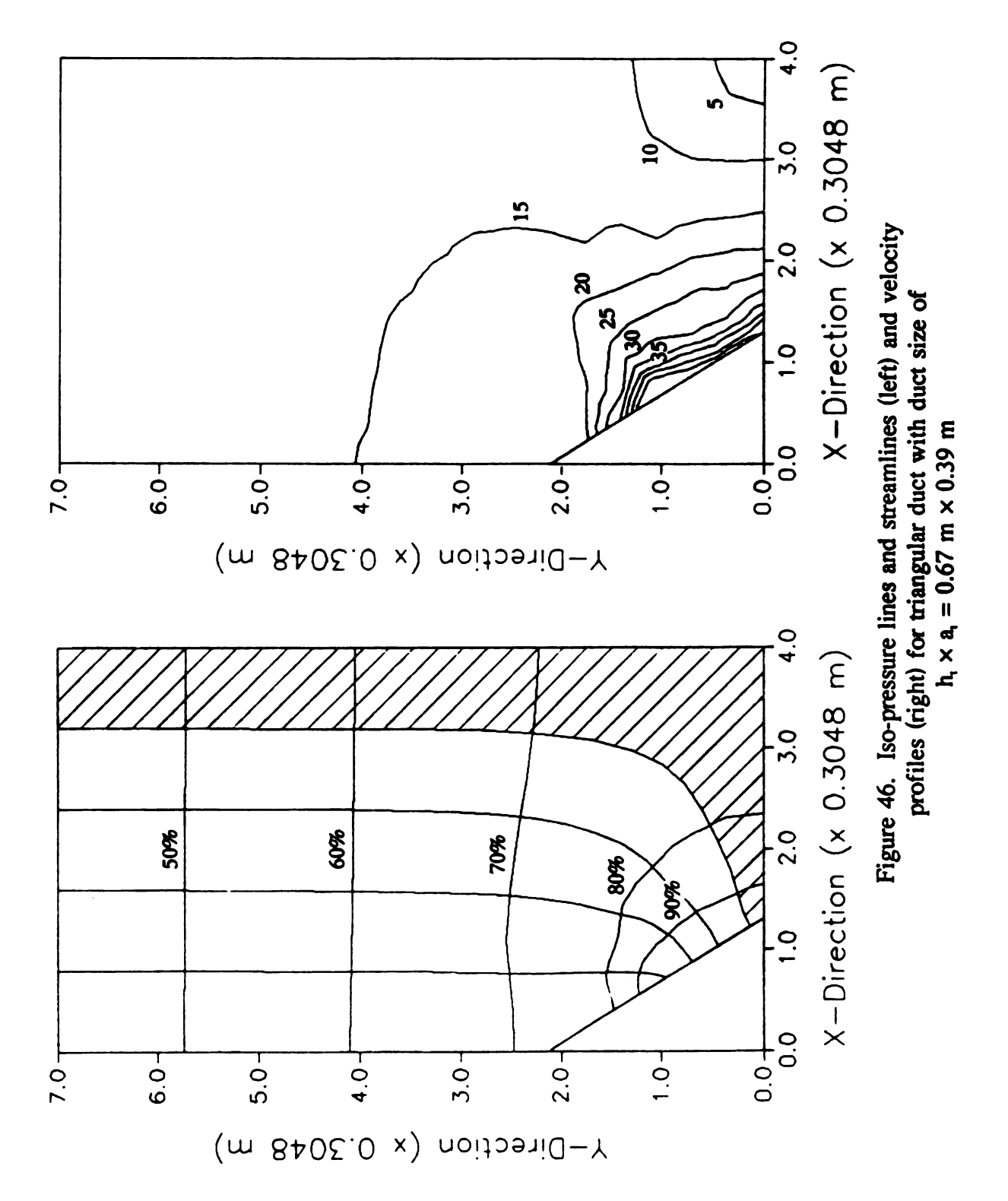
Comparing the effect on air flow patterns of the in-floor rectangular duct with different duct sizes, it is noted that increasing duct size in the horizontal direction will be beneficial to the improvement of air flow condition in the storage. This result can be

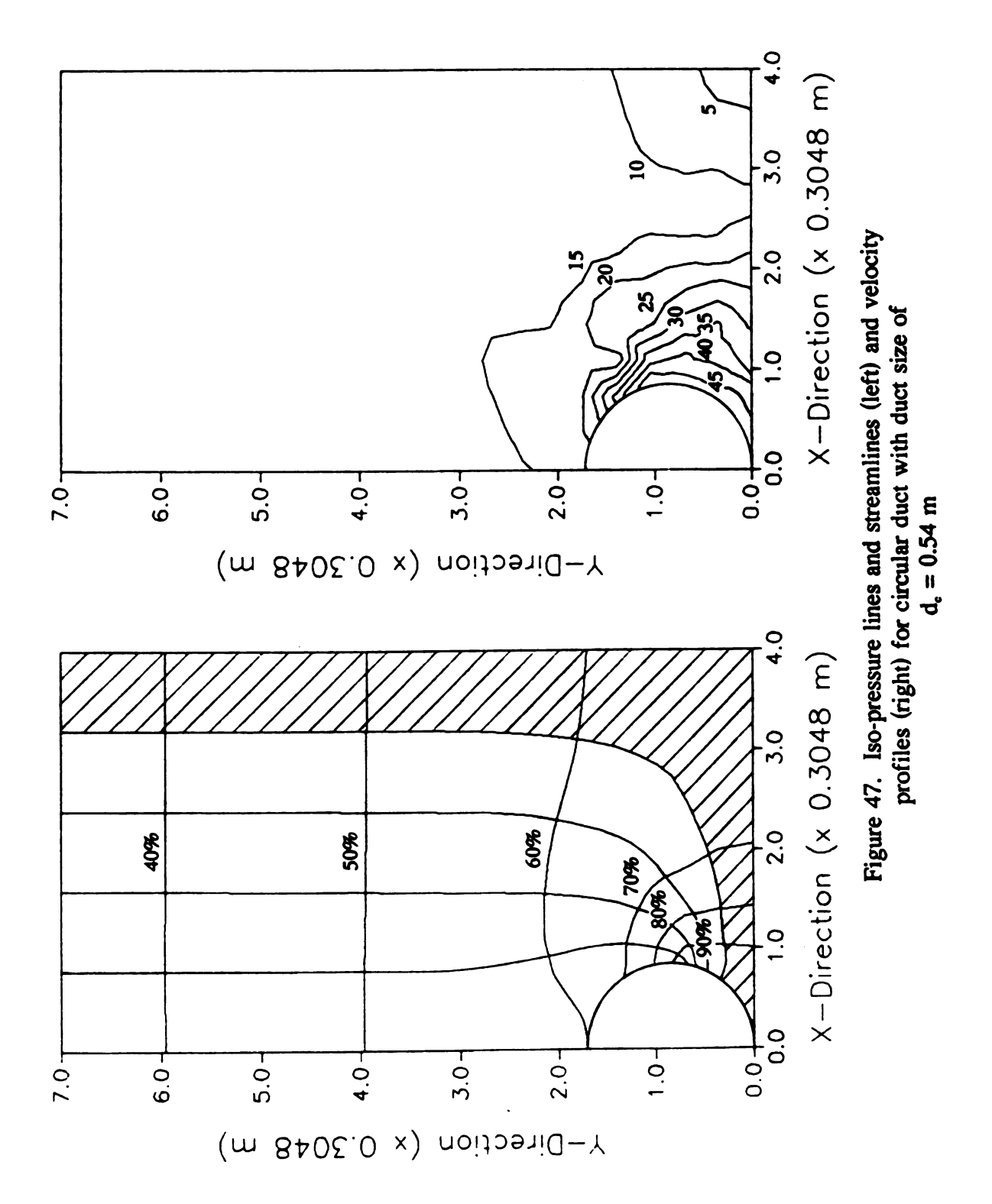
seen from the iso-pressure lines, streamlines and velocity profiles in Figures 43, 51 and 52 for in-floor rectangular ducts with three duct sizes. Therefore, from an air ventilation point of view, it is desirable for in-floor rectangular duct to have a larger width than its depth. But some researchers (Wilson, 1976) suggested that an in-floor rectangular duct with larger depth than its width will reduce the length of the cover planks.

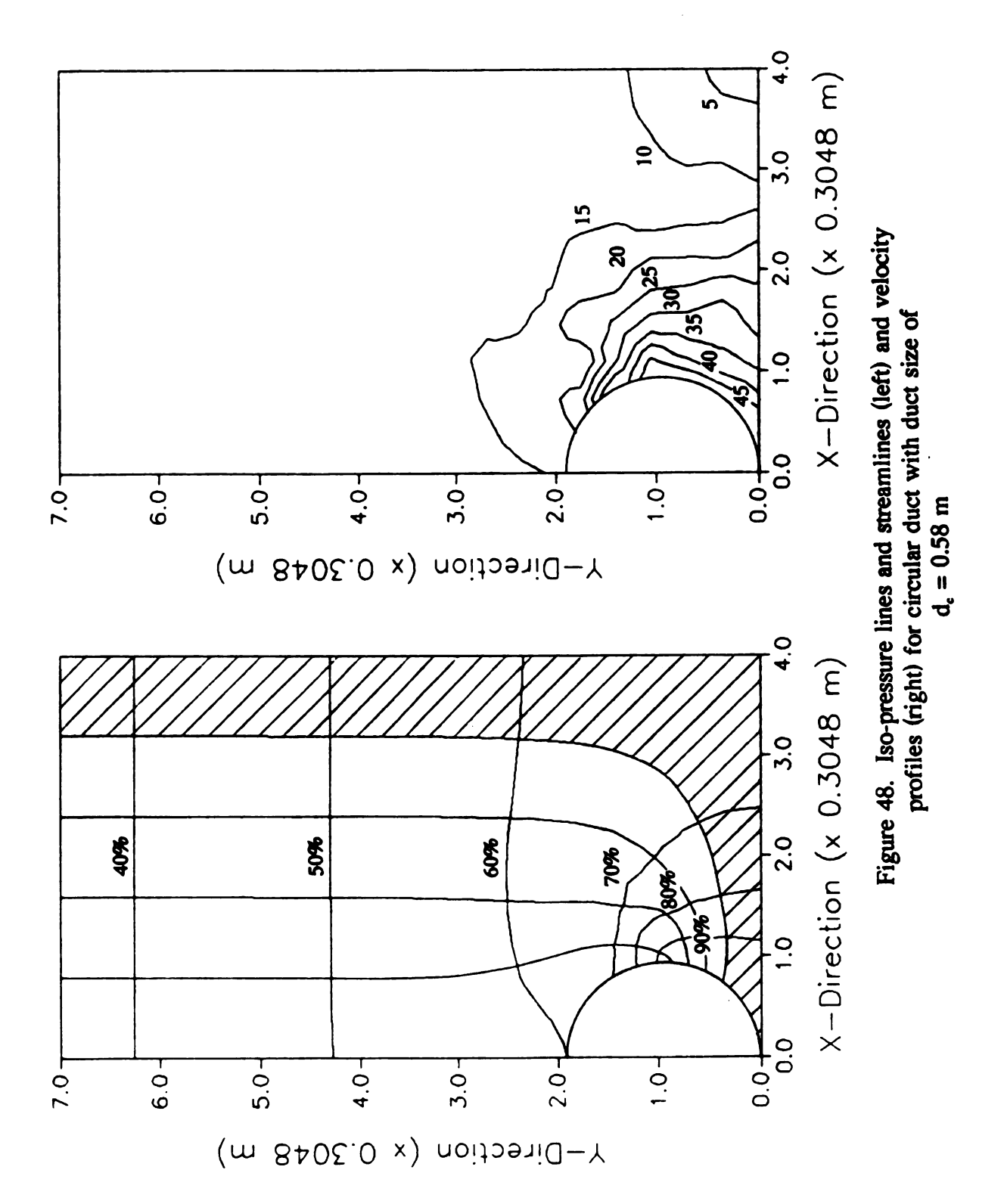
Table 9. The effect of duct size on air flow patterns: related data and Figure numbers

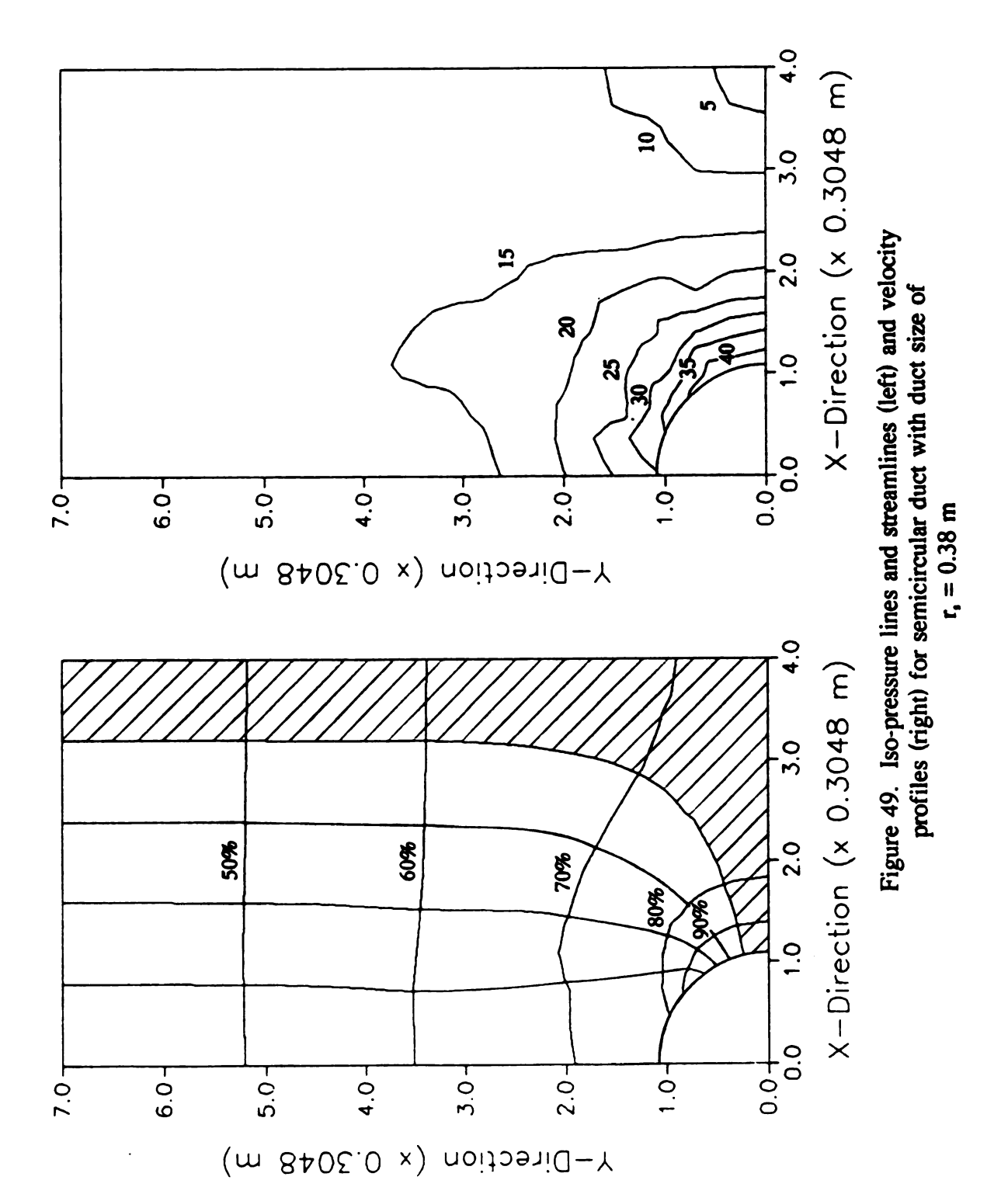
Duct shapes	Duct sizes (m)	Shaded area over total area (%)	Flow rate for shaded area (%)	Figure No. referring to iso-pressure lines, streamlines and velocity profiles
Triangular duct	0.59 × 0.34	27.0	20.0	Fig. 34
Triangular duct	0.64 × 0.36	26.2	20.0	Fig. 45
Triangular duct	0.67 × 0.39	25.0	20.0	Fig. 46
Circular duct	0.51	27.0	20.0	Fig. 37
Circular duct	0.54	26.8	20.0	Fig. 47
Circular duct	0.58	26.5	20.0	Fig. 48
Semicircular duct	0.36	27.0	20.0	Fig. 40
Semicircular duct	0.38	26.8	20.0	Fig. 49
Semicircular duct	0.41	26.7	20.0	Fig. 50
Rectangular duct	0.32 × 0.32	27.0	20.0	Fig. 43
Rectangular duct	0.34 × 0.34	26.5	20.0	Fig. 51
Rectangular duct	0.36 × 0.36	26.1	20.0	Fig. 52

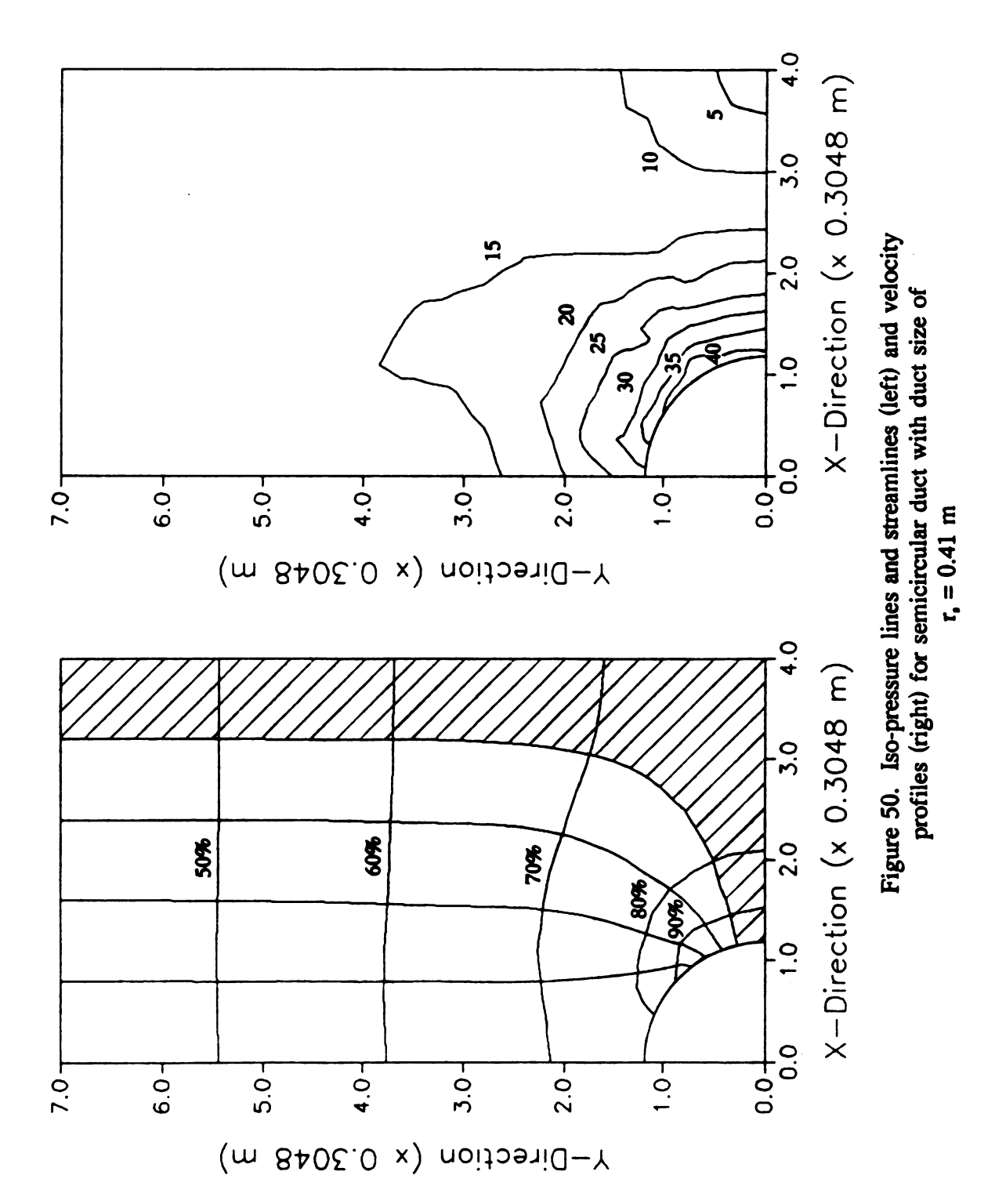


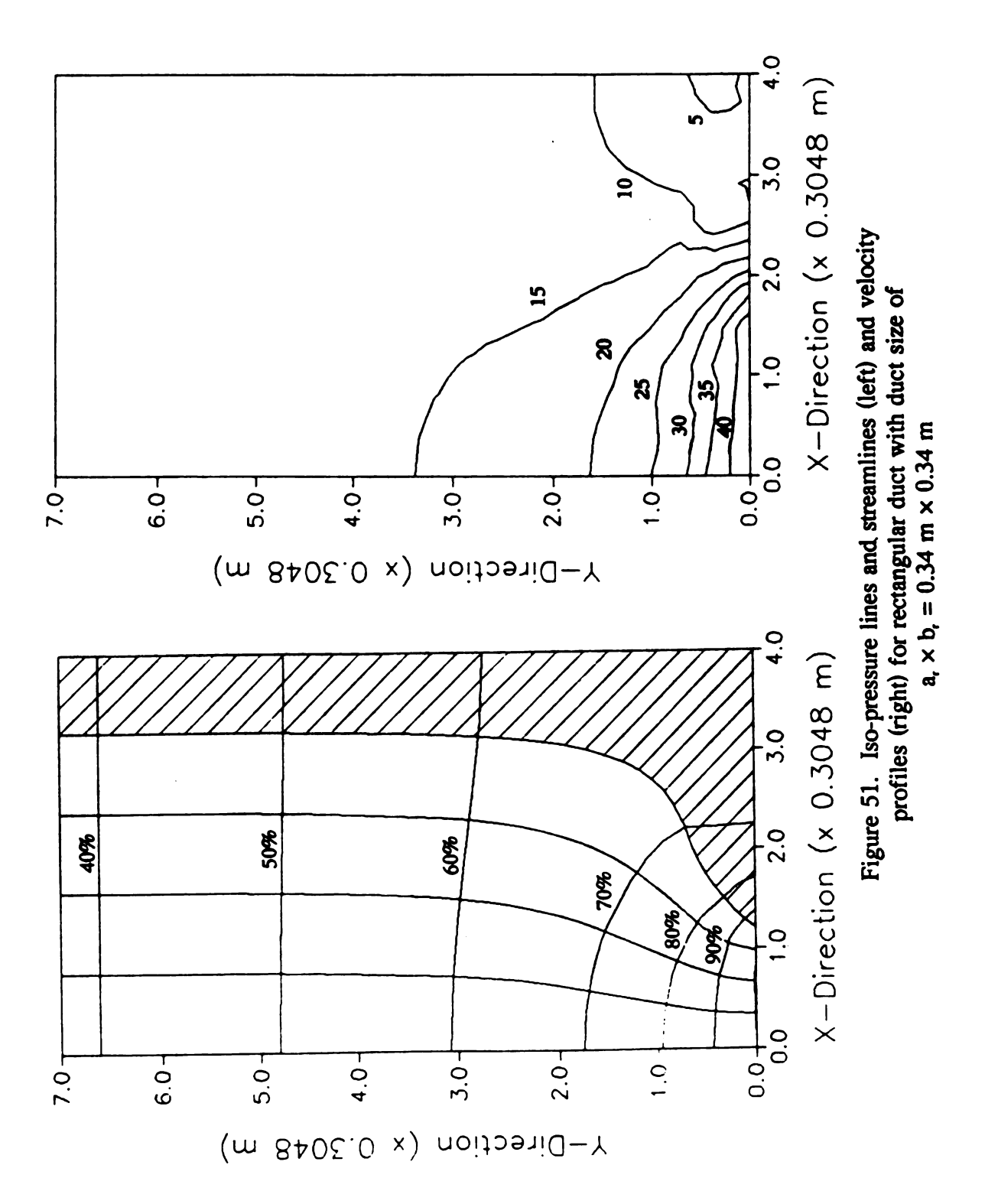


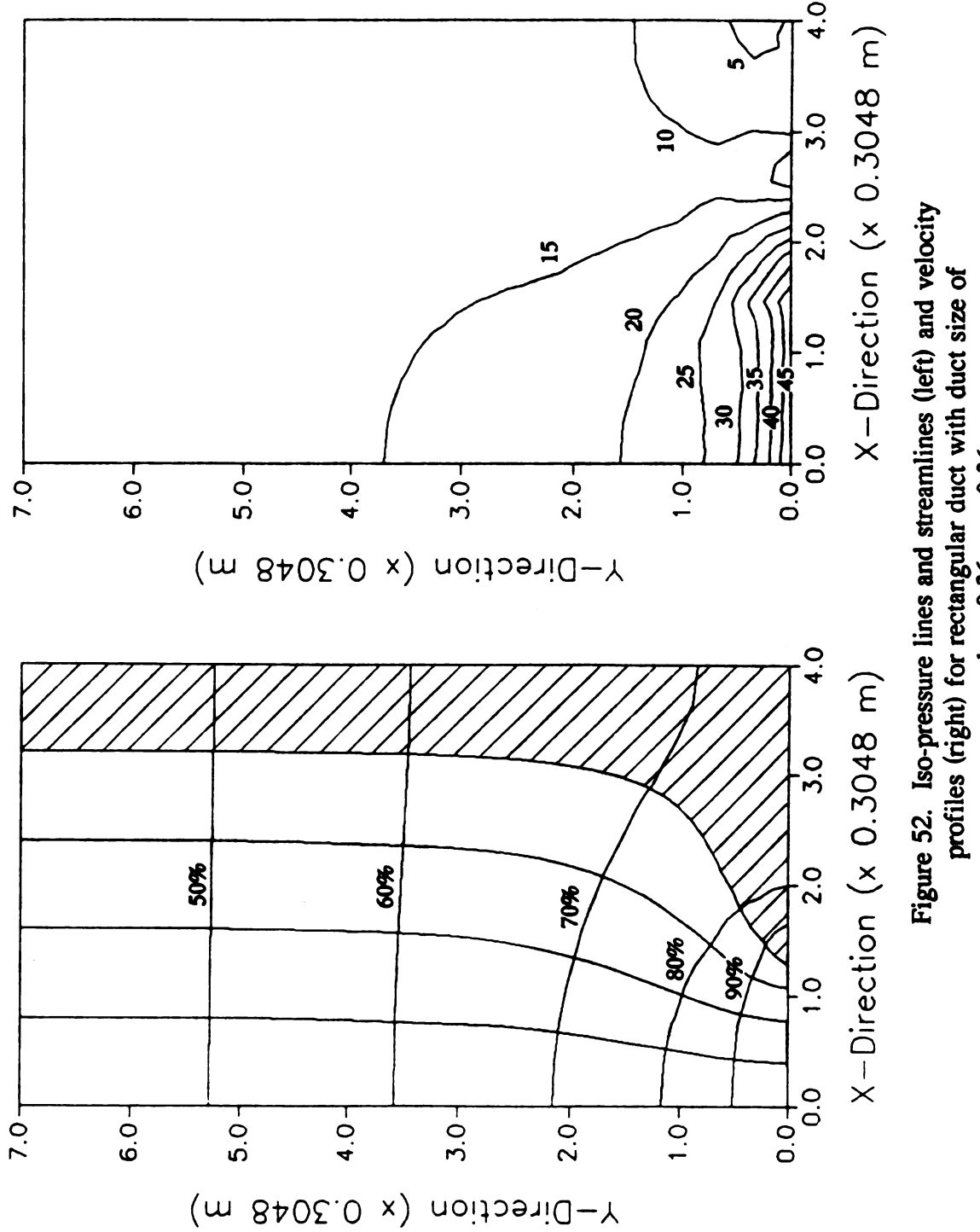












profiles (right) for rectangular duct with duct size of a, x > b, $z = 0.36 \text{ m} \times 0.36 \text{ m}$

4.2.3 The effect of potato pile depth on air flow patterns

To illustrate the effect of potato pile depth on air flow patterns, the potato storage with the triangular duct was selected as an example. The duct pressure was 125 Pa, the duct size was 0.59 m × 0.34 m, and the duct spacing was 2.4 m for all three potato piles. The iso-pressure lines, streamlines and velocity profiles are shown in Figures 53. 34 and 54 for potato pile depths of 3.1 m, 4.3 m and 5.5 m, respectively. Suppose the air flow rates are equal. Detailed observation reveals that the pressure gradient in the lower right region in Figure 54 is less than that in Figure 34 which in turn is less than in Figure 53. Therefore, lower pile depth has better air flow in the middle lower region between two adjacent ducts. The patterns of streamlines in the lower region of the crosssection are the same for these three pile depths. The percentages of shaded area over the total cross-sectional area shown in Figures 53, 34 and 54 are 27%, and the percentage flow rates per unit thickness are 20%. Because the pile depths are not the same, we may extend the shaded area to the top of the pile, so that we can take the total depth (not only the region under 2.1 m) of potato pile into consideration. In doing so it turns out that the air flow path line in the storage with higher depth is longer than in the storage with lower depth. Because it will take longer time for air travelling through the higher potato pile than through the lower pile when the air flow rates are the same, a potato pile with a lower depth is favorable for having good aeration condition.

Generally the air velocity value is very low in the region near the lower right corner in the cross-section. But the storage with lower pile depth has a relatively larger air velocity in this region than with higher pile depth. This observation also confirms the

comparison of iso-pressure lines and air flow path lines. Air ventilation in the shaded area can be improved when the pile depth is decreased.

The depth of a potato pile is limited not only by the requirement of maintaining an adequate air ventilation condition within the pile, but also by the consideration of reducing pressure on the lower layer potatoes and on the ducts. Other factors limiting potato pile depth include the requirement that there be a clearance between the top layer of potato pile and the ceiling of the storage. This clearance is necessary for inspection of potatoes, for circulation and mixing of the air, for installation of cooling equipment, and for ease of loading and unloading potatoes.

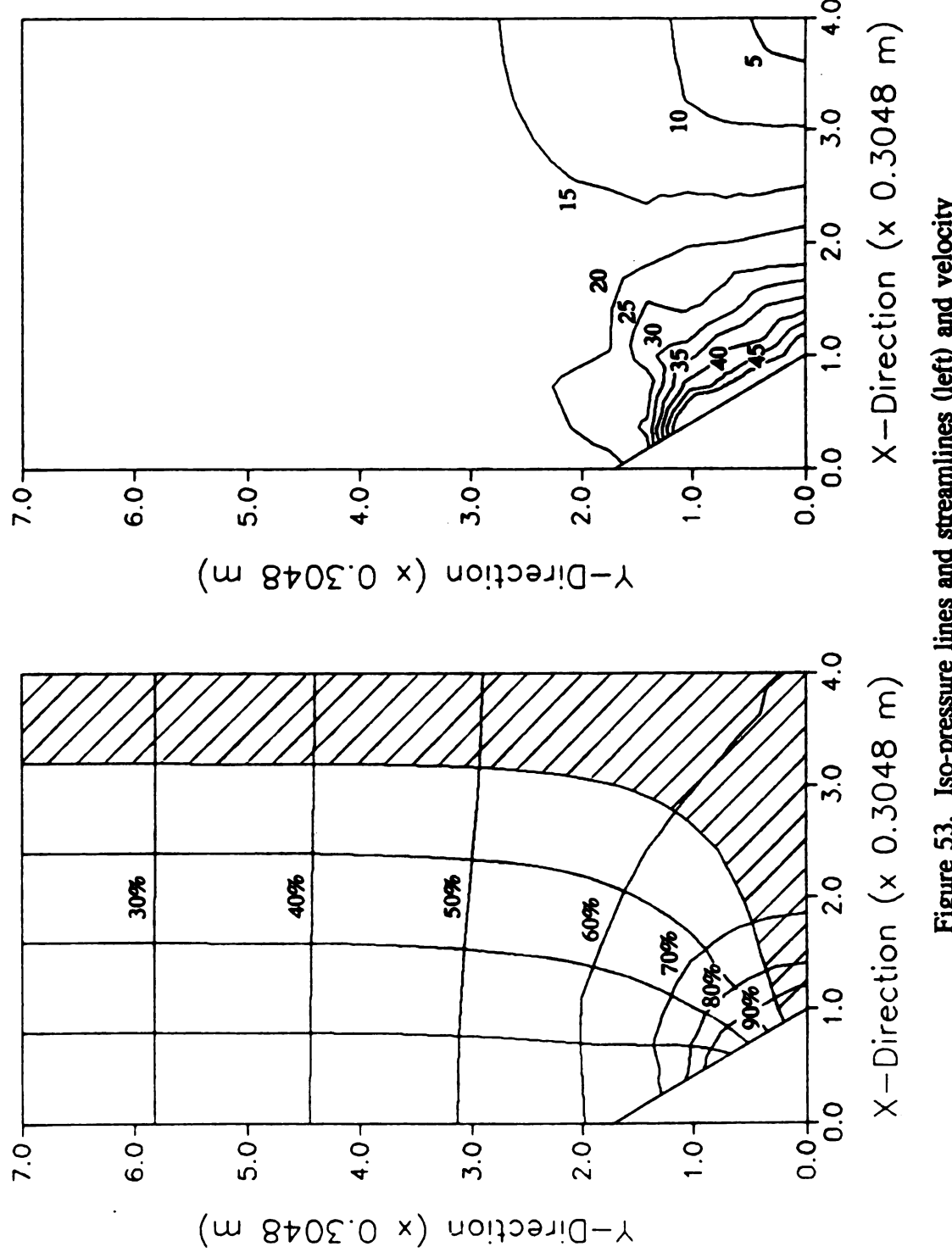


Figure 53. Iso-pressure lines and streamlines (left) and velocity profiles (right) for triangular duct with depth of potato pile of 3.1 m

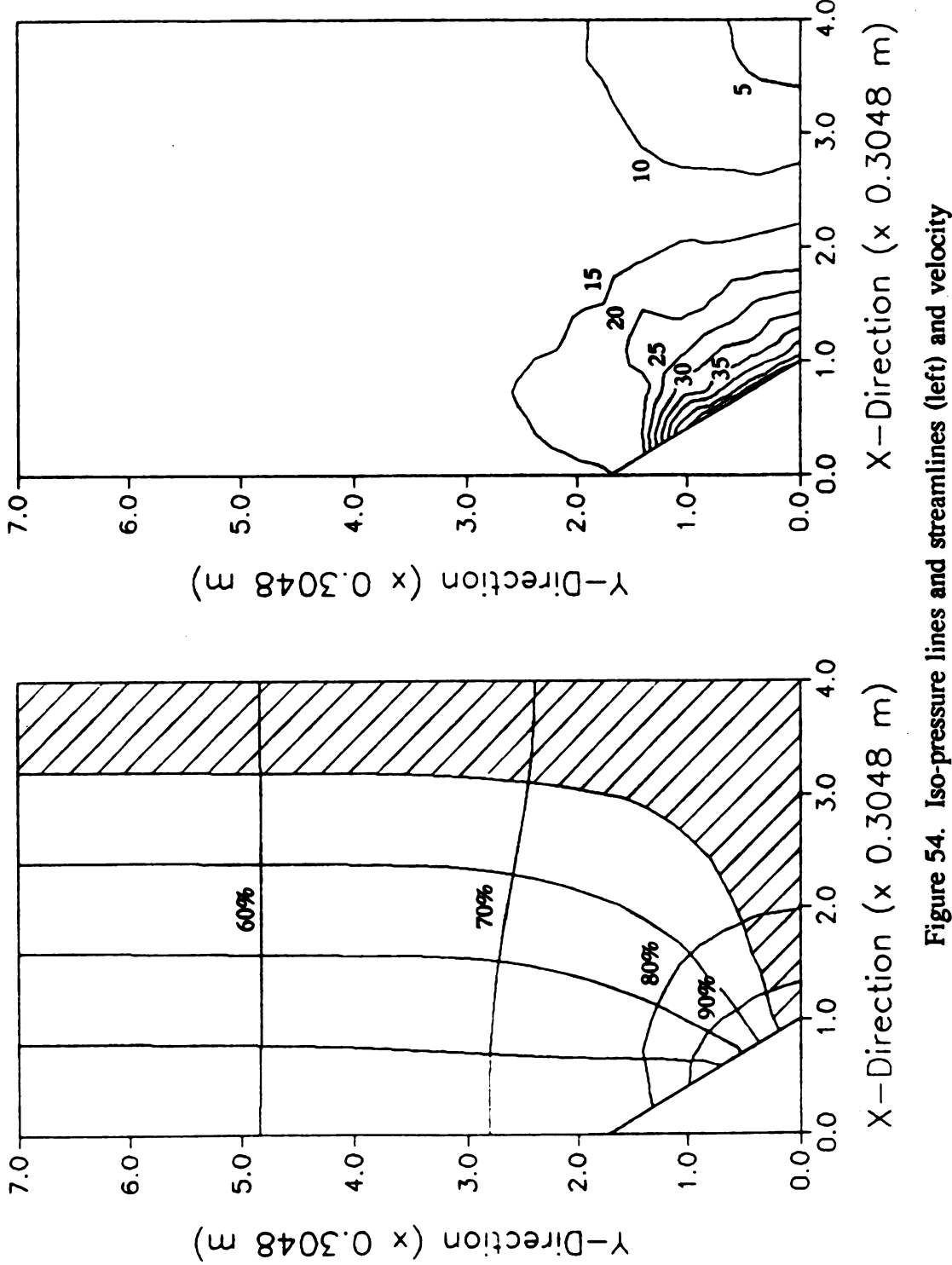


Figure 54. Iso-pressure lines and streamlines (left) and velocity profiles (right) for triangular duct with depth of potato pile of 5.5 m

4.2.4 The effect of duct pressure on air flow patterns

To compare the effect of different duct pressures on air flow patterns, three duct pressures (125 Pa, 250 Pa and 375 Pa) were chosen. The duct spacing was 2.4 m and the depth of the potato pile was 4.3 m. The duct size for the triangular duct was $h_1 \times a_2$ = 0.59 m \times 0.34 m, for the circular duct is d_e = 0.51 m, for the semicircular duct was $r_{\star} = 0.36$ m, and for the in-floor rectangular duct was $a_{\tau} \times b_{\tau} = 0.32$ m $\times 0.32$ m. The iso-pressure lines and streamlines for these three duct pressures are almost the same as those shown in Figures 34, 37, 40 and 43 for triangular ducts, circular ducts, semicircular ducts and in-floor rectangular ducts, respectively. The velocity profiles are different only near the duct opening and in the lower right corner for these three duct pressures. There are no distinct differences in the velocity profiles in other parts of the potato pile, so they are not presented here. The main reason for having the same isopressure lines and streamlines for different duct pressures is that the coefficients A and B in Equation [13] are suitable for a certain range of pressure gradients and velocity values. If the changes of pressure gradient and velocity value fall within the same range, then they will show a linear relationship in log-log scale. In this case, A and B remain unchanged. Especially when the pressure gradient and velocity value are high, the coefficients A and B related to potato pile are usually less sensitive. This trend can be seen from Table 7.

The use of higher pressure than required in the duct system is not recommended. Increasing duct pressure will increase the air velocity at the duct opening, therefore it will cause turbulence and uneven air distribution. At the same time, high air velocity will

also result in more pressure head loss and more energy consumption.

4.2.5 The effect of duct shape on air flow patterns

Before the effect of the duct shape on air flow patterns can be analyzed, it is important to note that these ducts must have an equivalent duct size. That is to say their cross-sectional areas should be the same. The duct size for the triangular duct was h, X $a_c = 0.59 \text{ m} \times 0.34 \text{ m}$, for the circular duct was $d_c = 0.51 \text{ m}$, for the semicircular duct was $r_{s} = 0.36$ m, and for the in-floor rectangular duct was $a_{r} \times b_{r} = 0.32$ m $\times 0.32$ m. Other variables were set at the following levels: the duct spacing was 2.4 m, the duct pressure was 125 Pa and the depth of the potato pile was 4.3 m. Under these conditions, the iso-pressure lines, streamlines and velocity profiles for triangular duct, circular duct, semicircular duct and in-floor rectangular duct are shown in Figures 34, 37, 40 and 43, respectively. We can see that the pressure distributions for these four duct configurations show different patterns. But it is common that a very low pressure gradient exists in the lower right region of the cross-section. The percentages of shaded area over the total cross-sectional area for the four duct shapes are exactly the same. They are all equal to 27% as listed in Table 8. The percentage flow rates per unit thickness are also the same with the value of 20%. Air flow conditions in the middle lower region between two adjacent ducts are independent of the duct shape used as long as the cross-sectional areas are the same for different duct shapes. It should be noted here that the size, orientation and location of the duct opening may affect the air flow patterns within the storage. But if the cross-sectional area and the total air flow rate per unit thickness across this crosssection are the same, then the shaded areas for different duct shapes under present study will show a similar air flow pattern.

The pressure distributions directly above the duct vary for the four duct shapes under study. The regions above circular duct and semicircular duct experience high pressure drop, while pressure distributions above triangular duct and in-floor rectangular duct are relatively uniform. Comparing the velocity profiles for the four duct shapes, the velocity distribution for an in-floor rectangular duct appears very uniform. This is because most of the air discharged from the duct opening will travel in the normal direction due to inertia, while only a part of the air may flow in the tangential direction of the opening. In this sense, the triangular and rectangular ducts are favorable for obtaining uniform air flow above the ducts.

4.2.6 The effect of the distance to the duct entrance on air flow patterns

Three-dimensional pressure and velocity distributions mean that the pressure contour lines and the velocity profiles in potato storage are different from one cross-section to another. This is mainly due to the fact that the distributions of potato tuber size and porosity in the pile are inhomogeneous and the static pressures along the lateral duct are not constant. When air moves along a duct, a part of it will be discharged through the duct opening into the potato storage. Therefore the air flow rate along the duct will be gradually decreased. If the cross-section of the duct is uniform, then the velocity in the duct will also be decreased accordingly. The decreased velocity will in turn cause a pressure regain along the duct. But according to Equations [69] and [70], the resistance

of the duct internal surface to air flow will cause the pressure head losses along the duct.

To evaluate the effect on air flow patterns of the distance from a given cross-section in the potato pile to the duct entrance, three distances of 2.0 m, 6.0 m and 10 m were selected. Again a triangular duct was used as an example. The duct spacing was equal to 2.4 m, the duct size was 0.59 m × 0.34 m, and the depth of the potato pile was 4.3 m. The general tendency of the effect of increasing the distance was equivalent to the effect on air flow patterns of increasing duct pressure values as described in Section 4.2.4. All the plots of iso-pressure lines and streamlines are very close to those shown in Figure 34, and are not presented. Because of the pressure regain along the duct, the velocities at the duct opening and in the lower region of the potato pile for different cross-sections were not the same. High velocity difference between the cross-sections will also cause a nonuniform air flow in the potato pile. This should be avoided.

Theoretically a uniform pressure along the lateral duct can be obtained by using a tapered duct or stepped duct (Allen, 1974). But practically it may not be feasible, since making a tapered duct may cost more than making the uniform one.

CHAPTER 5

CONCLUSIONS AND RECOMMENDATIONS

5.1 Conclusions

Equations [13], [36] and [37] together with proper coefficients A and B are the useful mathematical models for predicting air flow phenomena within a potato storage.

The finite element method is an effective tool in solving nonlinear partial differential equations, through which the effect of various factors on air flow patterns in a potato storage can be analyzed.

Uniform air flow usually exists in the upper region of a potato pile where the depth of the potato pile H_P is equal to or greater than the spacing L_d between two adjacent ducts. Nonuniform air flow dominates over the lower region of a potato pile where the depth of the potato pile H_P is less than the duct spacing L_d .

In the lower region of the potato pile, the area having a relatively good air ventilation situation is that above the lateral duct. The area with the poorest aeration condition is usually located in the middle lower region between two adjacent ducts, where the pressure shows a remarkable variation, the air flow path is the longest and the velocity is the lowest.

Duct spacing has a significant effect on air flow patterns in a potato storage.

Decreasing duct spacing is generally favorable for having more uniform air distribution

in the potato pile and is preferable for improving the air ventilation condition in the middle lower region between two adjacent ducts. But decreasing duct spacing will increase the duct numbers, thus increasing the cost of the investment for the duct system. Decreasing duct spacing will also reduce the effective floor area and will slightly lower the storage capacity.

Duct size also has a marked effect on air flow patterns in a potato storage. Increasing duct size will achieve similar results as decreasing duct spacing. A larger duct is usually preferred to improve air flow situations both in the duct system and in the storage. A small duct is unfavorable for the air ventilation efficiency. When ducts with different sizes must deliver air at the same flow rate, the smaller duct will have a higher air velocity than the large one. High air velocity will not only cause turbulence and uneven air flow in the duct system, but also increase the pressure head loss and energy consumption.

Because a potato pile with a lower depth has a shorter air flow path than one with a higher depth, it requires less time to bring the entire pile to the same temperature or same relative humidity if the same air flow rate per metric ton was used. Therefore, it will have more efficient air ventilation and air circulation in the potato pile and in the whole storage, respectively. The depth of the potato pile is limited not only by the requirement of maintaining adequate air ventilation, but also by the considerations of reducing pressure on the lower layer potatoes and on the duct and having a proper clearance between the top layer of the potato pile and the ceiling of the potato storage.

The iso-pressure lines, presented as a percentage of the duct pressure, and the streamlines for three different duct pressures of 125 Pa, 250 Pa and 375 Pa, have shown

very similar patterns. Duct pressure had little effect on iso-pressure lines and streamlines.

But the use of a higher pressure in the duct system is not recommended, as it will cause more pressure head loss and energy consumption.

Under present study, the percentage shaded area over the cross-sectional area and the percentage air flow rate per unit thickness for the shaded area are similar for triangular duct, circular duct, semicircular duct and rectangular duct as long as these ducts have similar cross-sectional areas. In this case, the air ventilation condition in the middle lower region between two adjacent ducts is generally independent of the duct shape.

Among these four duct shapes, in-floor rectangular ducts tend to have a more uniform air ventilation condition in the storage than others. And from the air ventilation point of view, it is desirable for in-floor rectangular duct to have a larger width than its depth. The circular and semicircular ducts have shown a distinct pressure drop directly above the ducts where the air flow appears relatively uneven.

Air flow distribution along the duct axial direction is generally nonuniform. The effect of increasing distance from a given cross-section to the duct entrance on air flow patterns has been found to be equivalent to that of decreasing duct pressures on air flow patterns.

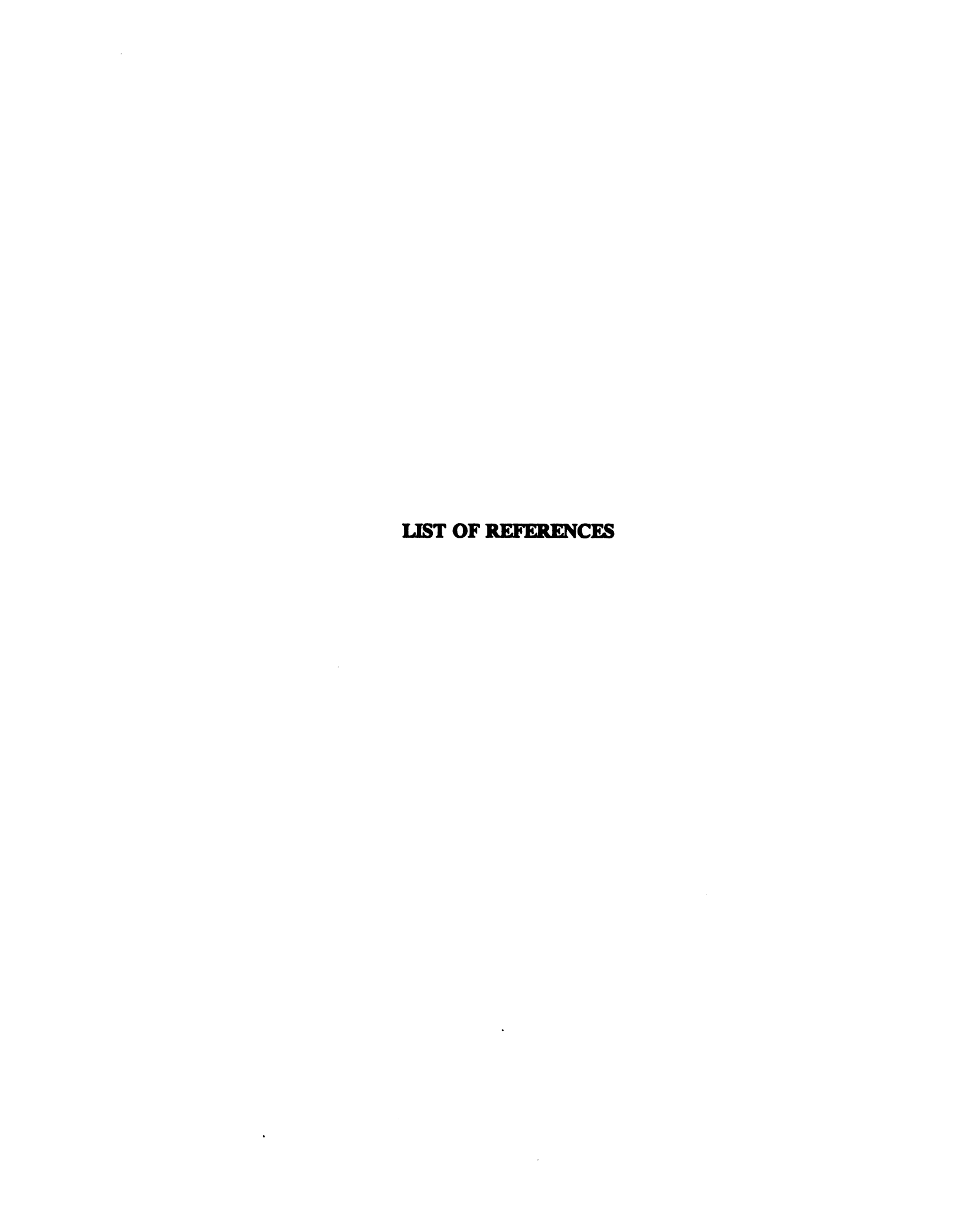
Generally, uniform air distribution can be approached and the air ventilation condition in potato pile can be improved through properly selecting the design parameters of the duct system and the potato storage. But uniform air flow in the lower region of the storage will never be achieved by a duct system.

5.2 Recommendations

The computer programs developed in this study can be used to analyze air flow patterns not only for potato storage but also for grain storages and hay piles.

The analysis of the effect of various factors on air flow patterns will be beneficial to the design and management of a potato storage. But other economic, technical and environmental factors should also be taken into consideration in the design.

Temperature distribution in a potato pile is a very important aspect in design and management of a potato storage. It is closely related to the heat transfer phenomena: conduction, convection and radiation that are taking place within the potato storage and between storage and environment. Therefore, further research on temperature distribution patterns in the potato pile is necessary.



LIST OF REFERENCES

- Akritidis, C. B. and A. J. Siatras. 1979. Resistance of pumpkin seeds to air flow. Transactions of the ASAE 22(6):1414-1416.
- Allen, D. 1974. Air flow distribution from tapered ducts. ASAE Paper No.74-6514. ASAE, St. Joseph, MI.
- Ames, W. F. 1965. Nonlinear partial differential equations in engineering. Academic Press, New York, NY.
- ANSYS Manual (revision 4.3), 1987. Swanson Analysis Systems, Inc. PA.
- ASAE Standards. 35th ed. 1988. Resistance to airflow of grains, seeds, other agricultural products, and perforated metal sheets. ASAE, St. Joseph, MI.
- Bakker-Arkema, F. W., R. J. Patterson and W. G. Bickert. 1969. Static pressure-airflow relationships in packed beds of granular biological materials such as cherry pits. Transactions of the ASAE 12(1):134-136,140.
- Barrowman, R. and D. S. Boyce. 1966. Air distribution from lateral ducts in barley. J. Agric. Eng. Res. 11(4):243-247.
- Bear, J. 1972. Dynamics of fluids in porous media. American Elsevier Inc. New York, NY.
- Bern, C. J. and L. F. Charity. 1975. Airflow resistance characteristics of corn as influenced by bulk density. ASAE Paper No.75-3510. ASAE, St. Joseph, MI.
- Boyce, D. S. and J. K. Davies. 1965. Air distribution from a lateral duct with different escape areas of barley. J. Agric. Eng. Res. 10(3):230-234.
- Brook, Roger C. 1991. Potato storage design and management. Agricultural Engineering Information Series, AEIS No. 581, File No. 18.144, Date 4/91. Cooperative Extension Service, Michigan State University, East Lansing, MI.
- Brooker, D. B. 1958. Lateral duct air flow paterns in grain drying bins. Agricultural Engineering 39(6):348-351.

- Brooker, D. B. 1961. Pressure patterns in grain-drying systems established by numerical methods. Transactions of the ASAE 4(1):72-74,77.
- Brooker, D. B. 1969. Computing air pressure and velocity distribution when air flows through a porous medium and nonlinear velocity-pressure relationships exist. Transactions of the ASAE 12(1):118-120.
- Bunn, J. M. and W. V. Hukill. 1963. Pressure pattern predictions for nonlinear air flow through porous media. Transactions of the ASAE 6(1):32-36.
- Burton, W. G. 1982. Post-harvest physiology of food crops. Longman Inc. New York, NY.
- Burton, W. G. 1989. The potato. John Wiley & sons, Inc. New York, NY.
- Calderwood, D. L. 1973. Resistance to airflow of rough, brown and milled rice. Transactions of the ASAE 16(3):525-527, 532.
- Campbell, J. G. 1962. Potato handbook. The Potato Association of America. New Brunswick, NJ.
- Cargill, B. F. 1976. The potato storage design, construction, handling and environmental control. Michigan State University, East Lansing, MI.
- Cargill, B. F. 1986. Importance of balanced air flow for quality potatoes for the chip market. The National Chipping Potato Seminar. Feb. 27-March 1, 1986, Boston, MA.
- Cargill, B. F., K. C. Price and T. D. Forbush. 1989. Requirements and recommendations for potato storage in the Midwest USA. In: Potato storage Technology and practice. Cargill, B. F., Roger C. Brook and Todd D. Forbush (editors). ASAE, St. Joseph, MI.
- Cash, J. N., R. Chase and A. Cameron. 1986. Application of potato carbohydrate analysis and CIPC interaction in a commercial growing and storage operation. 1986 Michigan Potato Research Report (Volume 18). Michigan State University Agricultural Experiment Station in cooperation with the Michigan Potato Industry Commission. Dewitt, MI.
- Cash, J. N., R. Chase and W. A. Keim. 1987. The interaction of potato carbohydrates, sprout inhibition and CO₂ exchange on chipping quality of commercially stored potatoes. 1987 Michigan Potato Research Report (Volume 19). Michigan State University Agricultural Experiment Station in cooperation with the Michigan Potato Industry Commission. Dewitt, MI.

- Chandra, P., L. D. Albright and G. E. Wilson. 1981. Pressure drop of unidirectional air flow through rock beds. Transactions of the ASAE 24(4):1010-1013, 1021.
- Chapman, J. E., R. V. Morey and J. L. Nieber. 1989. Airflow patterns in flat storage aeration systems. Transactions of the ASAE 32(4):1368-1376.
- Chapra, S. C. and R. P. Canale. 1988. Numerical methods for Engineers, second edition. McGraw-Hill Book Company, New York, NY.
- Churchill, R. V. and Brown, J. W. 1987. Fourier series and boundary value problems, 4th edition. McGraw-Hill Inc. New York.
- Cloud, H. A. 1976. Design criteria for the air handling and distribution system for potato storage. In: The potato storage design, construction, handling and environmental control. Cargill, B. F. (editor). Michigan State University, East Lansing, MI.
- Cloud, H. A. and R. V. Morey. 1980. Distribution duct performance for through ventilation of stored potatoes. Transactions of the ASAE 23(5):1213-1218.
- Collins T. 1953. Flow patterns of air through grain during drying. Agricultural Engineering 34(11):759-760, 768.
- Earl, H. 1976. The produce buyer's demands to the grower for processing potatoes. In:
 The potato storage design, construction, handling and environmental control.
 Cargill, B. F. (editor). Michigan State University, East Lansing, MI.
- Ergun, S. 1952. Fluid flow through packed columns. Chem. Eng. Prog. 48(2):89-94.
- Farmer, G. S., G. H. Brusewitz and R. W. Whitney. 1981. Resistance to airflow of bluestem grass seed. Transactions of the ASAE 24(2):480-483.
- FIDAP Manual (version 4.5), 1989. Fluid Dynamics International, Inc. IL.
- Finlayson, B. A. 1980. Nonlinear analysis in chemical engineering. McGraw-Hill Inc. New York, NY.
- Fletcher, C. A. J. 1984. Computational Galerkin methods. Spring-Verlay New York Inc. New York, NY.
- Forbush, Todd D. and Roger C. Brook. 1989. Ventilation rate affects on temperature, moisture and quality responses of stored potatoes. ASAE Paper No. 89-1631. ASAE, St. Joseph, MI.
- Gaffney, J. J. and C. D. Baird. 1977. Forced air cooling of bell peppers in bulk. Transactions of the ASAE 20(6):1174-1179.

- Gould, W. A. 1984. Snack manufacturers put quality first. In: Potato technology, Volume III. Snack Food Association. Alexandria, VA.
- Grama, S. N., C. J. Bern and C. R. Hurburgh, Jr. 1984. Airflow resistance of mixtures of shelled corn and fines. Transactions of the ASAE 27(1):268-272.
- Greenkorn, R. A. 1983. Flow phenomena in porous media-Fundamentals and applications in petroleum, water, and food production. Marcel Dekker Inc. New York, NY.
- Hall, C. W. 1955. Analysis of air flow in grain drying. Agricultural Engineering 36(4):247-250.
- Hammerschmidt, R. and A. C. Cameron. 1986. Influence of environmental factors on wound healing of potato tubers in relation to storage disorders. 1986 Michigan Potato Research Report (Volume 18). Michigan State University Agricultural Experiment Station in cooperation with the Michigan Potato Industry Commission. Dewitt, MI.
- Hammerschmidt, R. and A. C. Cameron. 1987. Influence of environmental factors on wound healing of potato tubers in relation to storage disorders. 1987 Michigan Potato Research Report (Volume 19). Michigan State University Agricultural Experiment Station in cooperation with the Michigan Potato Industry Commission. Dewitt, MI.
- Haque, E., G. H. Foster, D. S. Chung and F. S. Lai. 1978. Static pressure drop across a corn bed mixed with fines. Transactions of the ASAE 21(5):997-1000.
- Haque, E., D. S. Chung and G. H. Foster. 1980. Pressure and velocity field in airflow through packed bed of corn mixed with fines under non-Darcy flow conditions. ASAE Paper No.80-3016. ASAE, St. Joseph, MI.
- Hardenburg, R. E., A. E. Watada and C. Y. Wang. 1986. The commercial storage of fruits, vegetables, and florist and nursery stocks. USDA Agricultural Research Service, Agricultural Handbook No.66.
- Hariharan, S. I. and T. H. Houlden. 1986. Numerical methods for partial differential equations. John Wiley & Sons Inc. New York, NY.
- Hawkes, F. G. 1978. History of potato. from The potato crop: The scientific basis for improvement. Harris, P. M. (editor). Chapman and Hall Ltd. London.
- Henderson, S. M. 1943. Resistance of shelled corn and bin walls to air flow. Agricultural Engineering 24(11):367-369, 374.

- Henderson, S. M. 1944. Resistance of soybeans and oats to air flow. Agricultural Engineering 25(4):127-128.
- Hide, G. A. and D. H. Lapwood. 1978. Disease aspects of potato production. from: The potato crop: The scientific basis for improvement. Harris, P. M. (editor). Chapman and Hall Ltd. London.
- Hohner, G. A. and D. B. Brooker. 1965. An analog of grain cooling by cross-flow aeration in tall structures. Transactions of the ASAE 8(1):56-59, 62.
- Hukill, W. V. and N. C. Ives. 1955. Radial air flow resistance of grain. Agricultural Engineering 36(5):332-335.
- Hukill, W. V. and C. K. Shedd. 1955. Non-linear air flow in grain drying. Agricultural Engineering 36(7):462-466.
- Hunter, J. H. and E. C. Yaeger. 1972. Evaluation of crossflow circulation system for potato storages. ASAE Paper No.NA72-410. ASAE, St. Joseph, MI.
- Hunter, J. H. 1985. Heat of respiration and weight loss from potatoes in storage. ASAE Paper No.85-4035. ASAE, St. Joseph, MI.
- Husain, A. and T. P. Ojha. 1969. Resistance to the passage of air through rice. J. Agric. Eng. Res. 14(1):47-53.
- Incropera, F. P. and D. P. DeWitt. 1985. Introduction to heat transfer. John Wiley & Sons Inc. New York, NY.
- Ives, N. C., W. V. Hukill and R. A. Saul. 1959. Grain ventilation and drying patterns. Transactions of the ASAE 21(1):95-101.
- Jayas, D. S., S. Sokhansanj, E. B. Moysey and E. M. Barber. 1987. The effect of airflow direction on the resistance of canola (rapeseed) to airflow. Can. Agric. Eng. 29(2):189-192.
- Jindal, V. K. and T. L. Thompson. 1972. Air Pressure patterns and flow paths in twodimensional triangular-shaped piles of sorghum using forced convection. Transactions of the ASAE 15(4):737-741.
- Kardestuncer, H. (editor in chief) and D. H. Norrie (project editor). 1987. Finite element handbook. McGraw-Hill Inc. New York, NY.
- Kay, R. L., C. J. Bern and C. R. Hurburgh, Jr. 1989. Horizontal and vertical airflow resistance of shelled corn at various bulk densities. Transactions of the ASAE 32(2):733-736.

- Kelly, C. F. 1939. Method of drying grain on the farm. Agricultural Engineering 20(4):135-138.
- Khompos, V. 1983. Three-dimensional finite element analysis of the flow field in cylindrical grain storages. Ph.D. dissertation. Michigan State University, East Lansing, MI.
- Khompos, V., L. J. Segerlind and R. C. Brook. 1984. Pressure patterns in cylindrical grain storages. ASAE Paper No.84-3011. ASAE, St. Joseph, MI.
- Lai, F. S. 1980. Three-dimensional flow of air through nonuniform grain beds. Transactions of the ASAE 23(3):729-734.
- Lawton, P. J. 1965. Resistance to air flow of some common seeds. J. Agric. Eng. Res. 10(4):298-300.
- Leva, M. 1959. Fluidization. McGraw-Hill Inc. New York, NY.
- Marchant, J. A. 1976a. Prediction of fan pressure requirements in the drying of large hay bales. J. Agric. Eng. Res. 21(4):333-346.
- Marchant, J. A. 1976b. The prediction of airflows in crop drying systems by the finite element method. J. Agric. Eng. Res. 21(4):417-429.
- Matthies, H. J. and H. Peterson. 1974. New data for calculating the resistance of air flow of stored granular materials. Transactions of the ASAE 17(6):1144-1149.
- Miketinac, M. J. and S. Sokhansanj. 1985. Velocity-pressure distribution in grain bins-Brooker's model. Int. J. Num. Meth. Eng. 21(6):1067-1075.
- Miketinac, M. J., S. Sokhansanj and D. S. Jayas. 1986. Graphical analysis of airflow distribution in grain bins using the finite element method. Can. Agric. Eng. 28(1):23-30.
- Mitchell, N. and R. Rogers. 1976. Ventilation system and equipment designs for the Midwest storage. In: The potato storage design, construction, handling and environmetal control. Cargill, B. F. (editor). Michigan State University, East Lansing, MI.
- Muskat, M. 1937. The flow of homogeneous fluids through porous media. McGraw-Hill Inc. New York, NY.
- Neale, M. A. and H. J. M. Messer. 1976. Resistance of root and bulb vegetables to airflow. J. Agric. Eng. Res. 21(3):221-231.

- Neale, M. A. and H. J. M. Messer. 1978. Resistance of leafy vegetables and inflorescences to airflow. J. Agric. Eng. Res. 23(1):67-75.
- Nellist, M. E. and D. V. H. Rees. 1969. The resistance to airflow of dry and soaked vegetable seeds. J. Agric. Eng. Res. 14(4):344-349.
- Ortega, James M. 1987. Matrix theory. Plenum Press, A Division of Plenum Publishing Corporation. New York, NY.
- Osborne, L. E. 1961. Resistance to airflow of grain and other seeds. J. Agric. Eng. Res. 6(2):119-122.
- Patterson, R. J. 1969. Airflow-pressure drop characteristics of packed beds of biological particles. Master Thesis. Michigan State University, East Lansing, MI.
- Patterson, R. J., F. W. Bakker-Arkema and W. G. Bickert. 1971. Static pressure-airflow relationships in packed beds of granular biological materials such as grain-II. Transactions of the ASAE 14(1):172-174, 178.
- Pearson, Carl E. (editor) 1983. Handbook of applied mathematics, selected results and methods. Van Nostrand Reinhold Company Inc., New York, NY.
- Pierce, R. O. and T. L. Thompson. 1975. Airflow patterns in conical-shaped piles of grain. Transactions of the ASAE 18(5):946-949.
- Plissey, E. S. 1976. Philosophy of potato storage. from: The potato storage design, construction, handling and environmental control. Cargill, B. F. (editor). Michigan State University, East Lansing, MI.
- Rabe, D. L. and H. D. Currence. 1975. Air flow resistance and density of alfalfa leaves. Transactions of the ASAE 18(5):932-934, 938.
- Rabe, F. W. 1958. Aeration of grain in vertical bins. Agricultural Engineering 39(4):247-250.
- Rastovski, A., A. Van Es et al. 1987. Storage of potatoes: Post-harvest behaviour, store design, storage practice, handling. Pudoc Wageningen, Netherlands.
- Reddy, J. N. 1984. An introduction to the finite element method. McGraw-Hill, Inc. New York, NY.
- Sabersky, R. H., A. J. Acosta and E. G. Hauptmann. 1989. Fluid flow-A first course in fluid mechanics. Macmillan Publishing Company. New York, NY.

- Scheidegger, A. E. 1974. The physics of flow through porous media, 3rd edition. University of Toronto Press, Toronto.
- Seelig, R. A. 1972. Fruit & vegetable facts & pointers: POTATO. United Fresh Fruit & Vegetable Association, Washington, D. C.
- Segerlind, L. J. 1982. Solving the nonlinear airflow equation. ASAE Paper No.82-3017. ASAE, St. Joseph, MI.
- Segerlind, L. J. 1983. Presenting velocity-pressure gradient data for use in mathematical methods. Transactions of the ASAE 26(4):1245-1248.
- Segerlind, L. J. 1984. Applied finite element analysis, 2nd edition. John Wiley & Sons Inc. New York, NY.
- Shedd, C. K. 1945. Resistance of ear corn to air flow. Agricultural Engineering 26(1):19-20, 23.
- Shedd, C. K. 1951. Some new data on resistance of grains to air flow. Agricultural Engineering 32(9):493-495, 520.
- Shedd, C. K. 1953. Resistance of grains and seeds to air flow. Agricultural Engineering 34(9):616-619.
- Sheldon, W. H., C. W. Hall and J. K. Wang. 1960. Resistance of shelled corn and wheat to low air flows. Transactions of the ASAE 3(2):92-94.
- Smith, E. A. 1982. Three-dimensional analysis of air velocity and pressure in beds of grain and hay. J. Agric. Eng. Res. 27(2):101-117.
- Sneddon, I. N. (editor) 1976. Encyclopaedic dictationary of mathematics for engineers and applied scientists. Pergamon Press Ltd., New York, NY.
- Sowokinos, J. R. and D. A. Preston. 1988. Maintenance of potato processing quality by Chemical Maturity Monitoring (CMM). Station Bulletin 586-1988 (Item No. AD-SB-3441). Minnesota Agricultural Experiment Station, University of Minnesota. St. Paul, MN.
- Spencer, H. B. 1969. Pressure drop in on-floor duct drying systems. J. Agric. Eng. Res. 14(2):165-172.
- Staley, L. M. and E. L. Watson. 1961. Some design aspect of refrigerated potato storages. Can. Agrc. Eng. 3(1):20-22.

- Stirniman, E. J., G. P bodnar and E. N. Bates. 1931. Tests on resistance to the passage of air through rough rice in a deep bin. Agricultural Engineering 12(5):145-148.
- Stryer, Lubert. 1975. Biochemistry. W. H. Freeman and Company, San Francisco, CA.
- Thornton, R. E. and J. B. Sieczka. 1980. Commercial potato production in North America. Potato Association of America Handbook. Supplement to volume 57 of the American Potato Journal.
- USDA Agricultural statistics. 1989. United States Government Printing Office, Washington, D. C. 20402.
- Waelti, H. (1989). Potato storage and ventilation in the Pacific Northwest. In: Potato storage Technology and practice. Cargill, B. F., Roger C. Brook and Todd D. Forbush (editors). ASAE, St. Joseph, MI.
- Wilhelm, L. R., D. W. Jones and C. A. Mullins. 1978. Air flow resistance for snap beans. ASAE Paper No.78-3058. ASAE, St. Joseph, MI.
- Wilhelm, L. R., F. D. Tompkins and C. A. Mullins. 1981. Air flow resistance of lima beans and southern peas. ASAE Paper No.81-3034. ASAE, St. Joseph, MI.
- Wilkes, P. 1976. Potato storage viewpoints by a potato processor. In: The potato storage design, construction, handling and environmental control. Cargill, B. F. (editor). Michigan State University, East Lansing, MI.
- Wilson, E. B. 1967. Ventilation of potato storage structures. ASAE Paper No.67-439. ASAE, St.Joseph, MI.
- Wilson, E. B. 1976. Potato storage ventilation systems for the Pacific Northwest. In: The potato storage design, construction, handling and environmental control. Cargill, B. F. (editor). Michigan State University, East Lansing, MI.